



Current status of eV axion dark matter search

@FY2023 "What is dark matter? - Comprehensive study of the huge discovery space in dark matter" March 7, 2023, Kyoto University

Tohoku U.-> Tokyo Metropolitan U.

Wen Yin

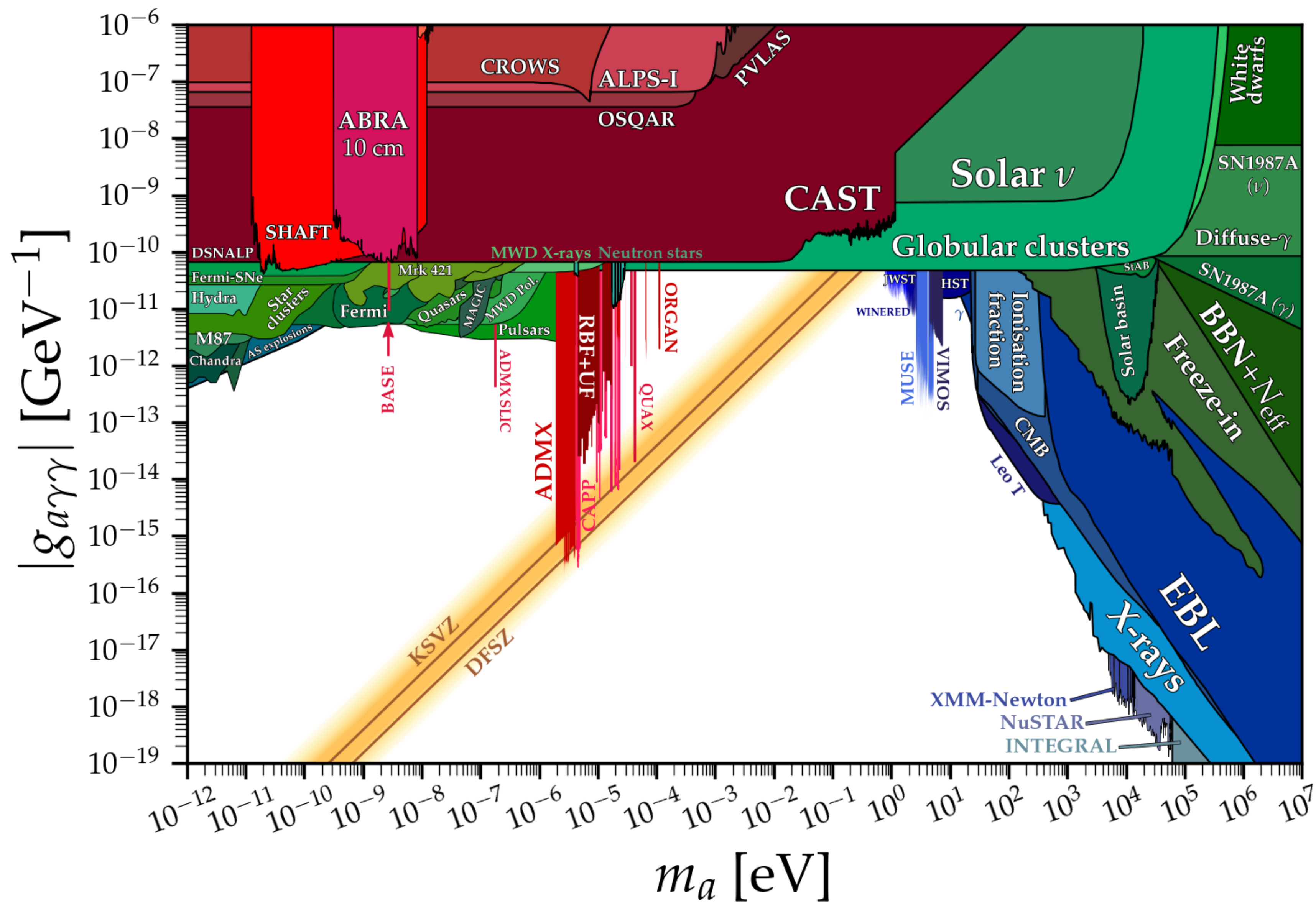
Based on Bessho, Ikeda, WY, 2208.05975

WY, Hayashi, 2305.13415,

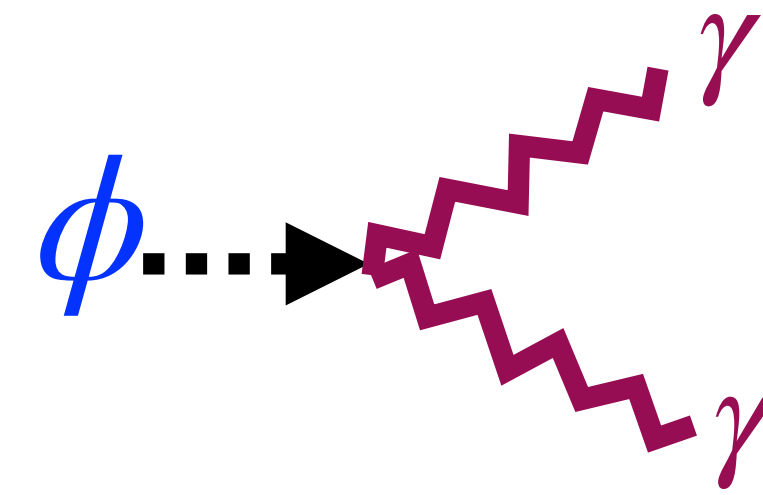
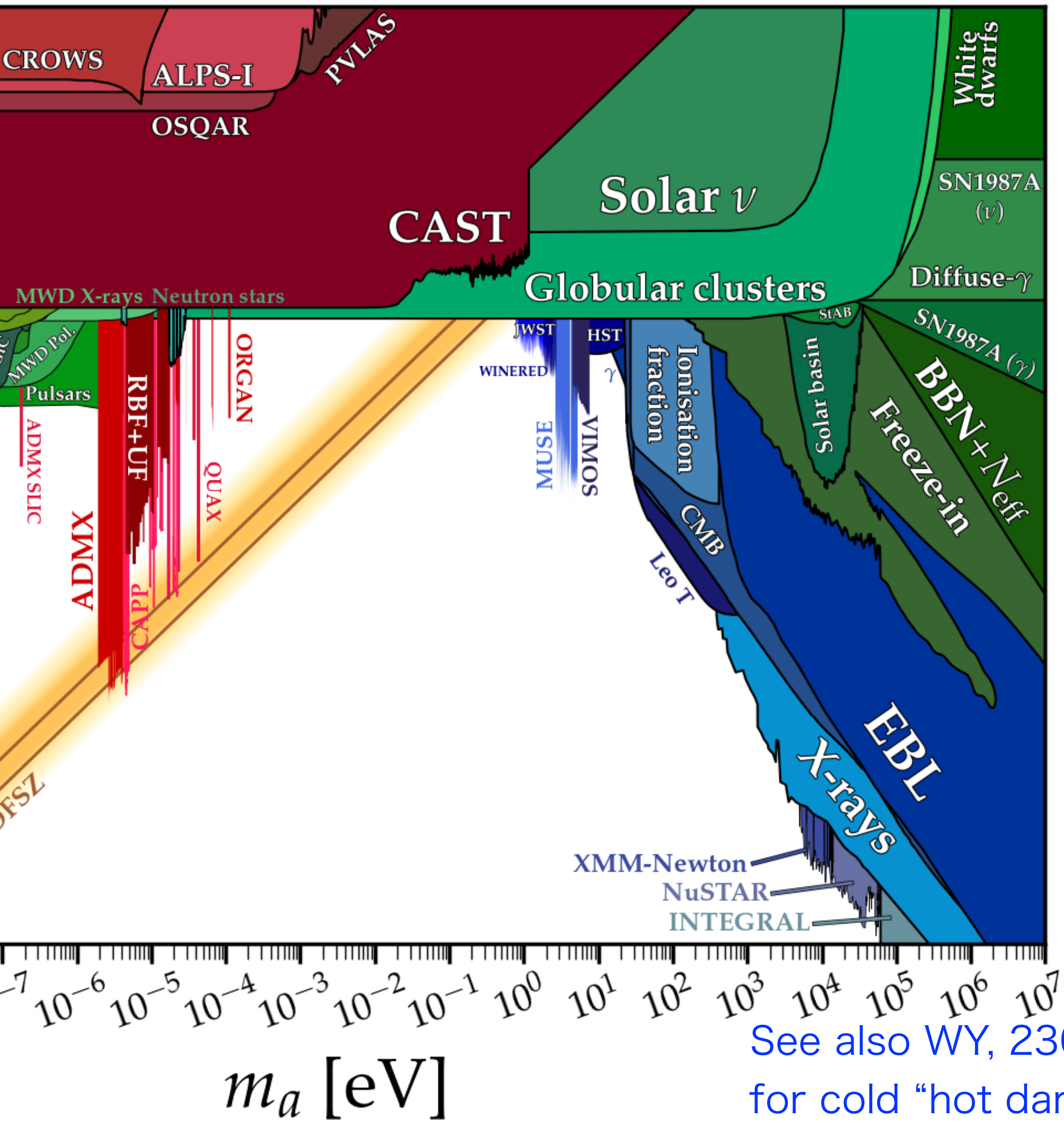
WY, Ikeda, Bessho, Kobayashi+WINERED team, 2402.07976

- **1. Introduction**

Axion Dark Matter



Why eV axion dark matter?



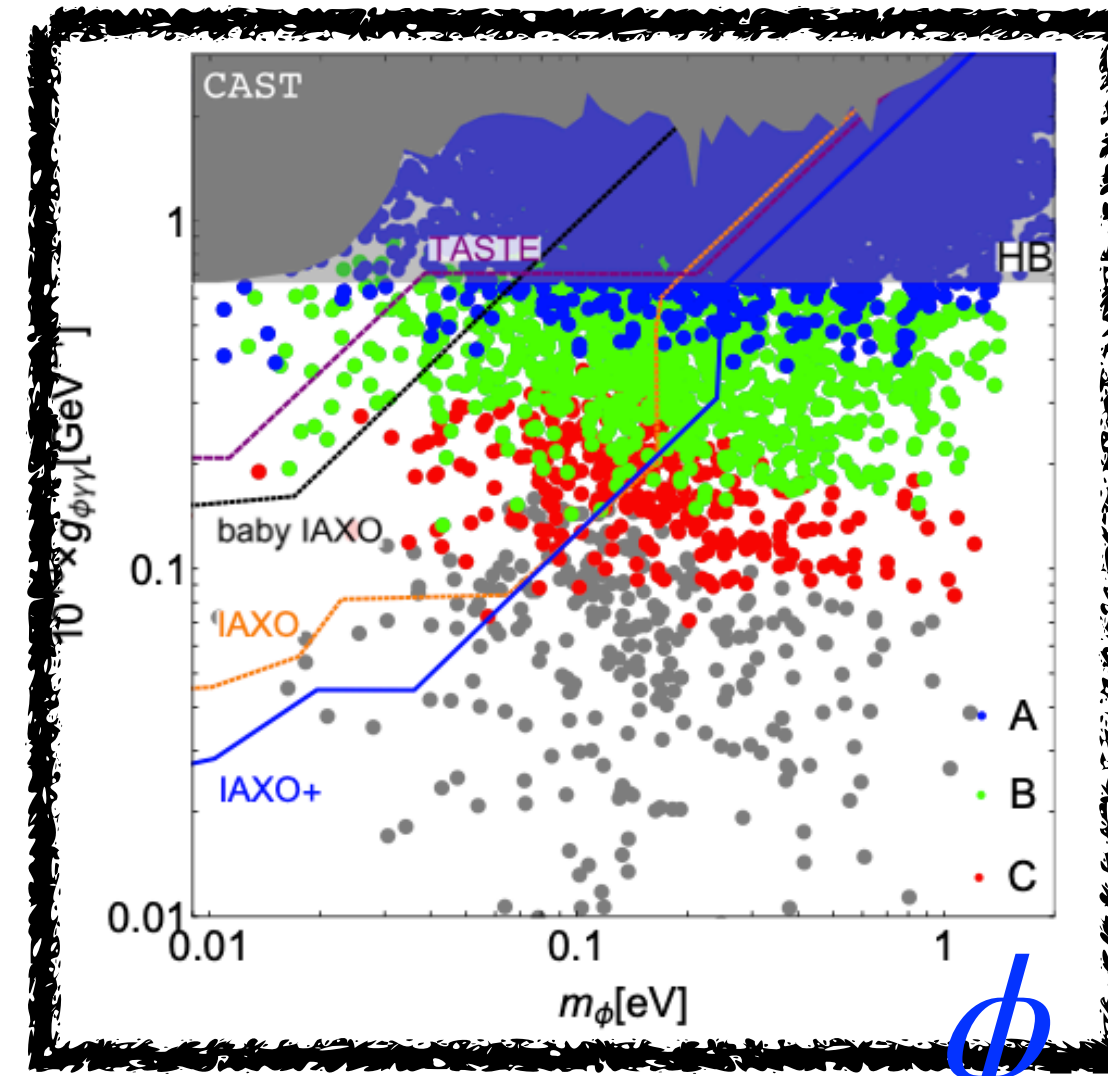
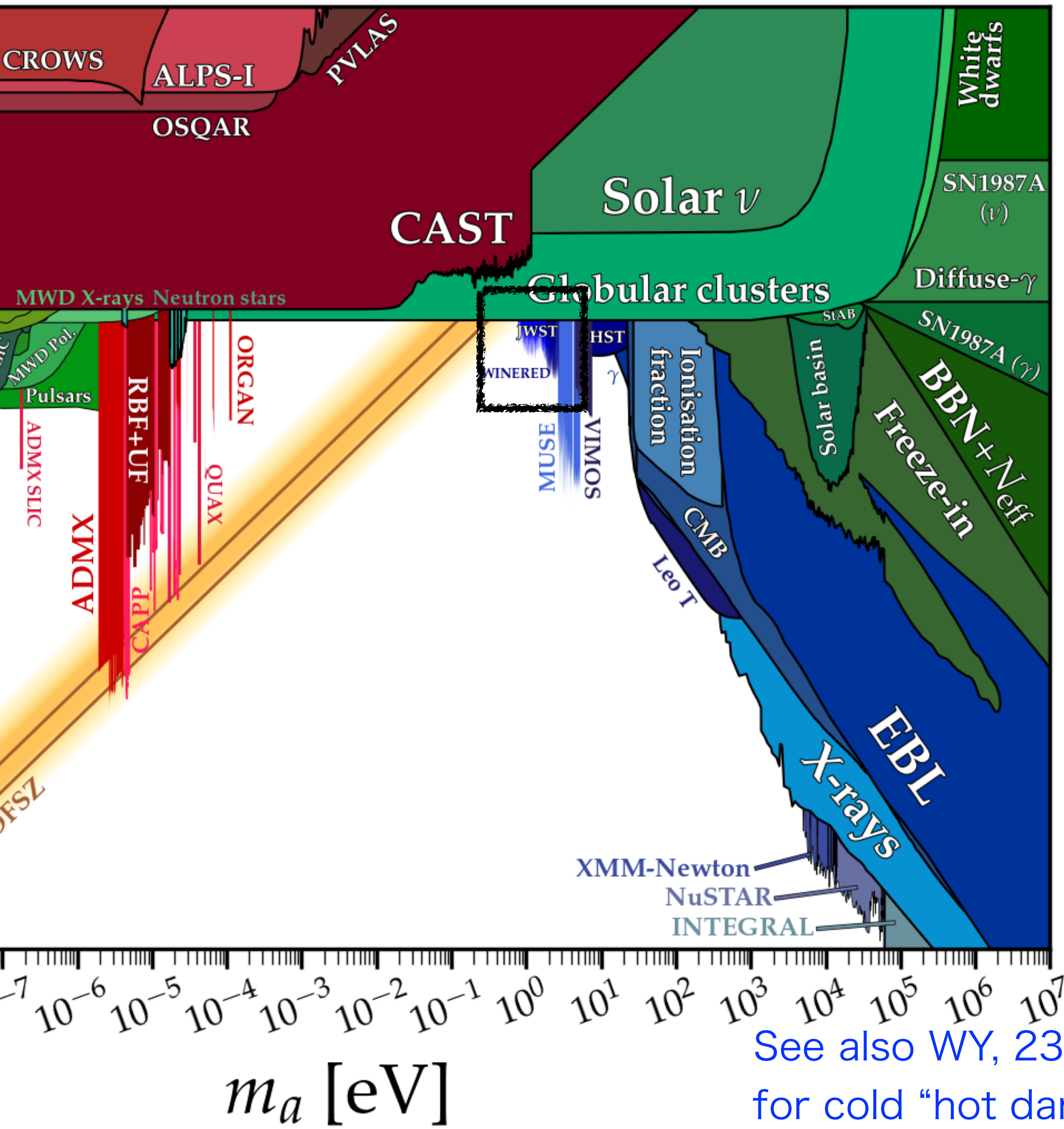
See also WY, 2301.08735
for cold “hot dark matter”

Why eV axion dark matter?

ALP miracle scenario:

Axion=Dark Matter=Inflaton

[Daido, Takahashi, WY, 1702.03284, 1710.11107](#)



See also [WY, 2301.08735](#)
for cold “hot dark matter”

Why eV axion dark matter?

ALP miracle scenario:

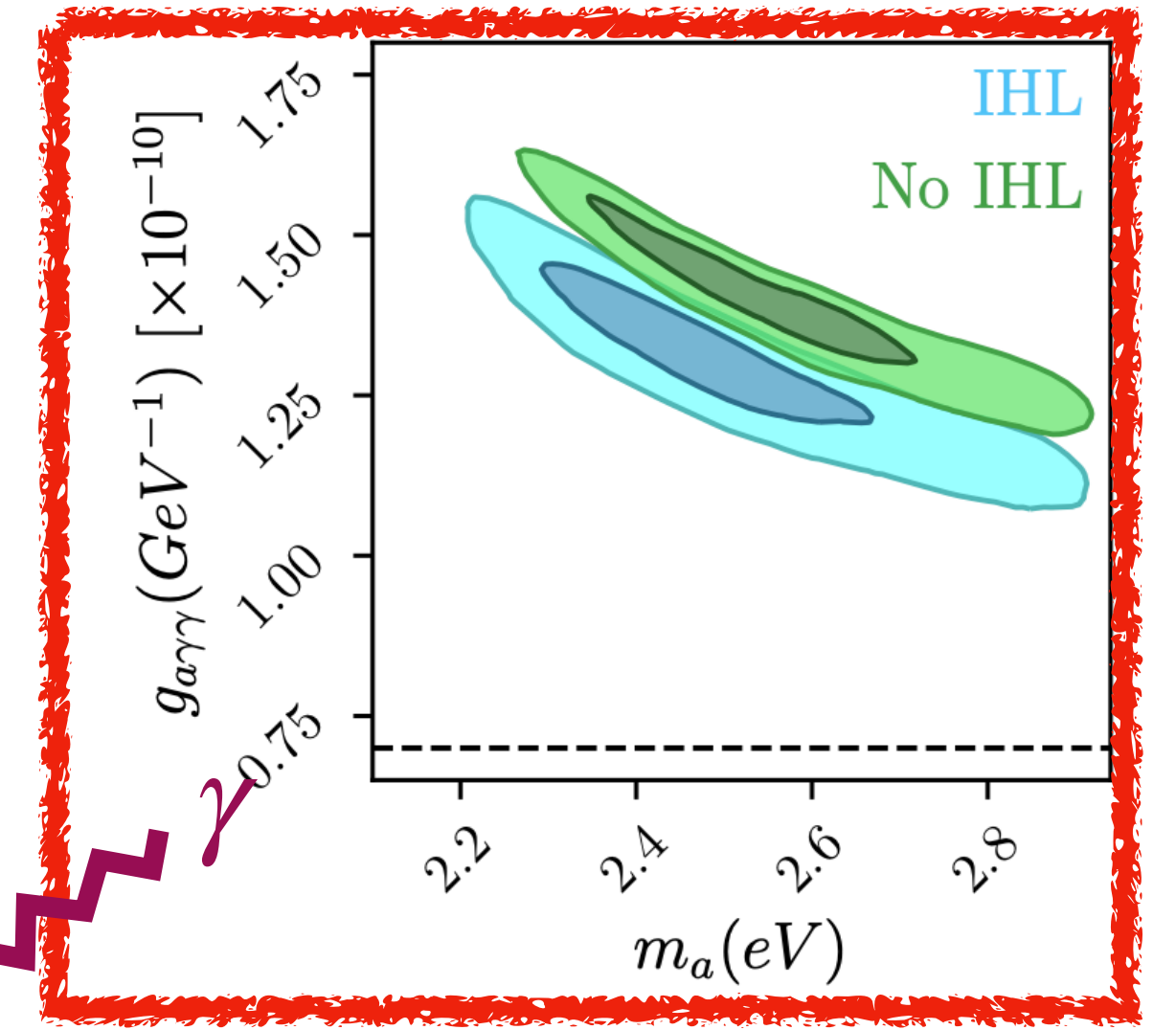
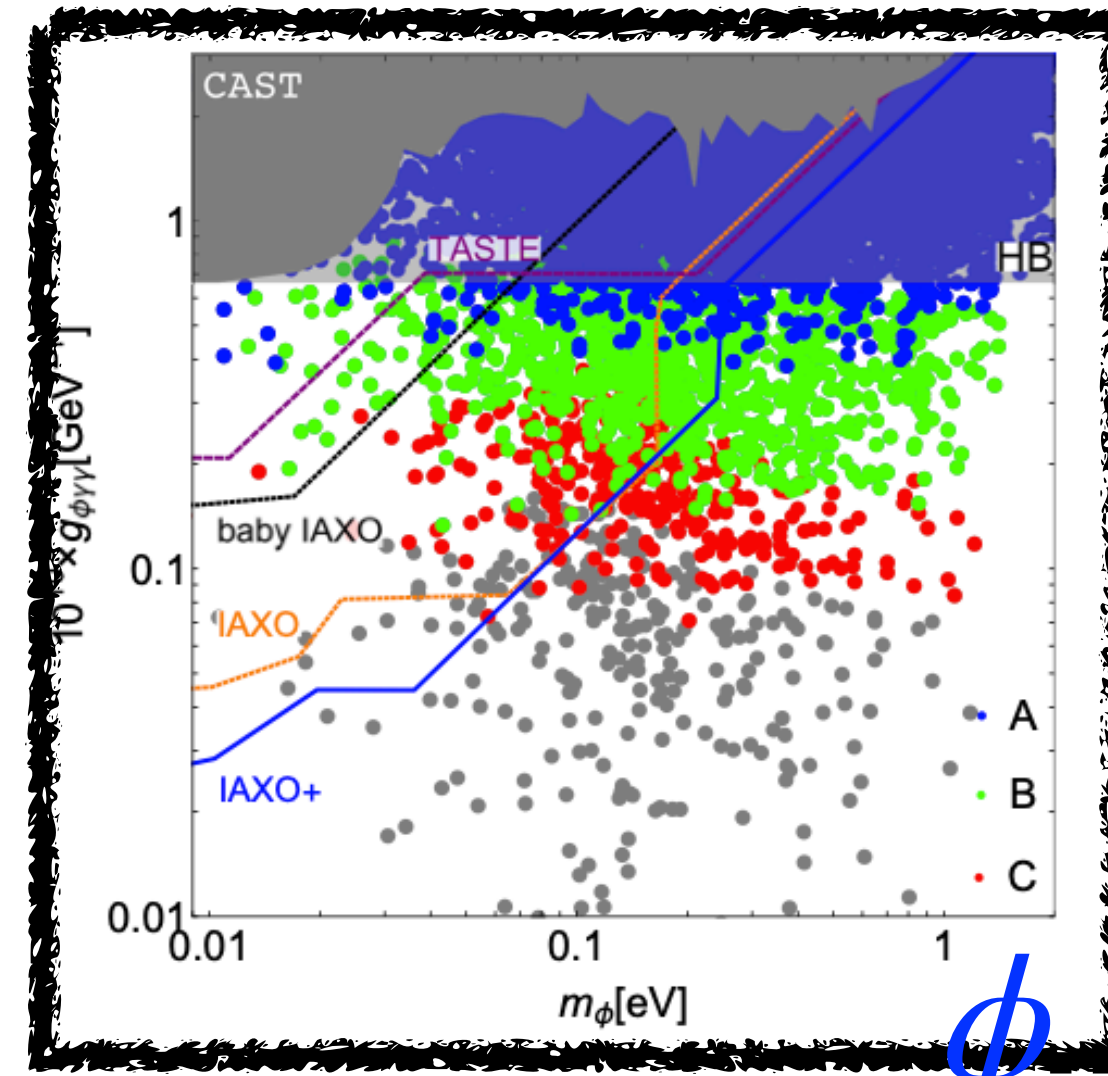
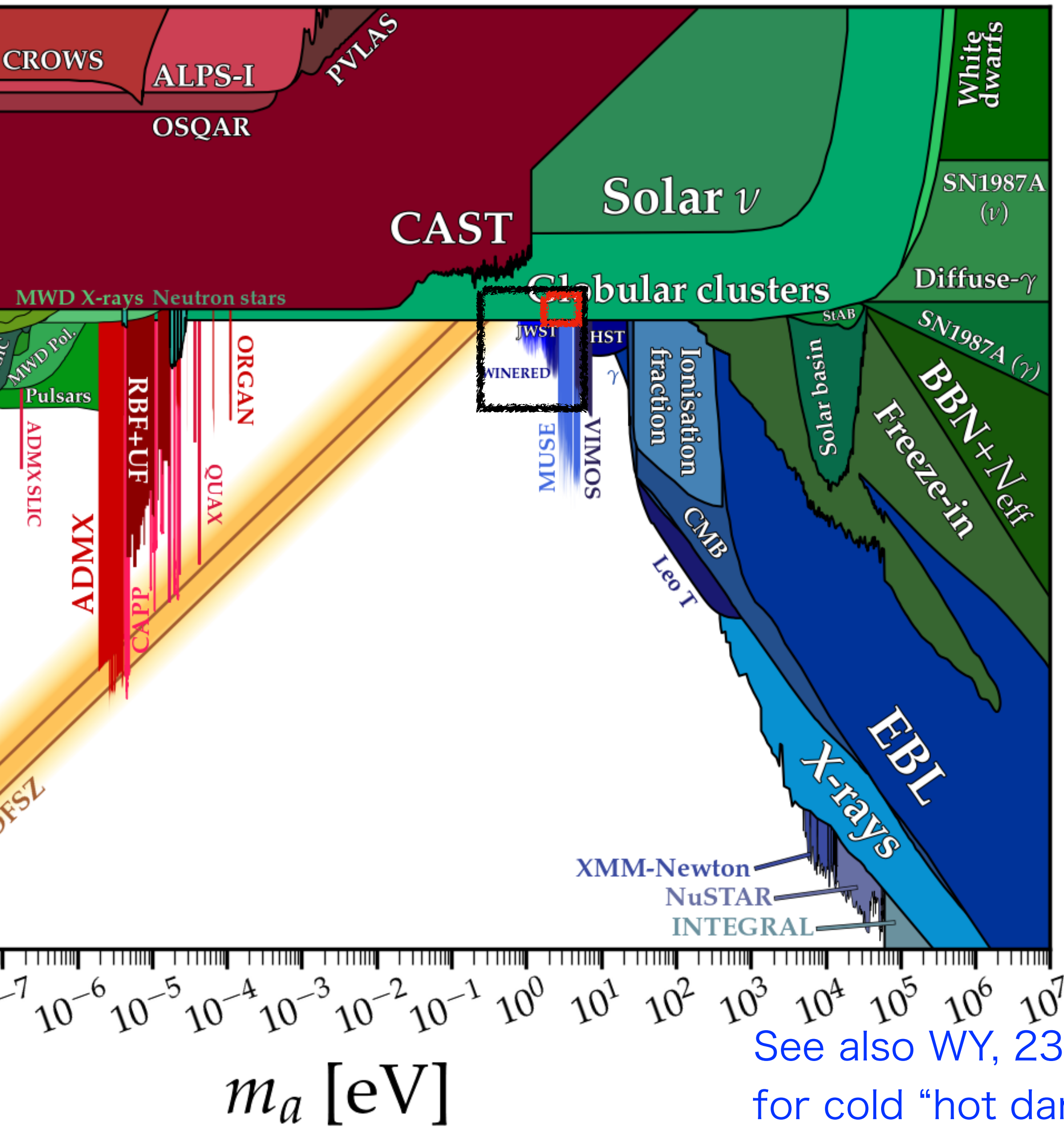
Axion=Dark Matter=Inflaton

Daido, Takahashi, WY, 1702.03284, 1710.11107

Anisotropic cosmic infrared

background [Gong et al 1511.01577](#),

[Caputo et al, 2012.09179](#)



See also [WY, 2301.08735](#)
for cold "hot dark matter"

Why eV axion dark matter?

ALP miracle scenario:

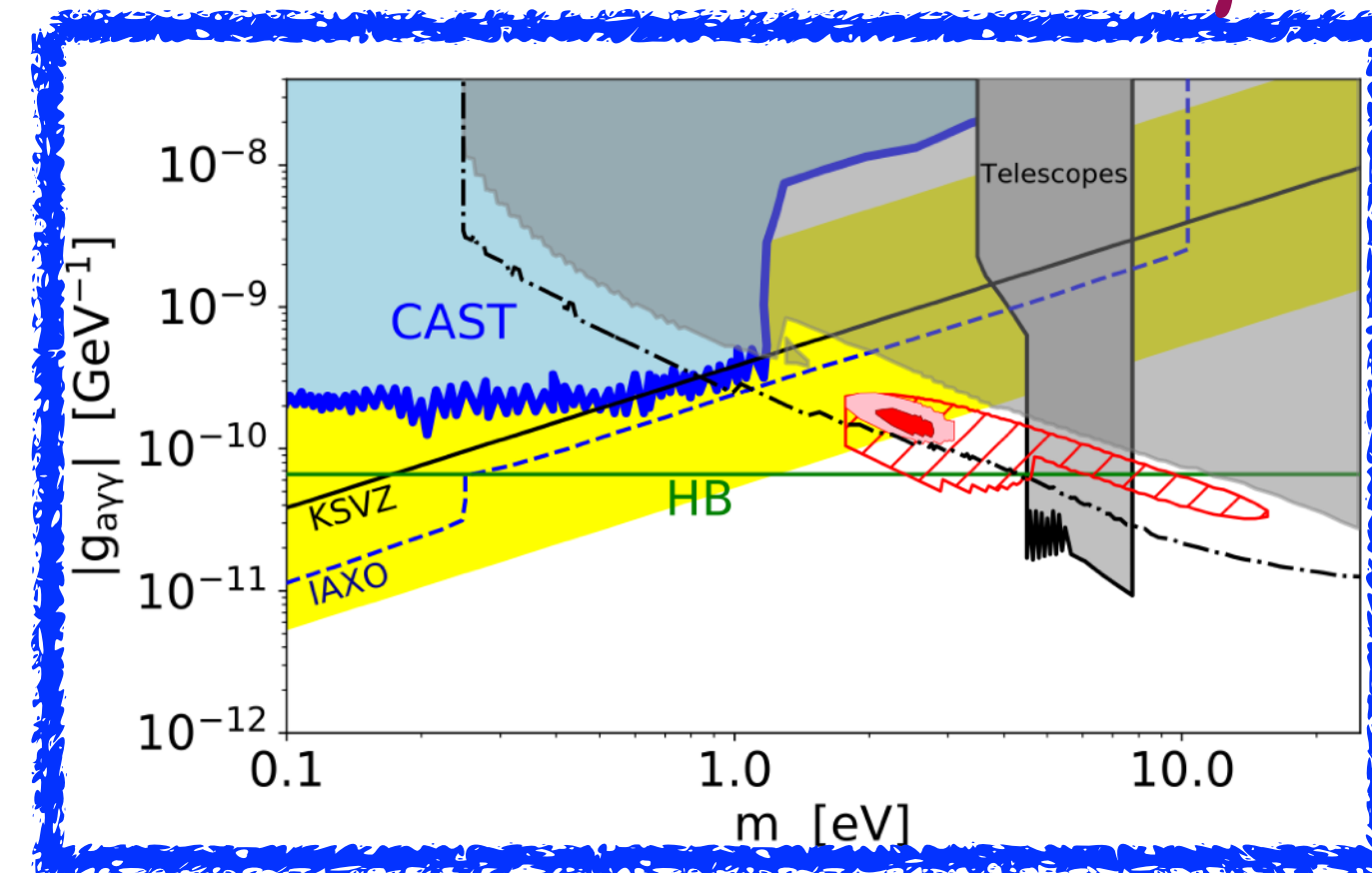
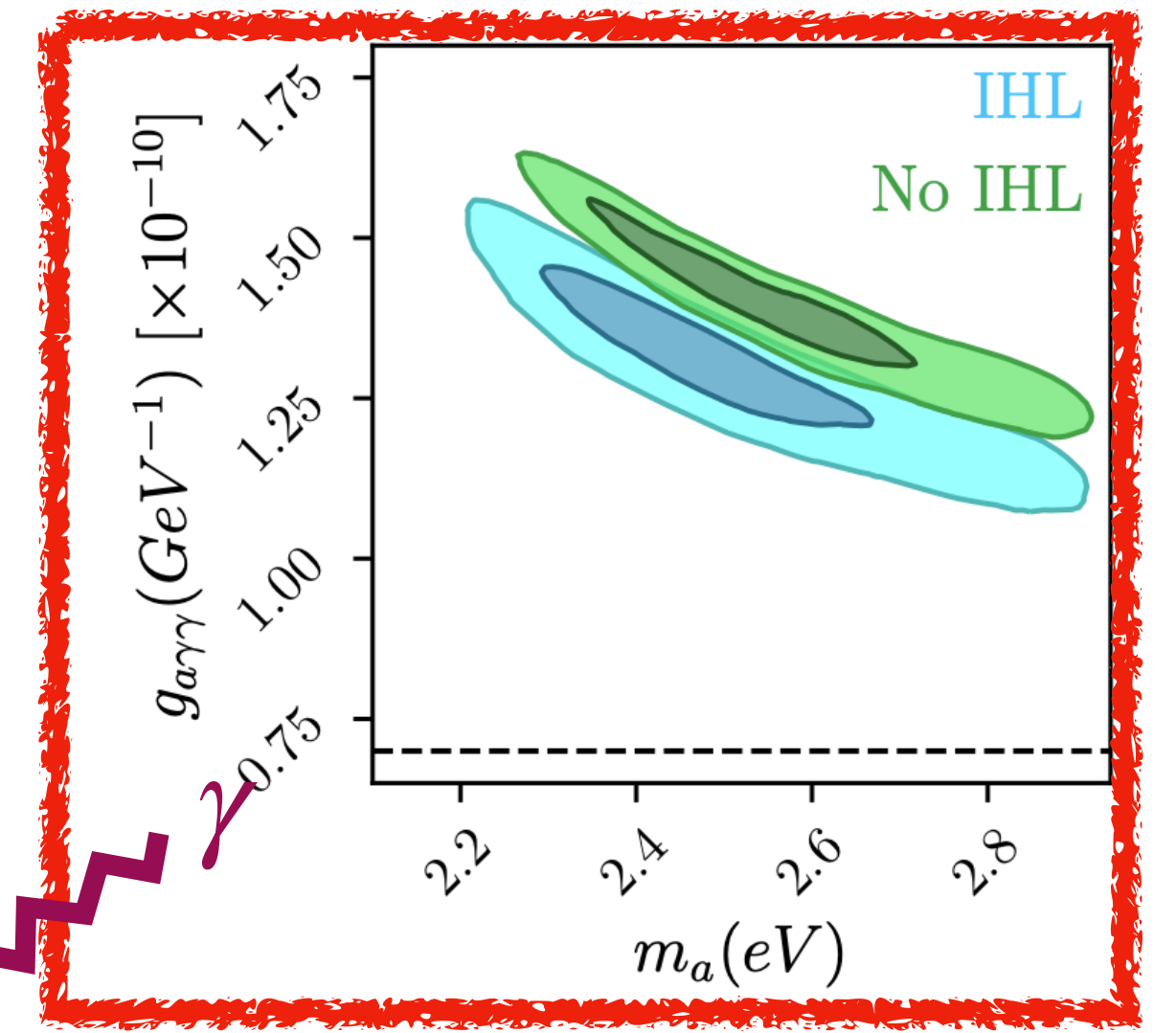
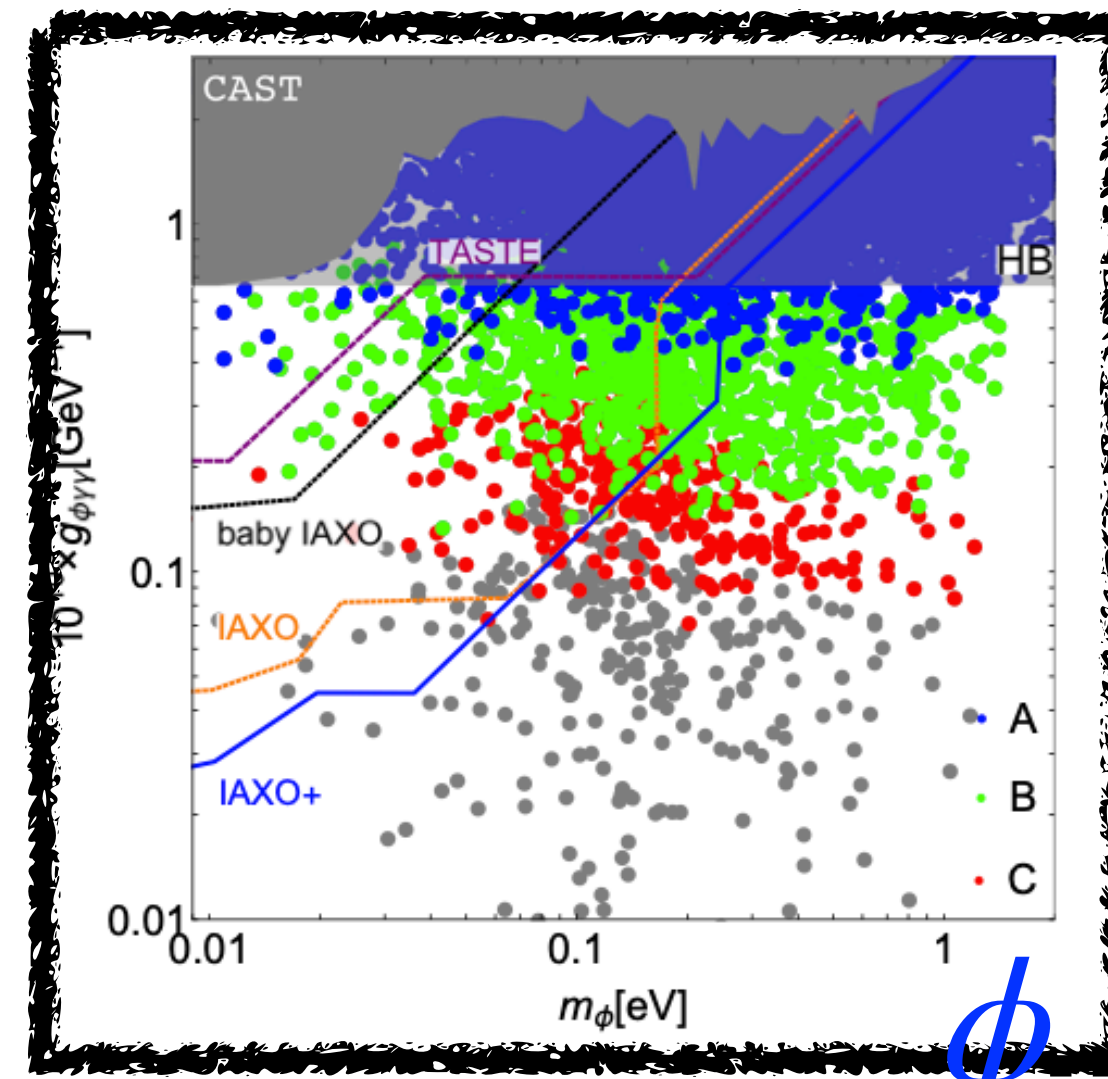
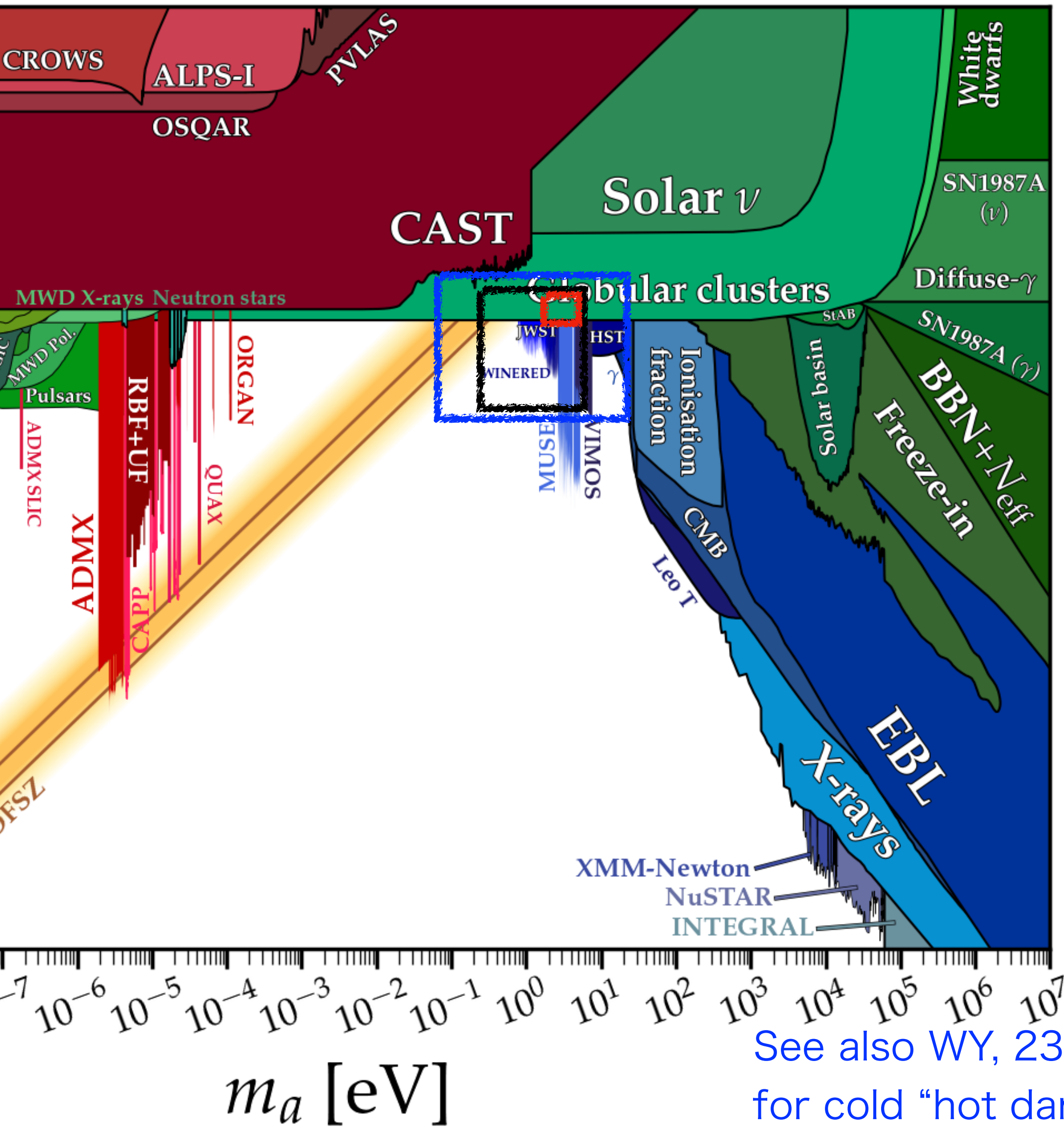
Axion=Dark Matter=Inflaton

Daido, Takahashi, WY, 1702.03284, 1710.11107

Anisotropic cosmic infrared

background [Gong et al 1511.01577](#),

[Caputo et al, 2012.09179](#)



Gamma-ray
attenuation

[Korochkin, Neronov, and Semikoz, 1911.13291](#)

See also [WY, 2301.08735](#)
for cold "hot dark matter"

Why eV axion dark matter?

ALP miracle scenario:

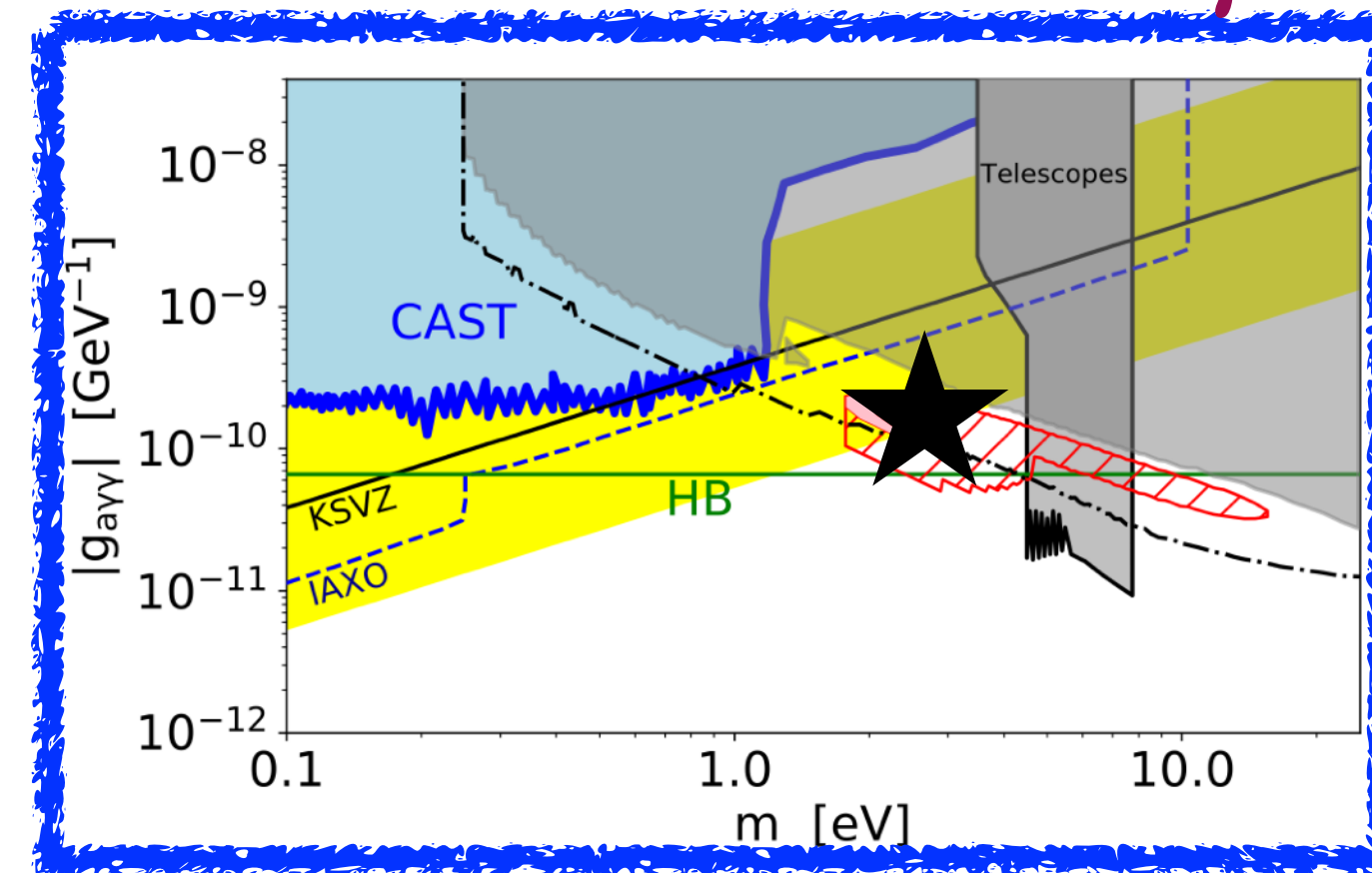
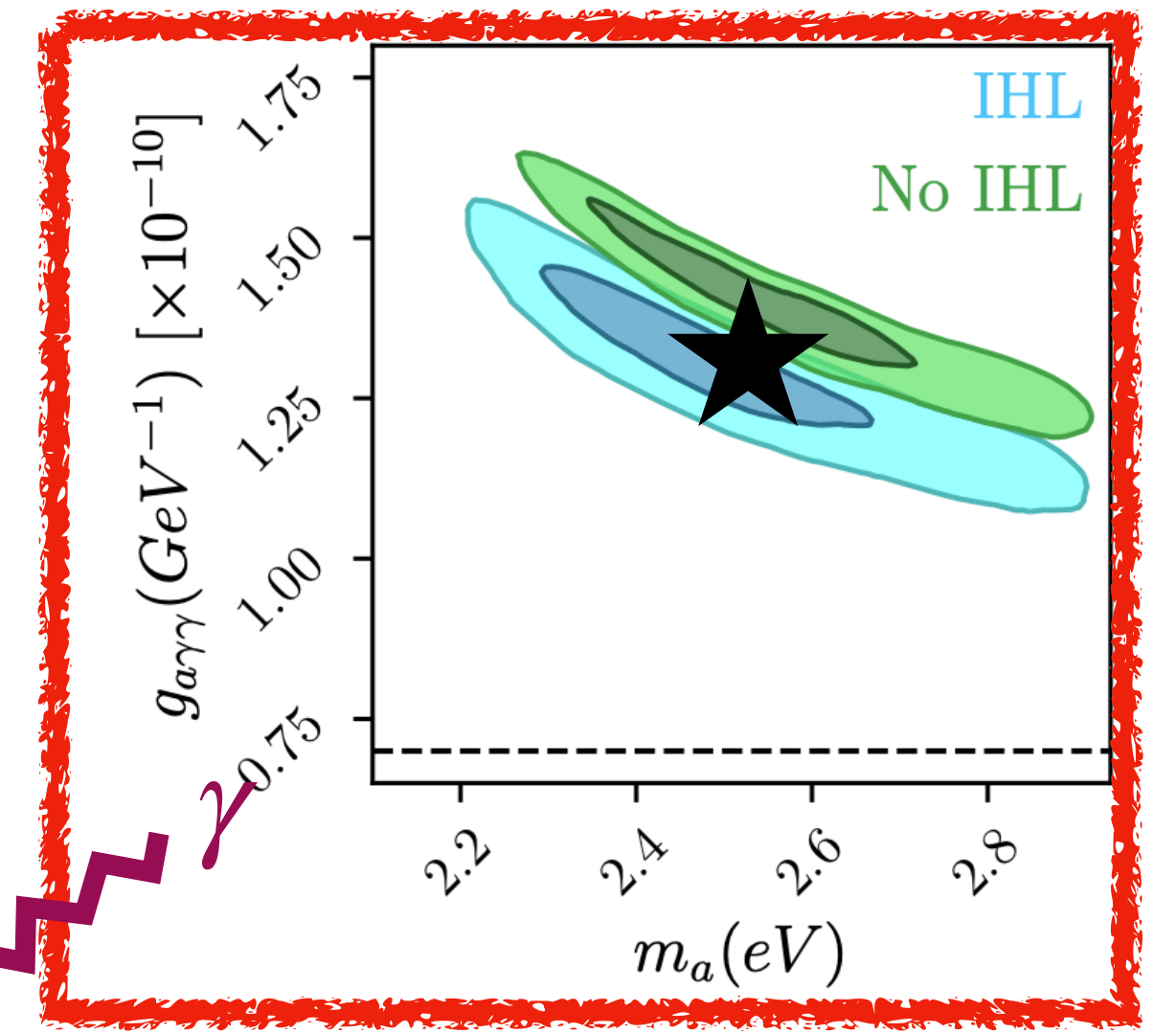
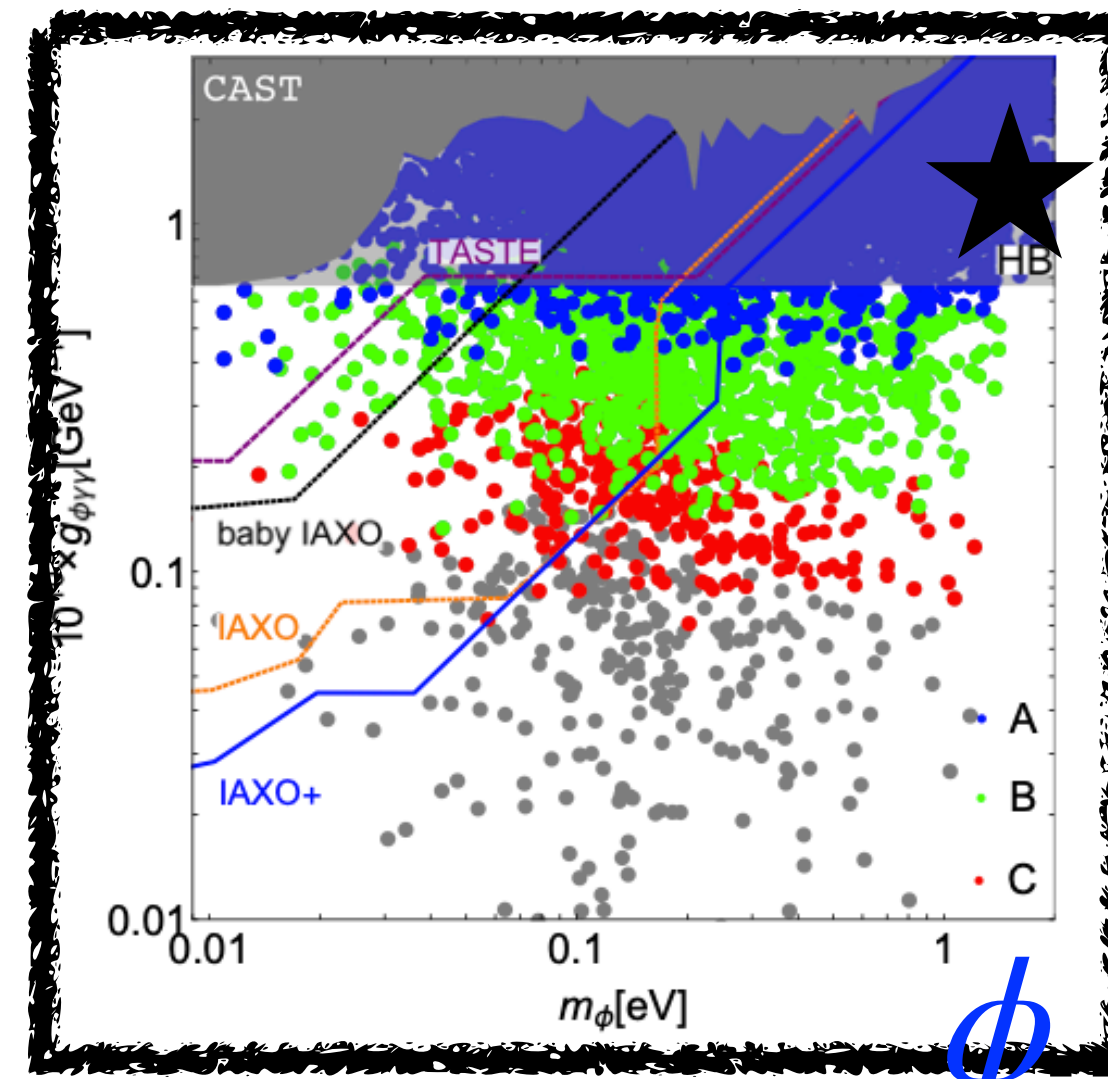
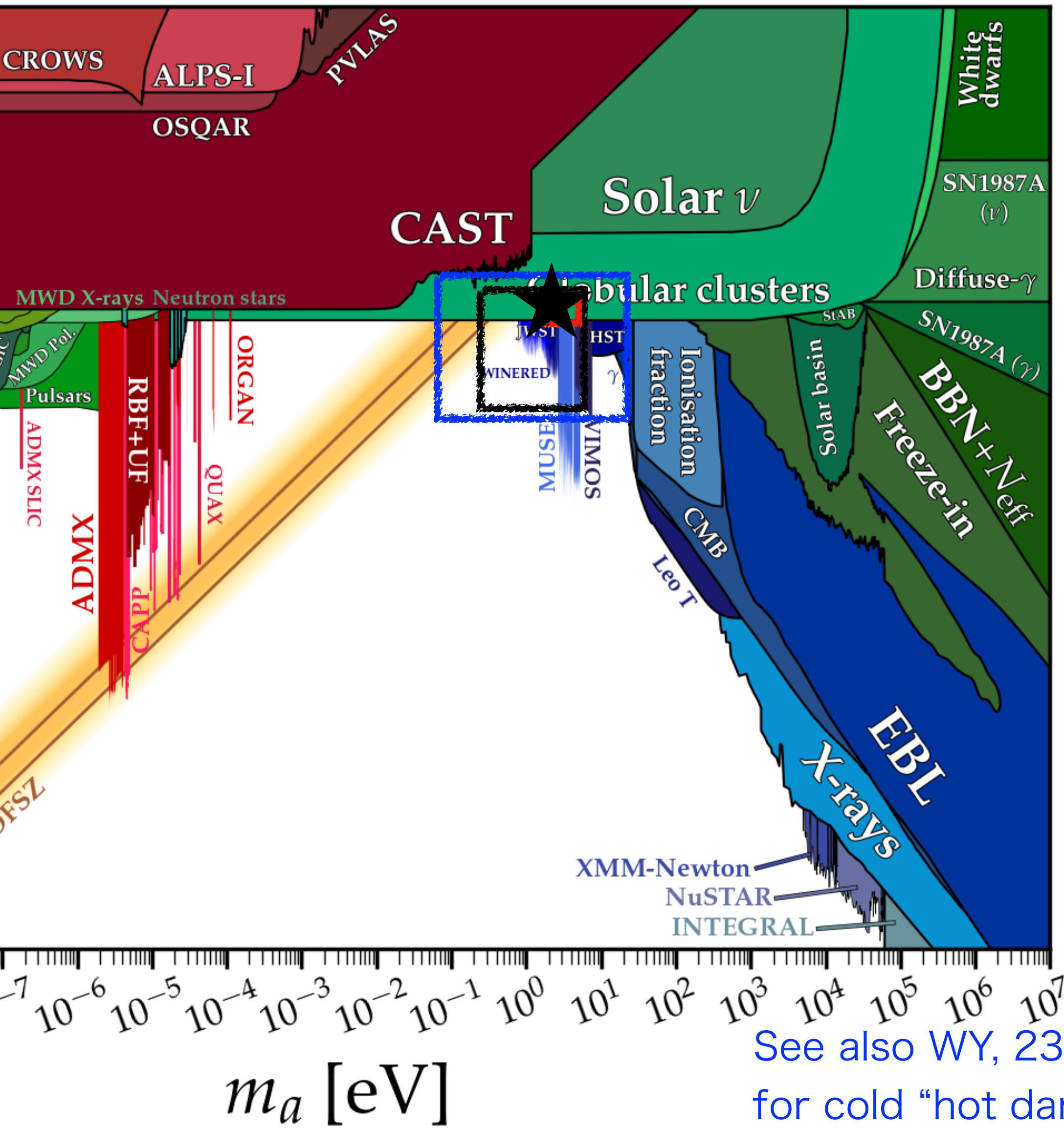
Axion=Dark Matter=Inflaton

Daido, Takahashi, WY, 1702.03284, 1710.11107

Anisotropic cosmic infrared

background [Gong et al 1511.01577](#),

[Caputo et al, 2012.09179](#)



Gamma-ray
attenuation

[Korochkin, Neronov, and Semikoz, 1911.13291](#)

See also [WY, 2301.08735](#)
for cold "hot dark matter"

Why eV axion dark matter?

ALP miracle scenario:

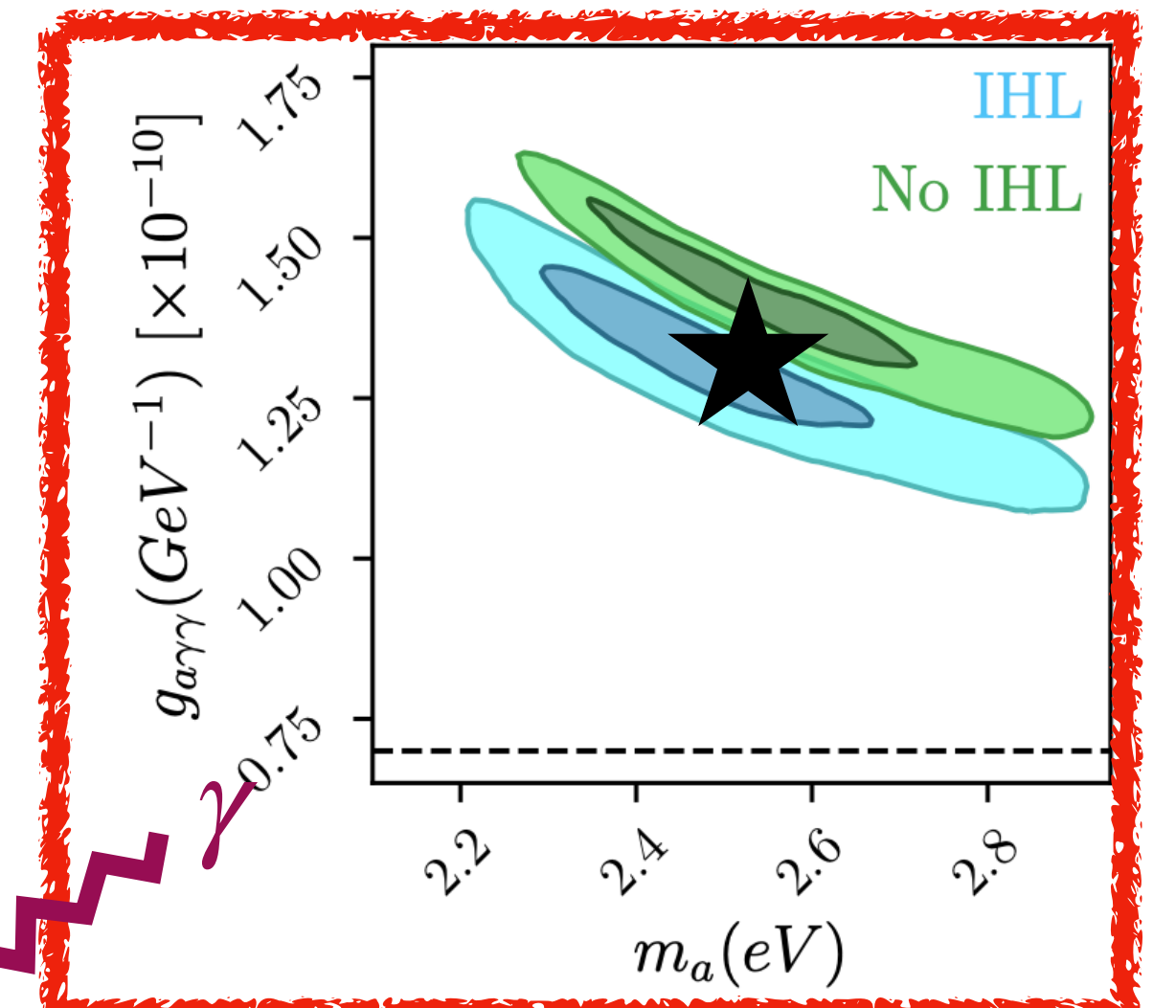
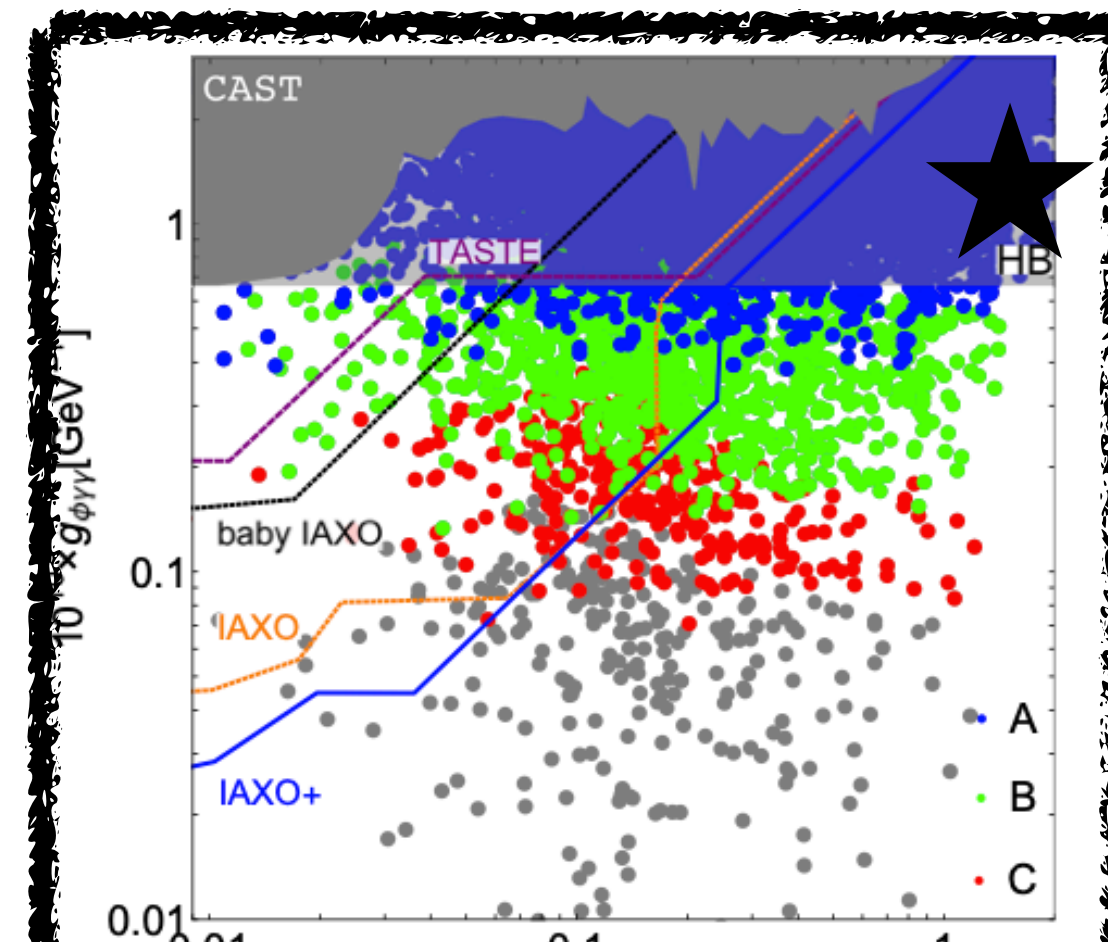
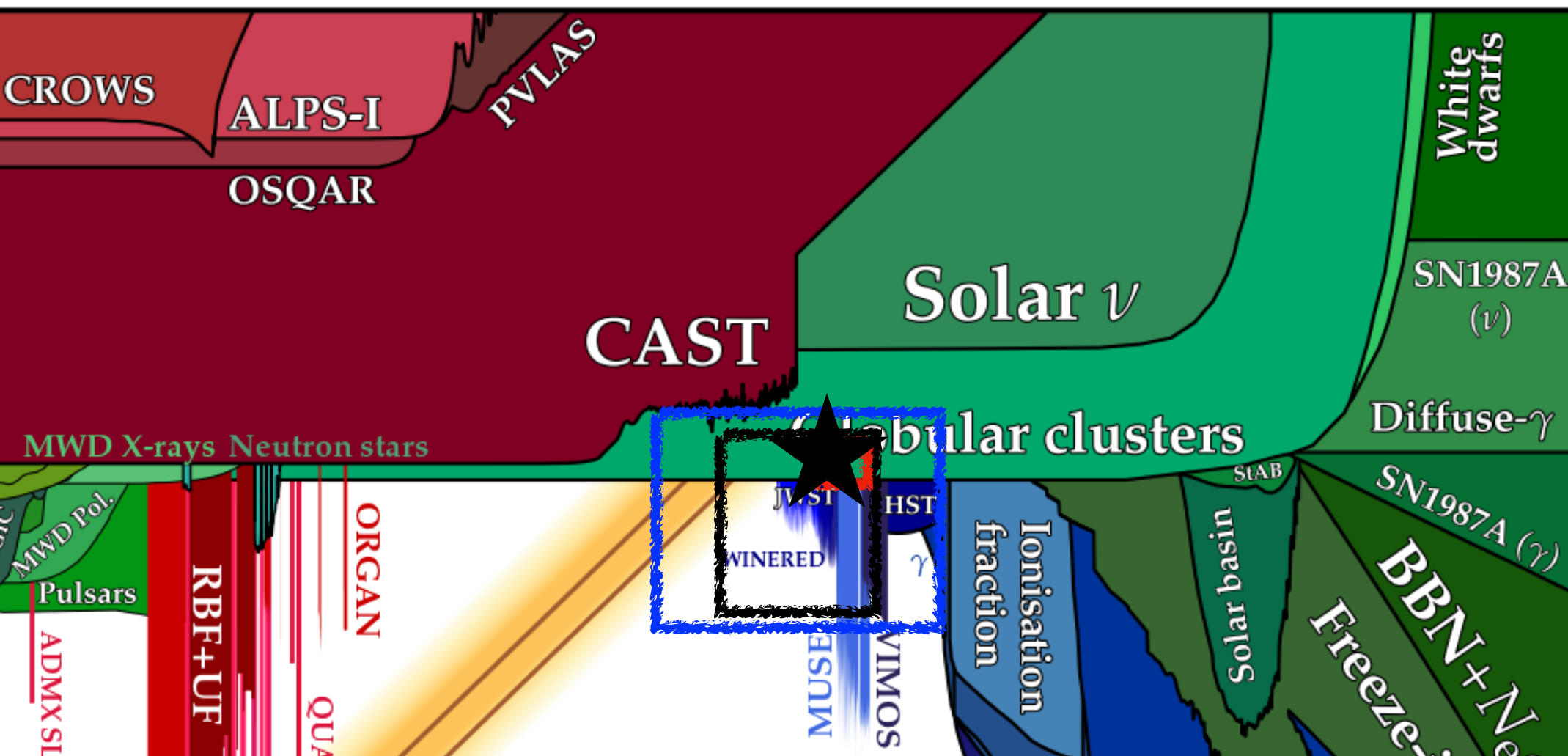
Axion=Dark Matter=Inflaton

[Daido, Takahashi, WY, 1702.03284, 1710.11107](#)

Anisotropic cosmic infrared

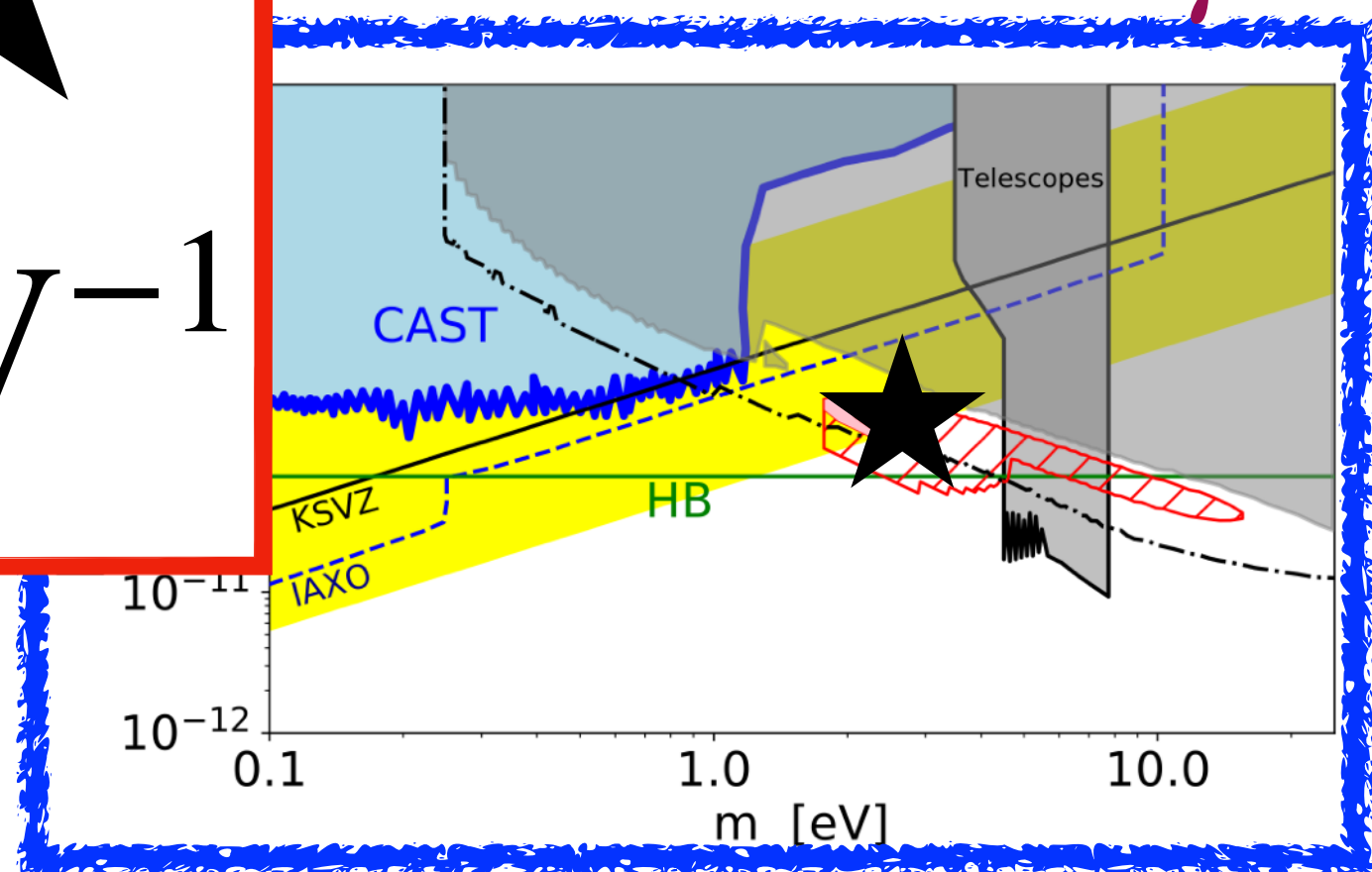
background [Gong et al 1511.01577,](#)

[Caputo et al, 2012.09179](#)



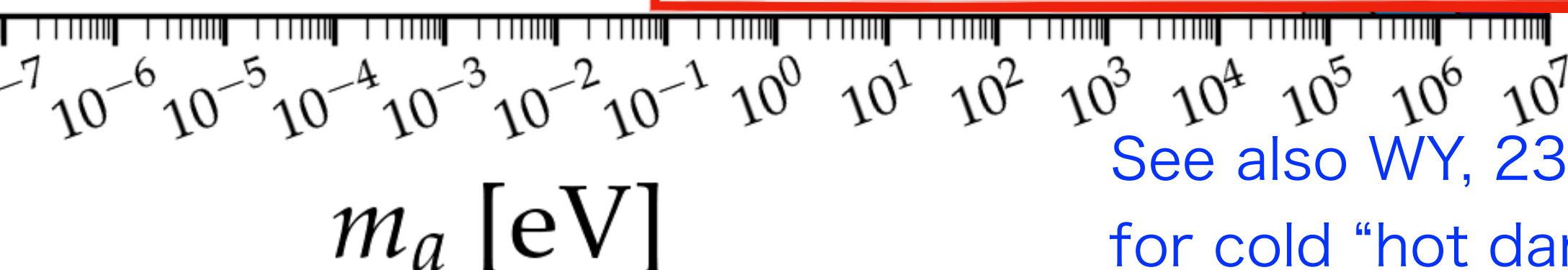
$$m_a \approx 2.5 \text{ eV},$$

$$g_{\gamma\gamma} \approx 1.5 \times 10^{-10} \text{ GeV}^{-1}$$



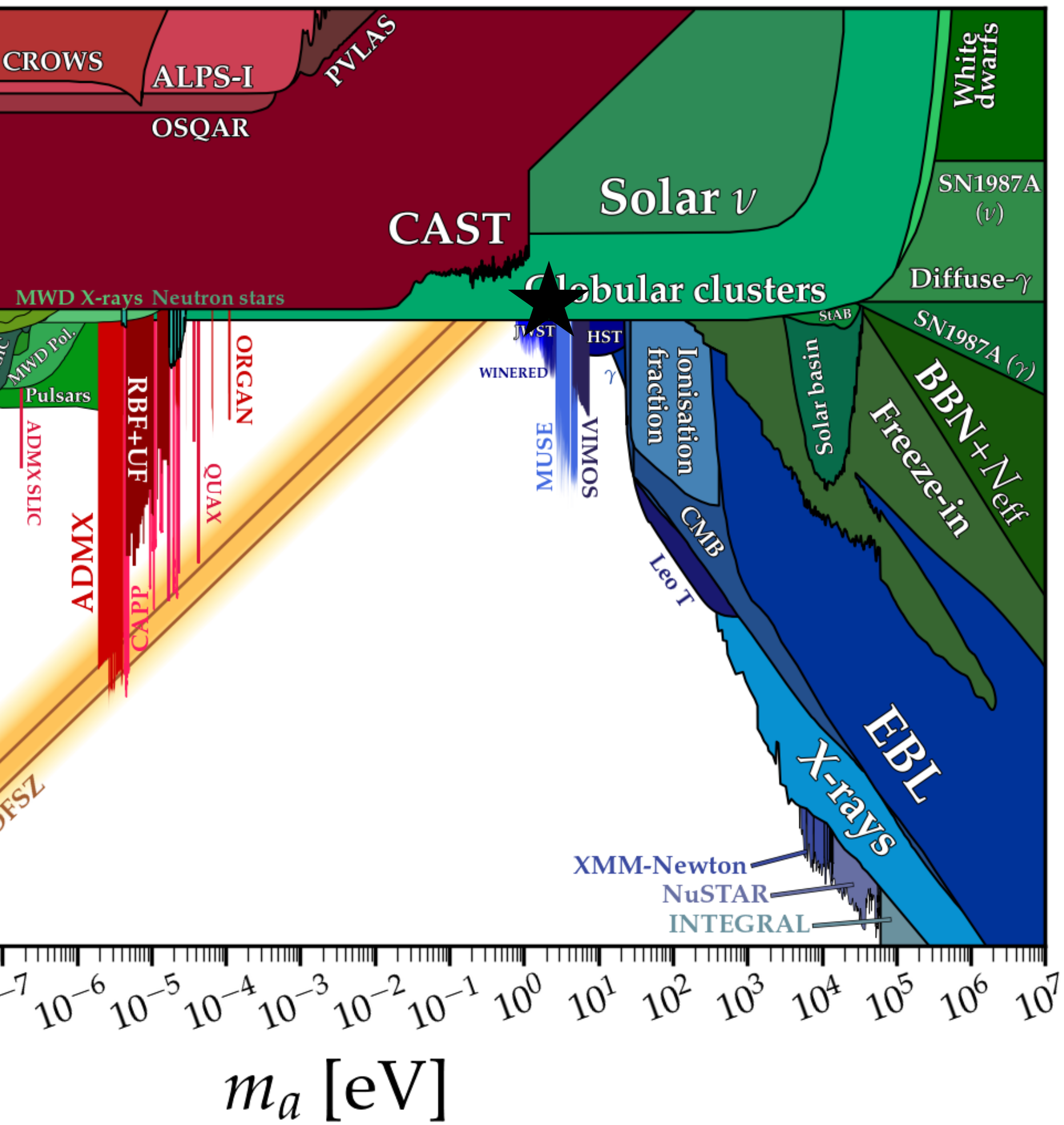
Gamma-ray attenuation

[Korochkin, Neronov, and Semikoz, 1911.13291](#)

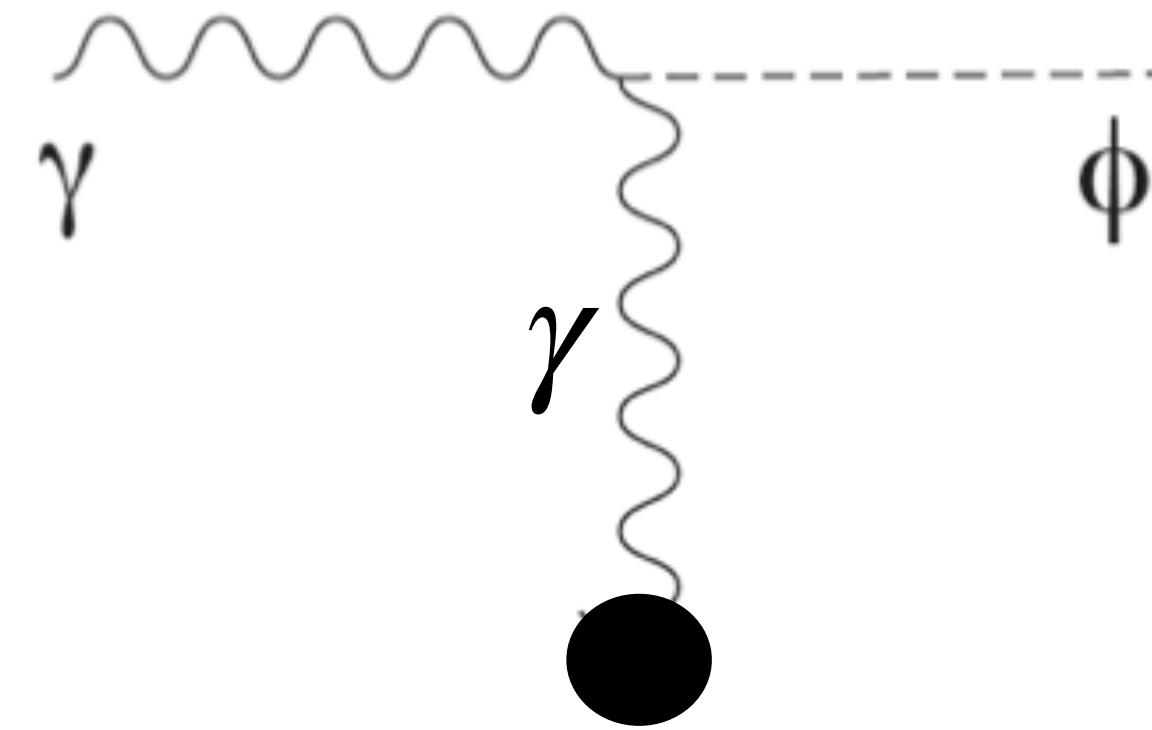


See also [WY, 2301.08735](#)
for cold "hot dark matter"

A comment on star cooling bound.

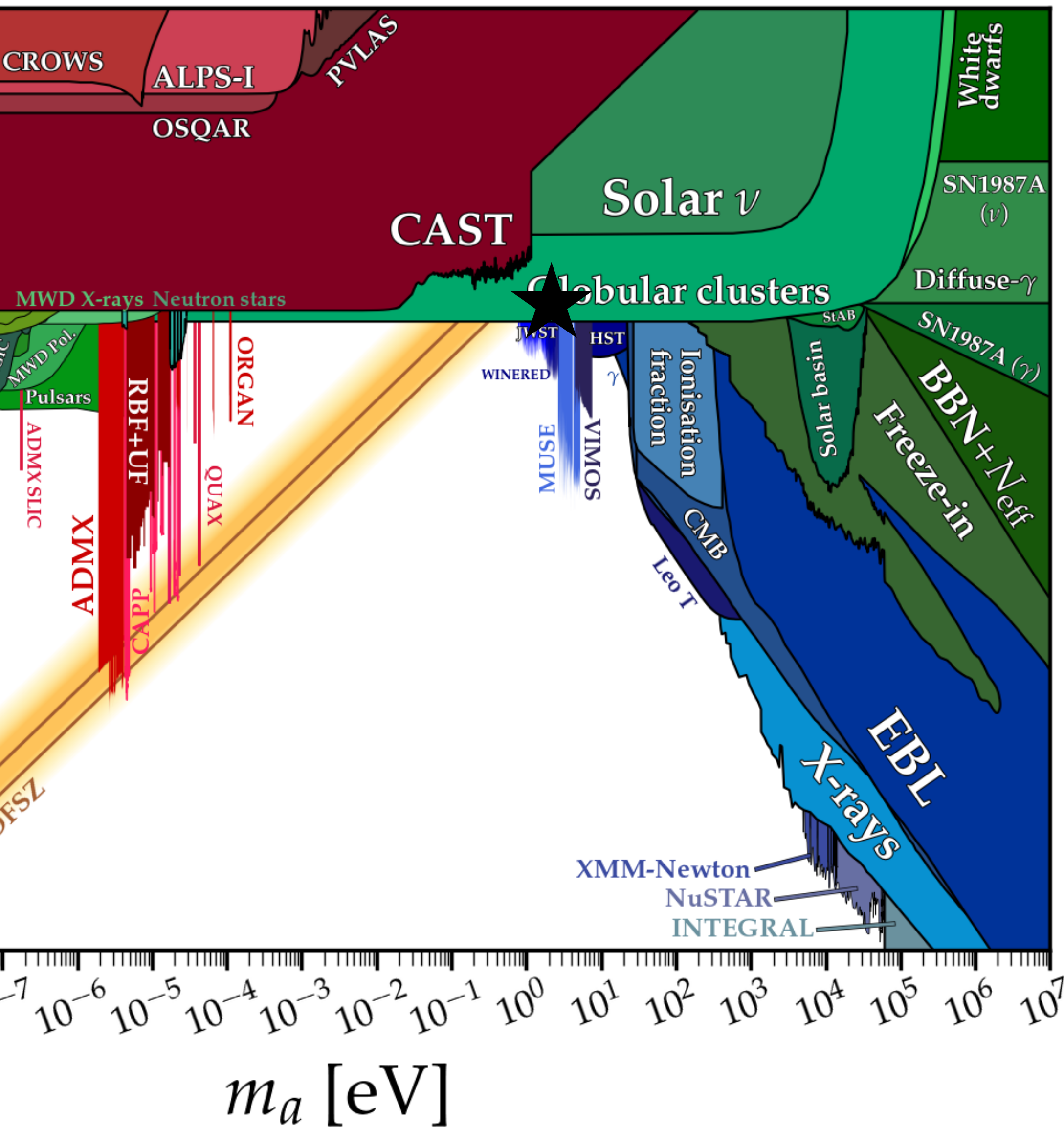


Axion coupling contributes to star cooling.

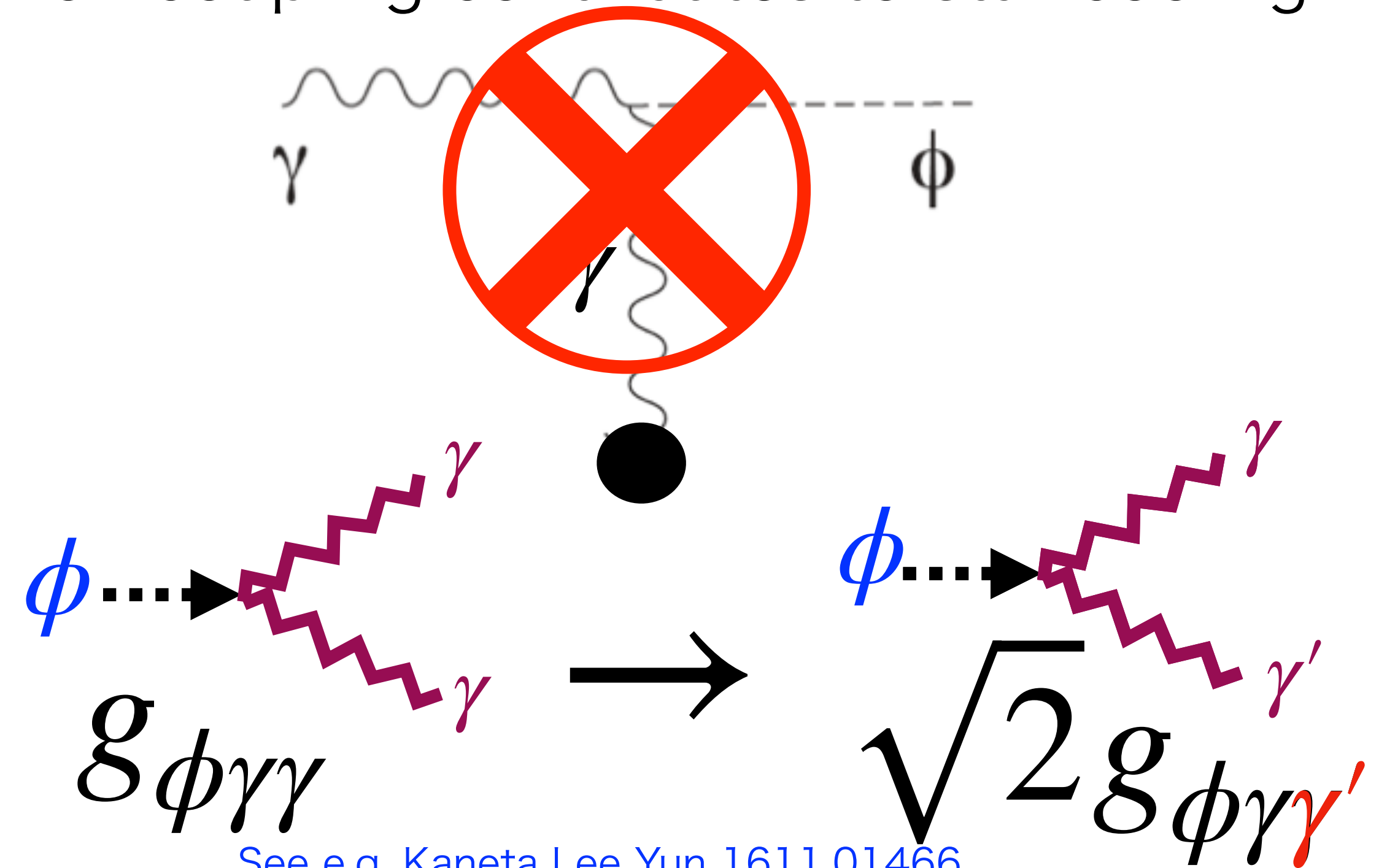


See e.g. Kaneta Lee Yun [1611.01466](#),
Kohri, Moroi, Nakayama, [1706.04921](#), Nakayama, WY [2205.01079](#)

A comment on star cooling bound.



Axion coupling contributes to star cooling.



See e.g. Kaneta Lee Yun [1611.01466](#),

Kohri, Moroi, Nakayama, [1706.04921](#), Nakayama, WY [2205.01079](#)

The coincidence holds.

(ALP miracle gives new prediction $\Delta N_{\text{eff}} \sim 0.1$ compared with the original one $\Delta N_{\text{eff}} \sim 0.03$.)

eV dark matter may be interesting.

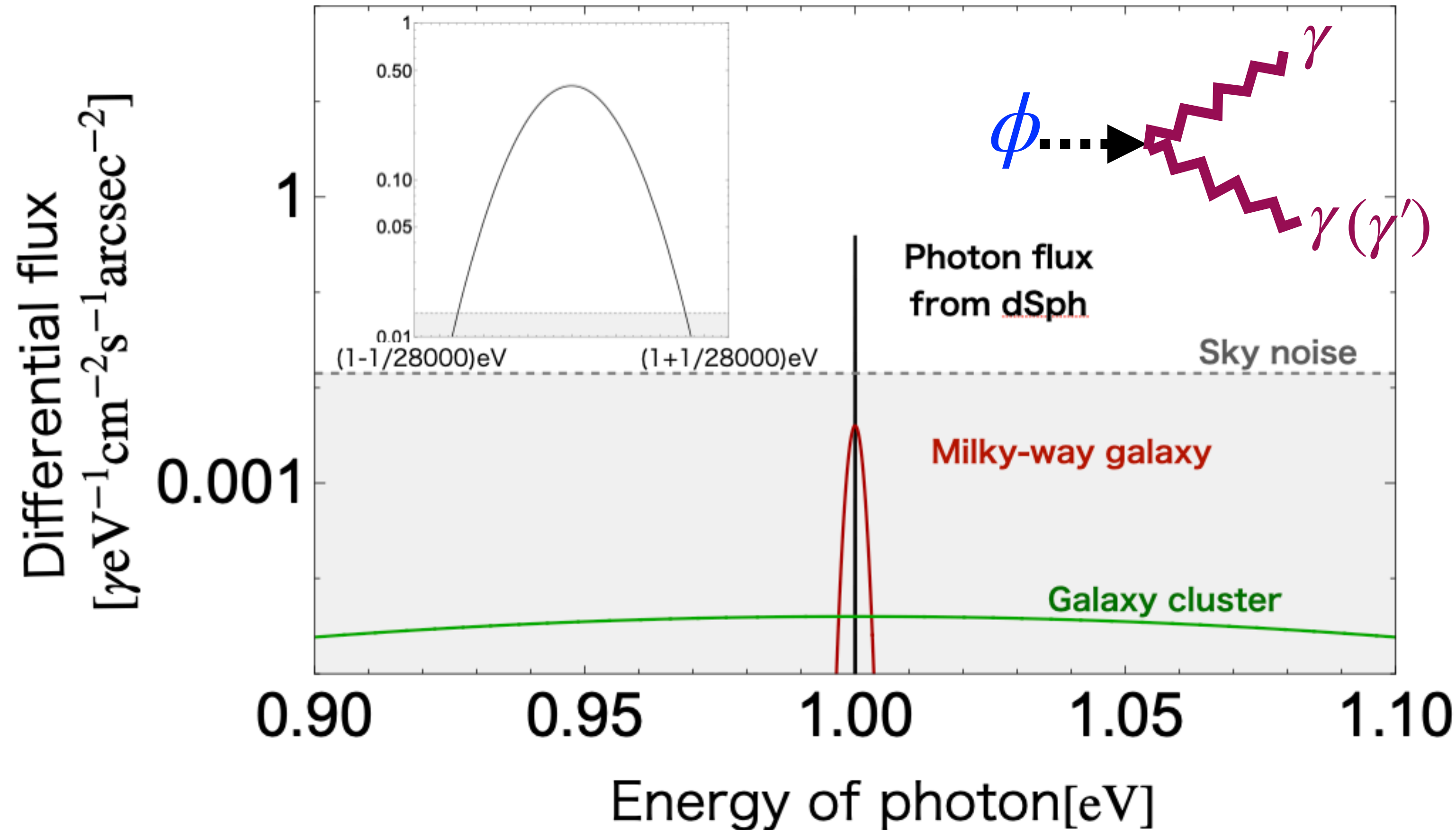
- **2. Indirect detection
with infrared spectrograph**

T. Bessho, Y. Ikeda, WY, 2208.05975
WY, Hayashi 2305.13415

DM line-like signal and background continuous spectrum can be distinguished by infrared spectrographs.

O(1)bin of high resolution spectrographs

DM mass = 2eV, Photon coupling = 10^{-10}GeV^{-1}



[T. Bessho, Y. Ikeda, WY, 2208.05975](#)

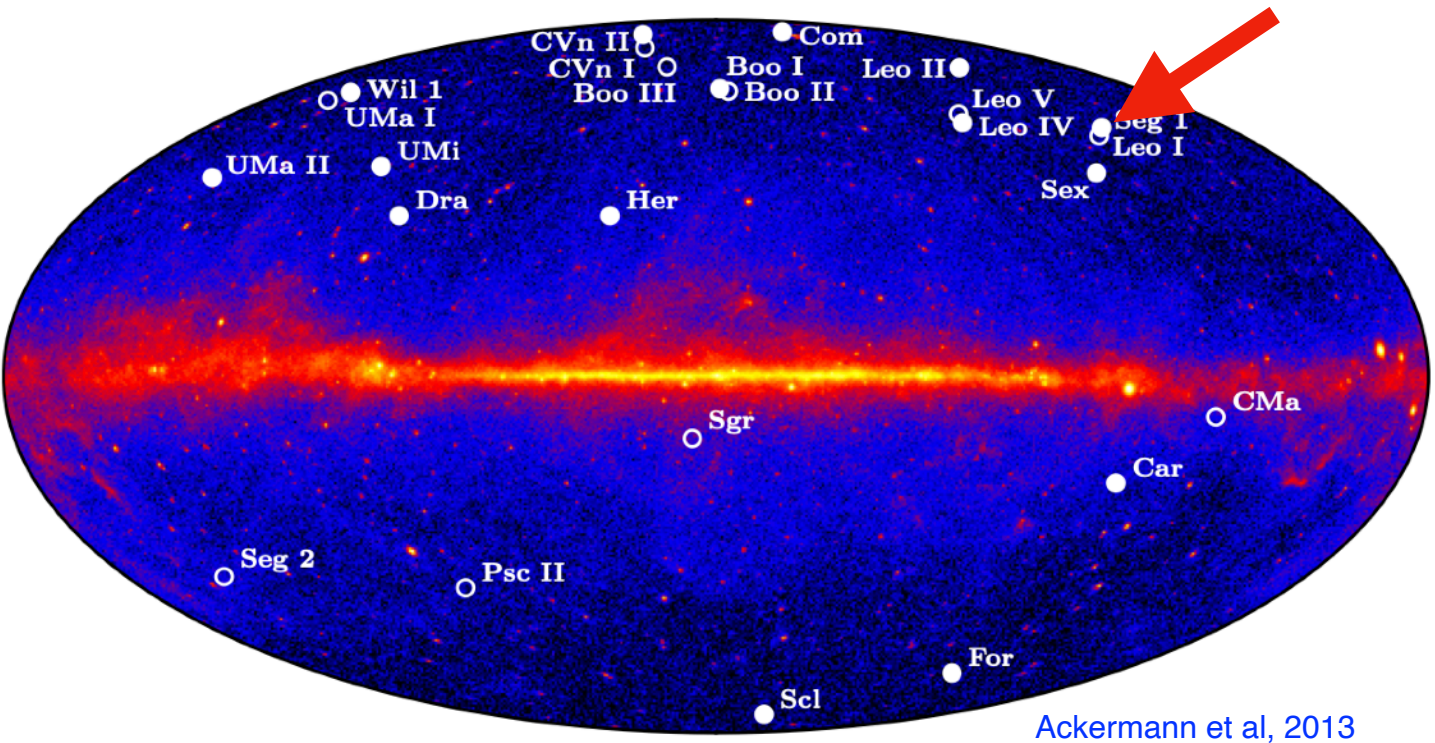
-DM signals from some dwarfs are **sky background free** for existing **high energy resolution** infrared spectrographs.

[T. Bessho, Y. Ikeda, WY, 2208.05975](#)

-With **high angular resolution** one can avoid seeing visible stars, while “see” the DM distribution from the decay photon in dwarfs.

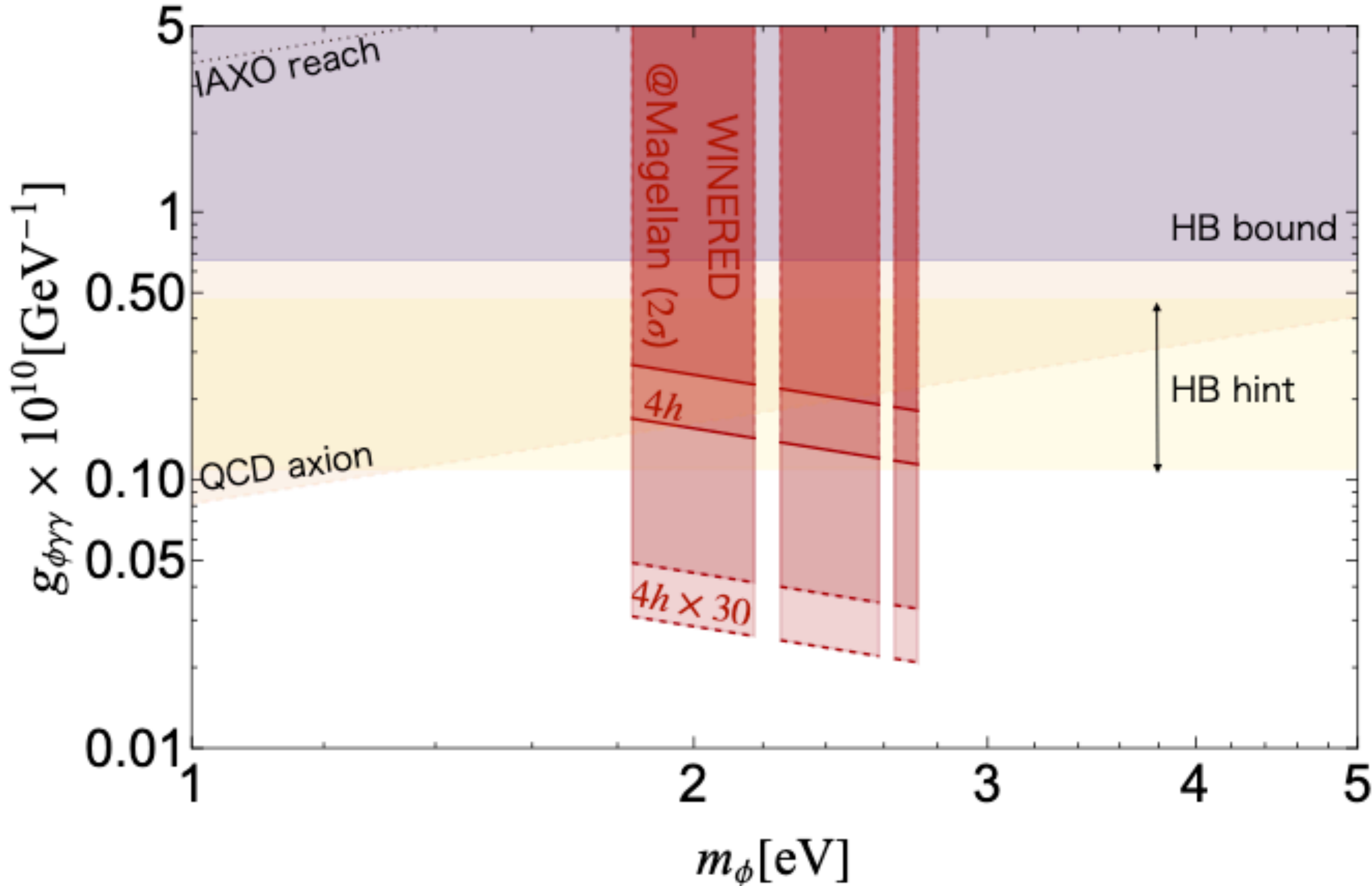
[WY, Hayashi, 2305.13415](#)

eV DM search with WINERED @ Magellan

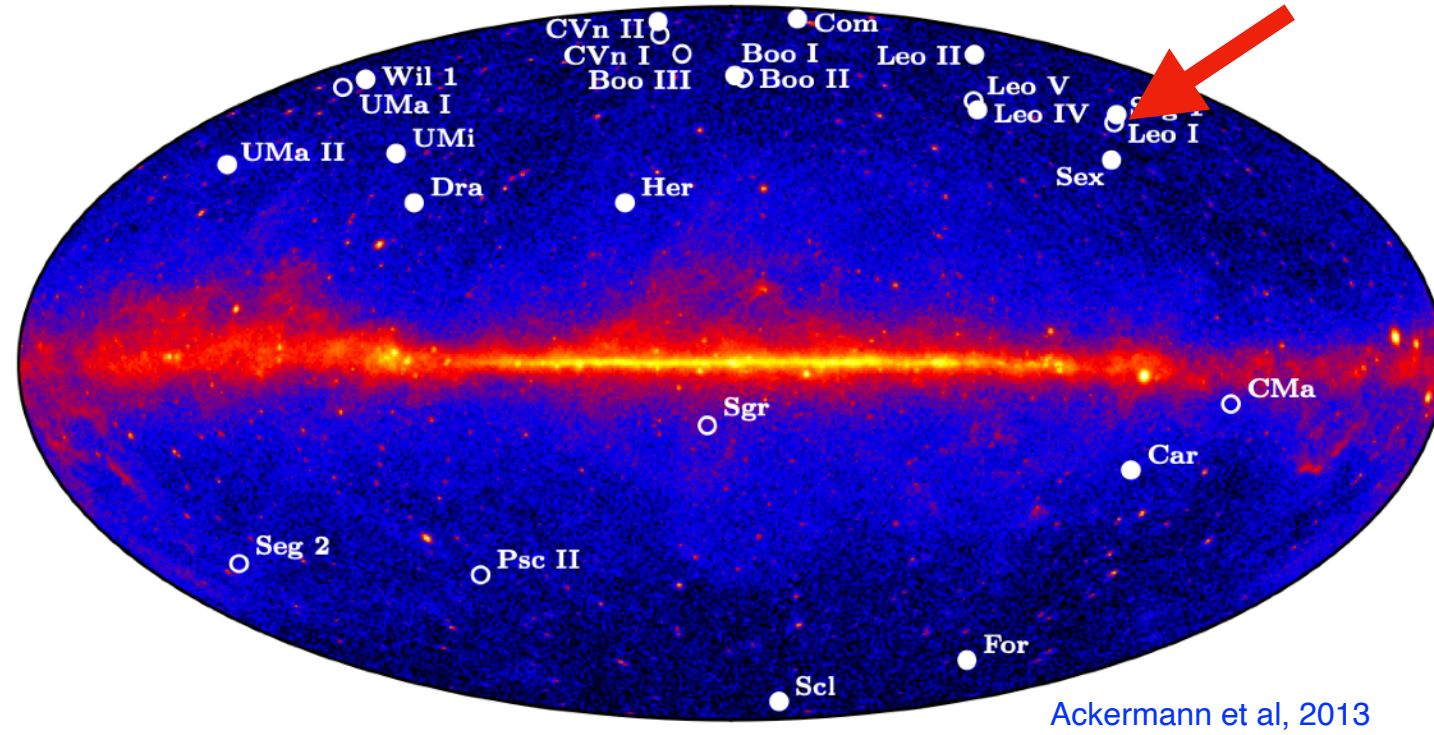


A high-resolution infrared spectrograph is one of the most efficient DM detectors.

$\lambda/\delta\lambda \sim 30000$ T. Bessho, Y. Ikeda, WY, 2208.05975



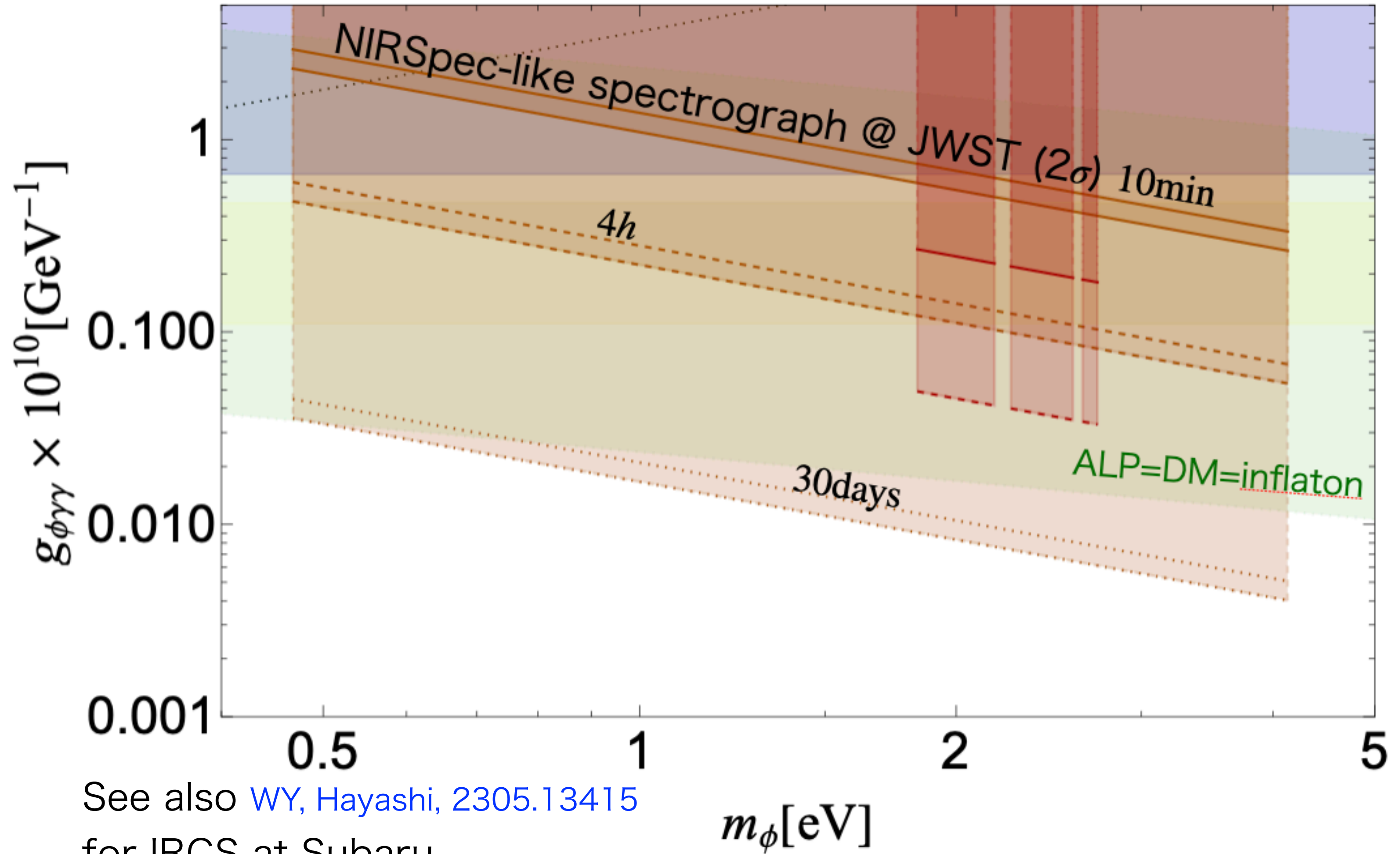
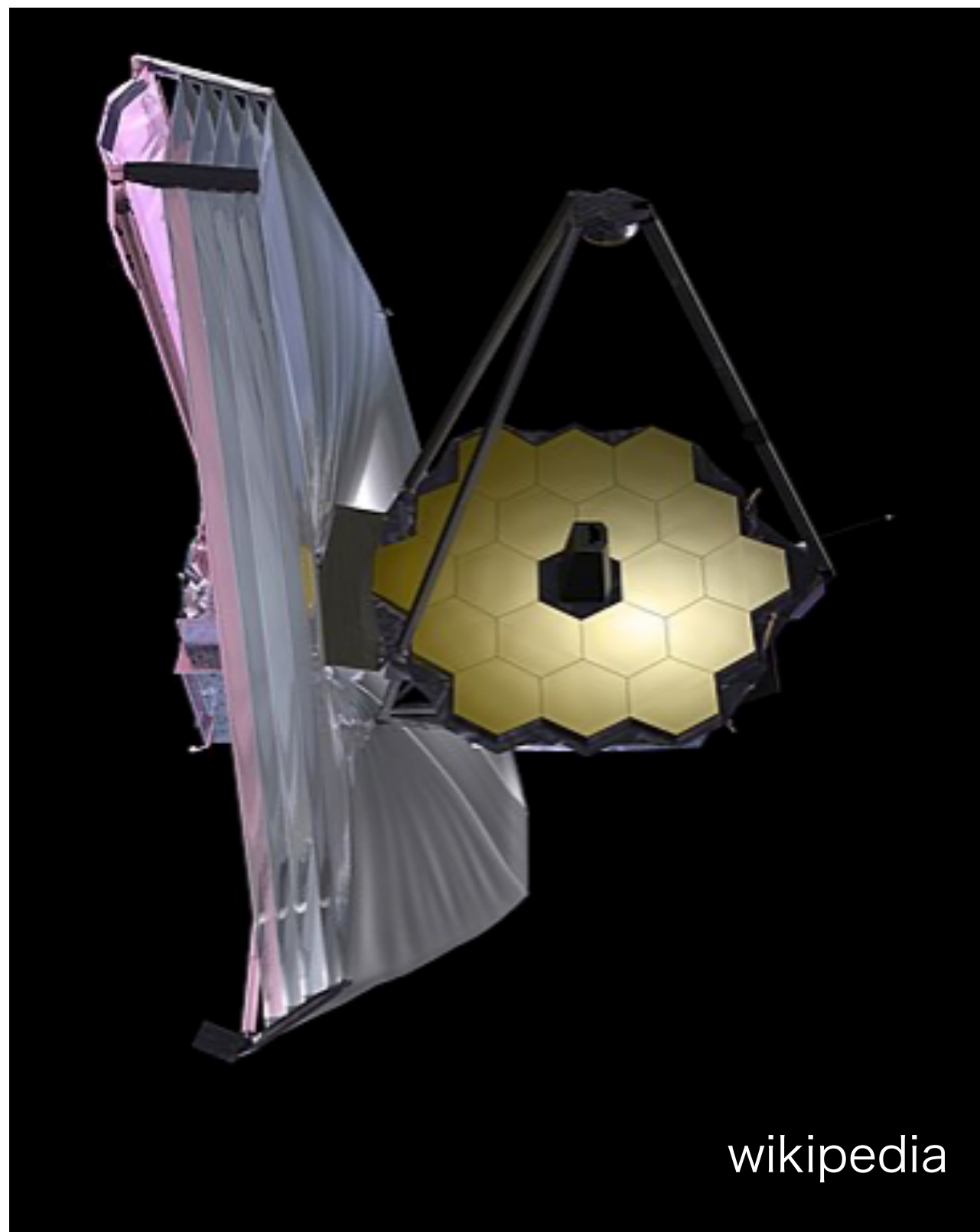
eV DM search with NIRSpec @ JWST



A high-resolution infrared spectrograph is one of the most efficient DM detectors.

$\lambda/\delta\lambda \sim 3000$ T. Bessho, Y. Ikeda, WY, 2208.05975

See also Janish, Pinetti, 2310.15395, Roy et al, 2311.04987 with blank sky data,



See also WY, Hayashi, 2305.13415 for IRCS at Subaru

• 3. Observations and results

$$\frac{\partial^2 \Phi_{\gamma,i}}{\partial \Omega \partial E} \simeq \frac{\partial_{\Omega} D[s, \Omega]}{4\pi} \frac{\Gamma_{\phi}}{m_{\phi}} \times \underline{2\delta(E - \frac{m_{\phi}}{2}(1 - v_i))} \times \underline{\eta}$$

Measured in

WY, Ikeda, Bessho, Kobayashi

+WINERED team, 2402.07976

Estimated in

WY, Hayashi

2305.13415

Measured in

WY, Ikeda, Bessho, Kobayashi

+WINERED team, 2402.07976

• 3. Observations and results

$$\frac{\partial^2 \Phi_{\gamma,i}}{\partial \Omega \partial E} \simeq \frac{\partial_{\Omega} D[s, \Omega]}{4\pi} \frac{\Gamma_{\phi}}{m_{\phi}} \times \underline{2\delta(E - \frac{m_{\phi}}{2}(1 - v_i))} \times \underline{\eta}$$

Measured in
WY, Ikeda, Bessho, Kobayashi
+WINERED team, 2402.07976

Estimated in
WY, Hayashi
2305.13415

Measured in
WY, Ikeda, Bessho, Kobayashi
+WINERED team, 2402.07976

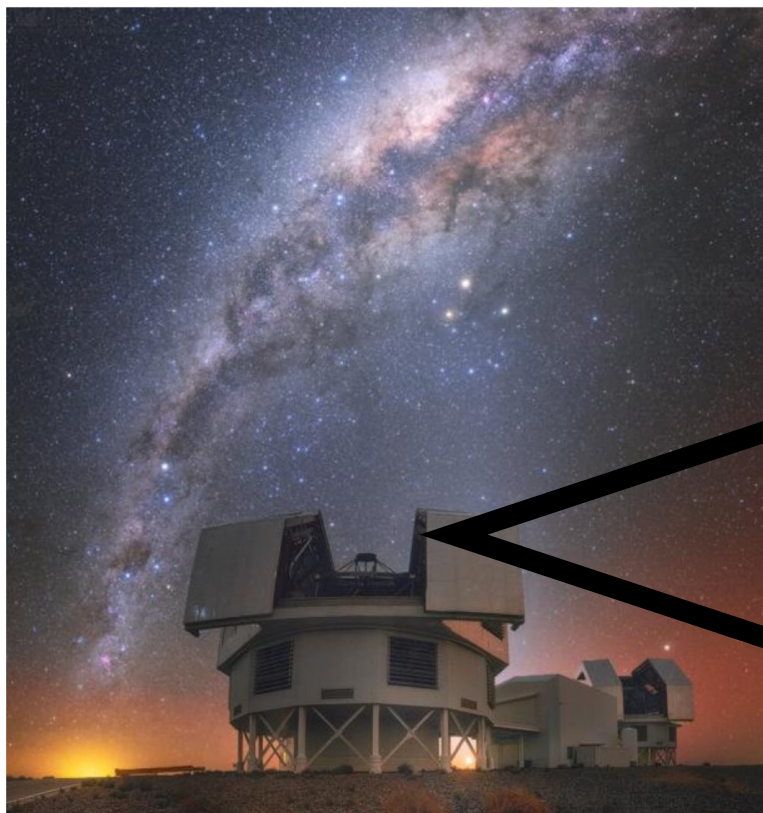


Bound on decay rate Γ_{ϕ} and thus $g_{a\gamma\gamma}$ (or $\sqrt{2}g_{a\gamma\gamma'}$)

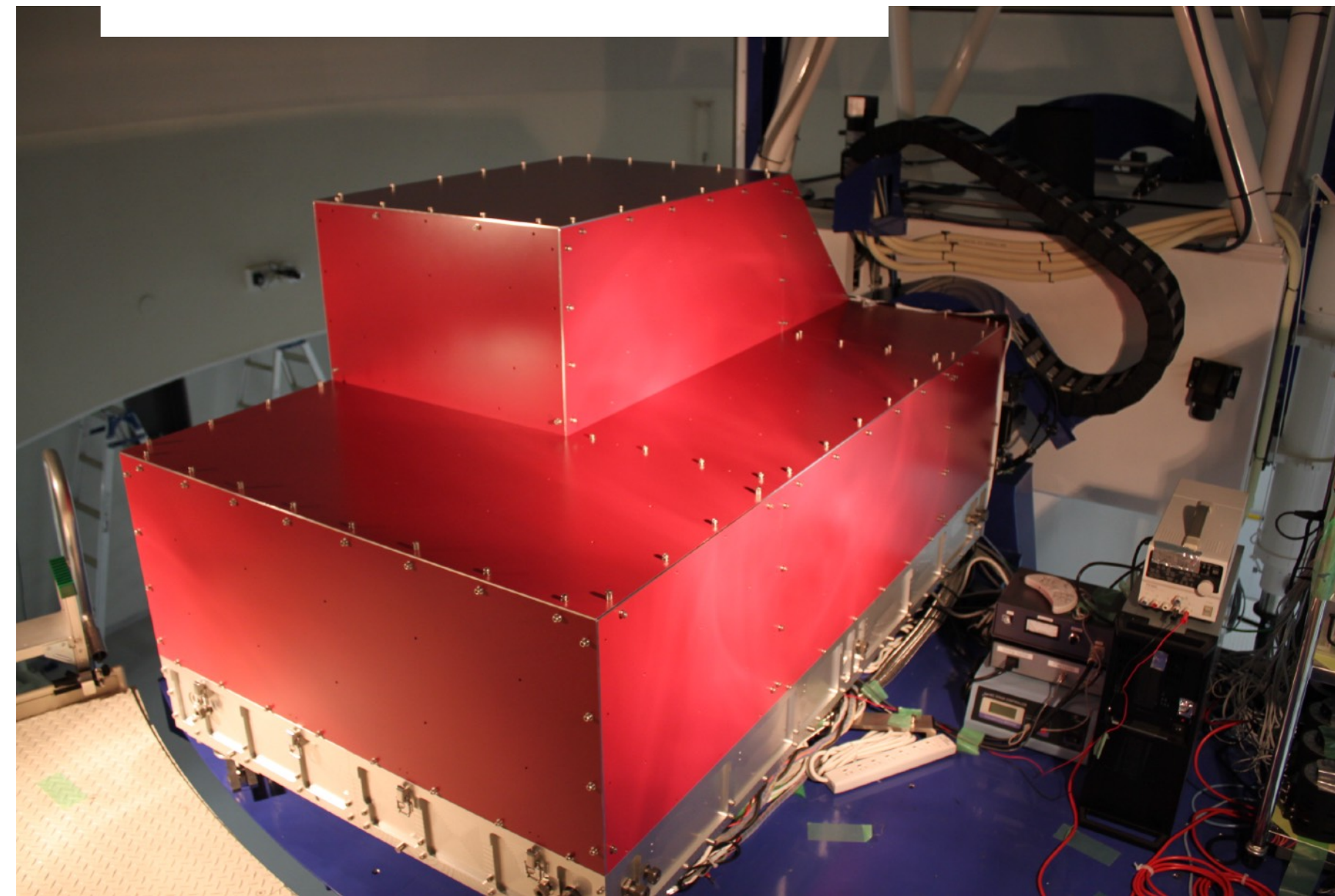
What we use: WINERED@ Magellan



Magellan



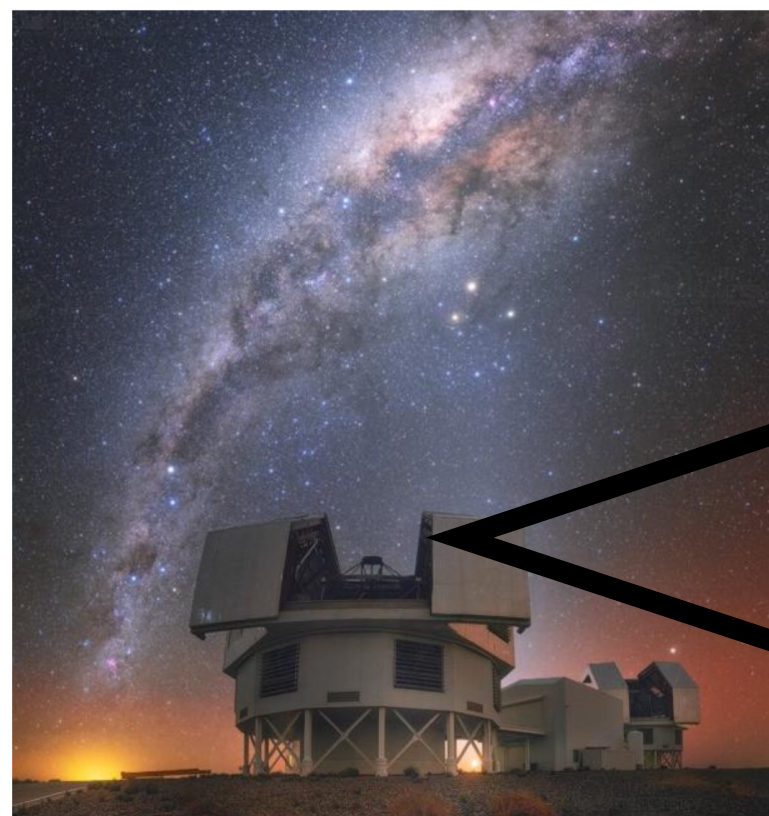
Ikeda et al 2006



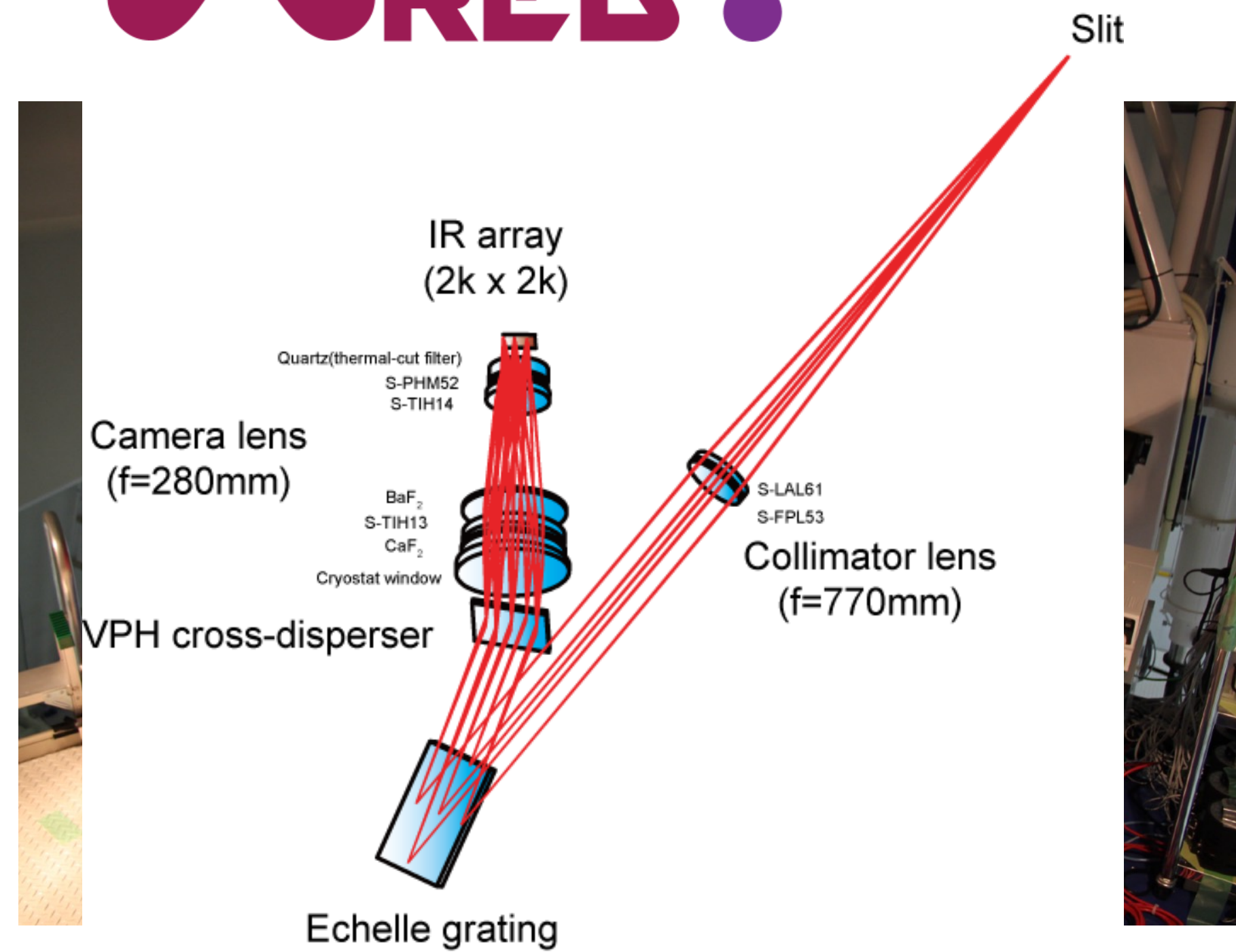
What we use: WINERED@ Magellan



Magellan



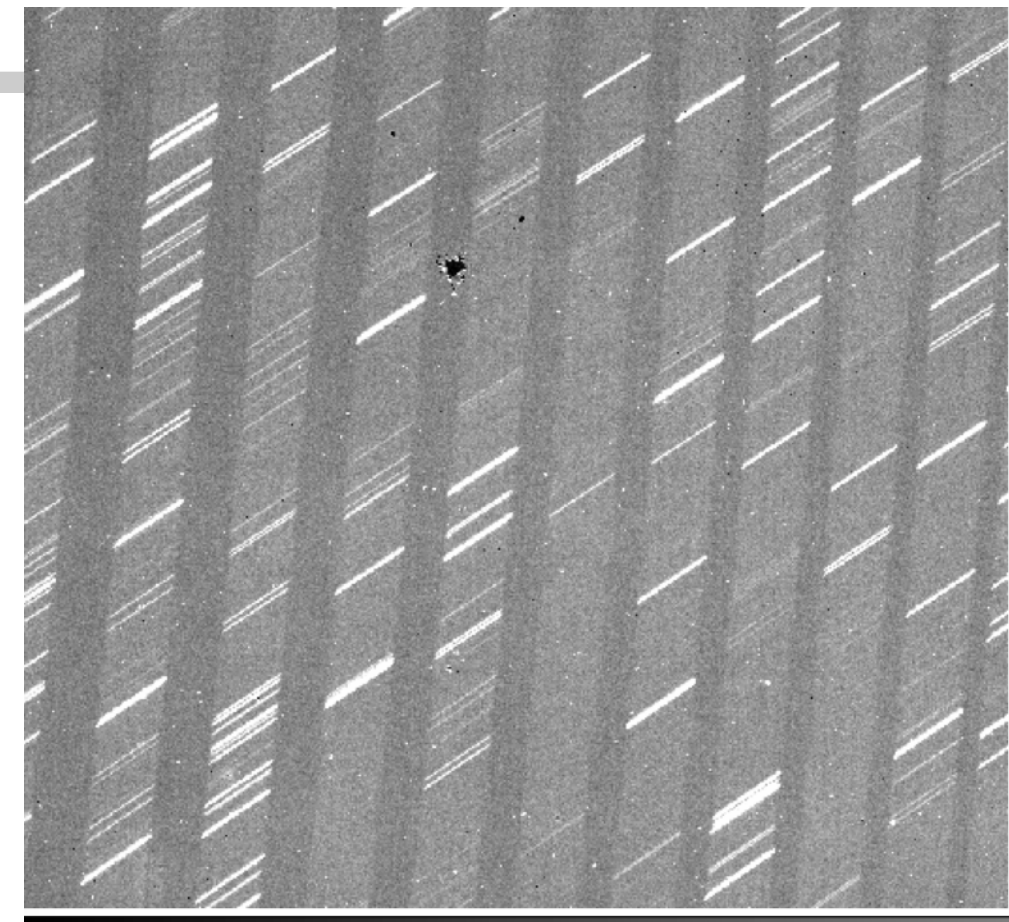
Ikeda et al 2006



What we use: WINERED@ Magellan

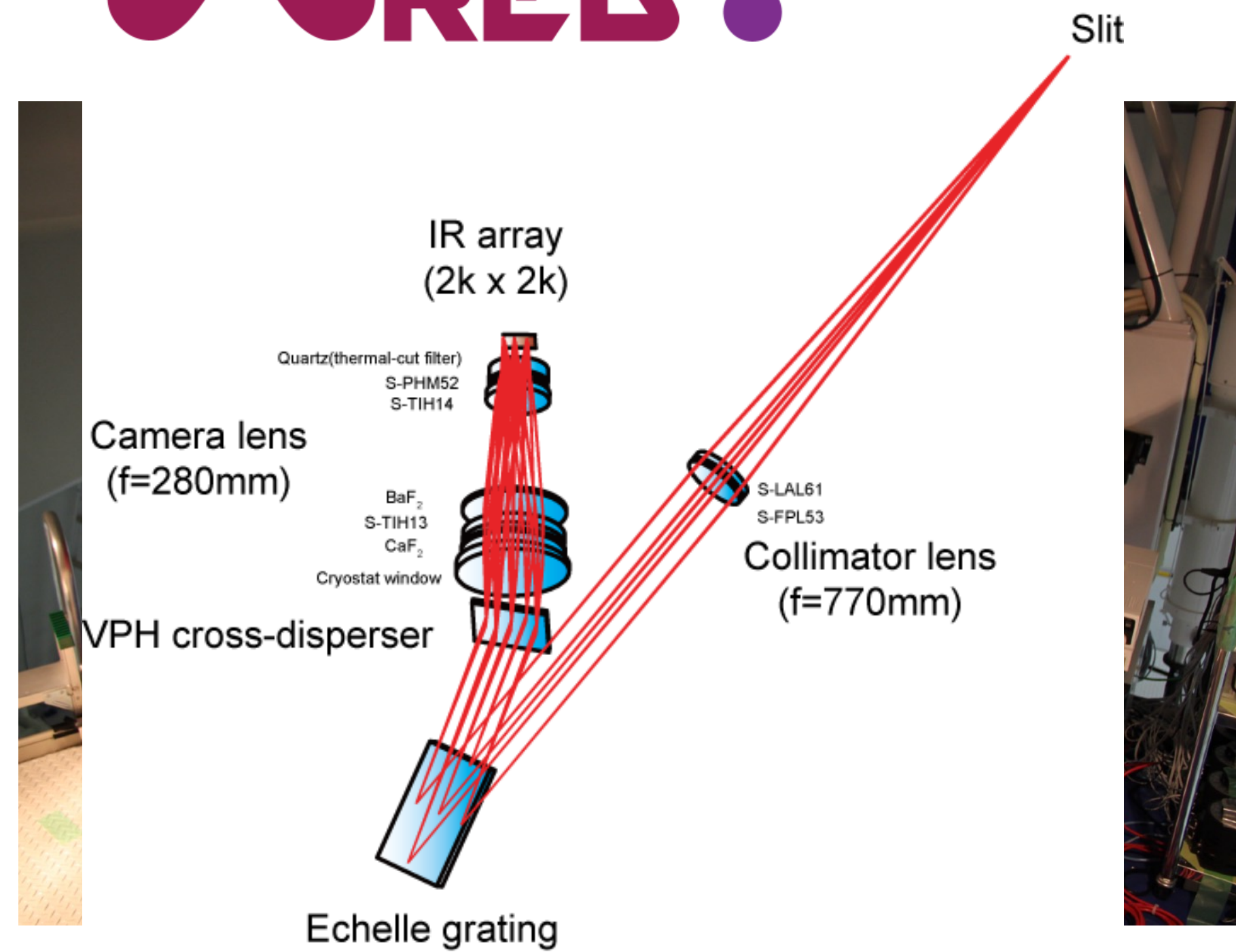


What we will obtain

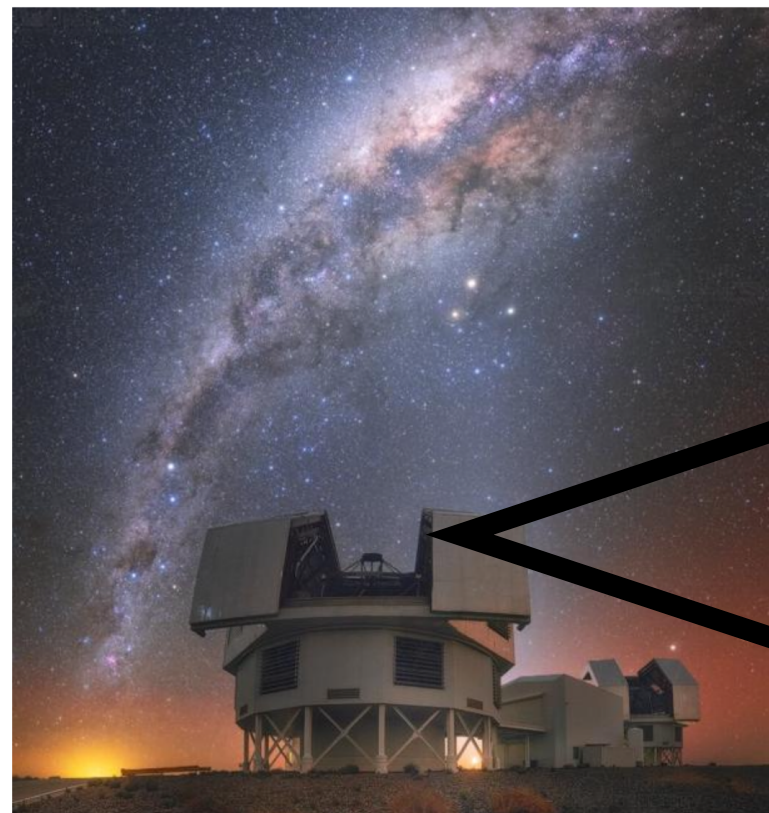


2nd diffraction

1st diffraction



Magellan



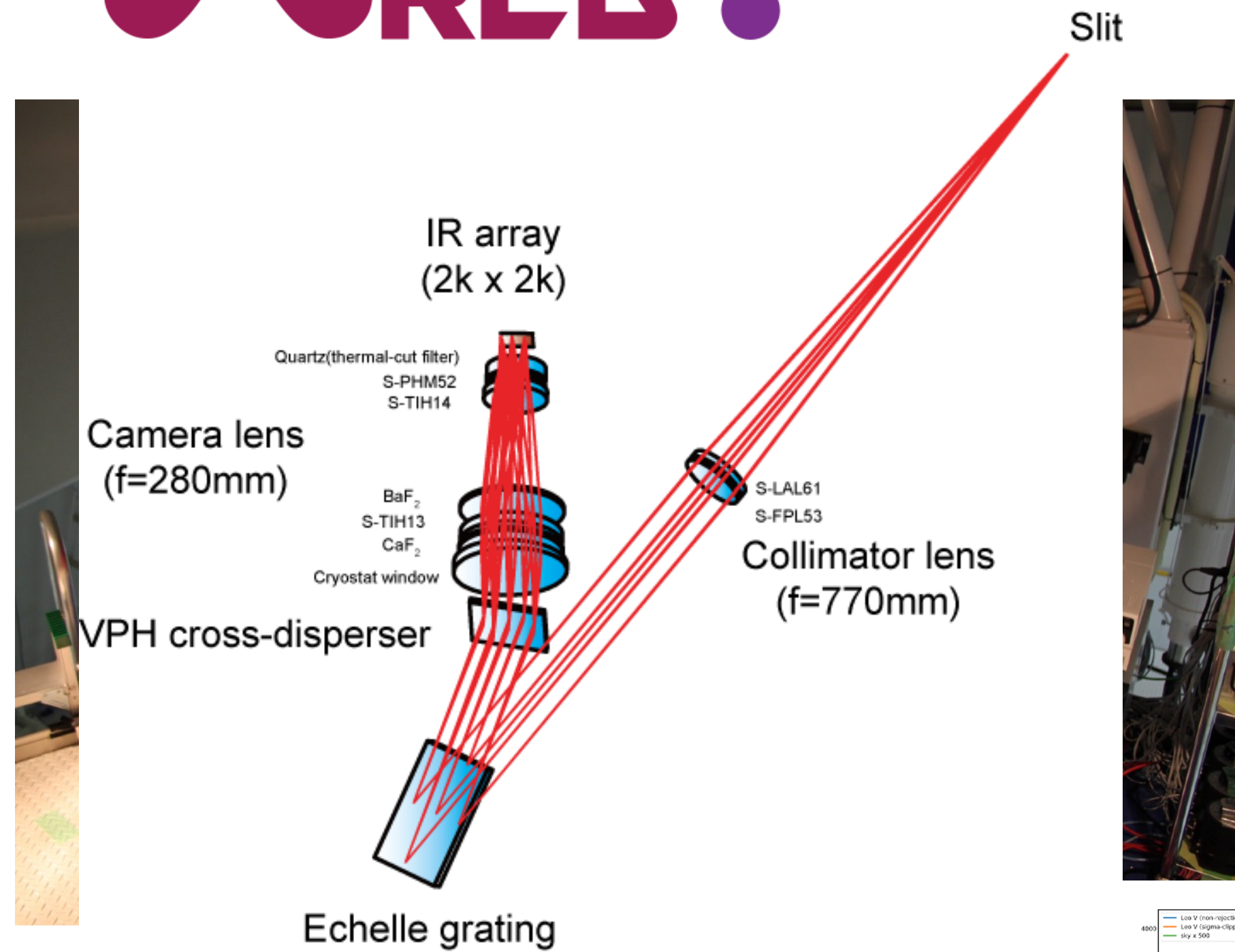
Ikeda et al 2006

What we use: WINERED@ Magellan

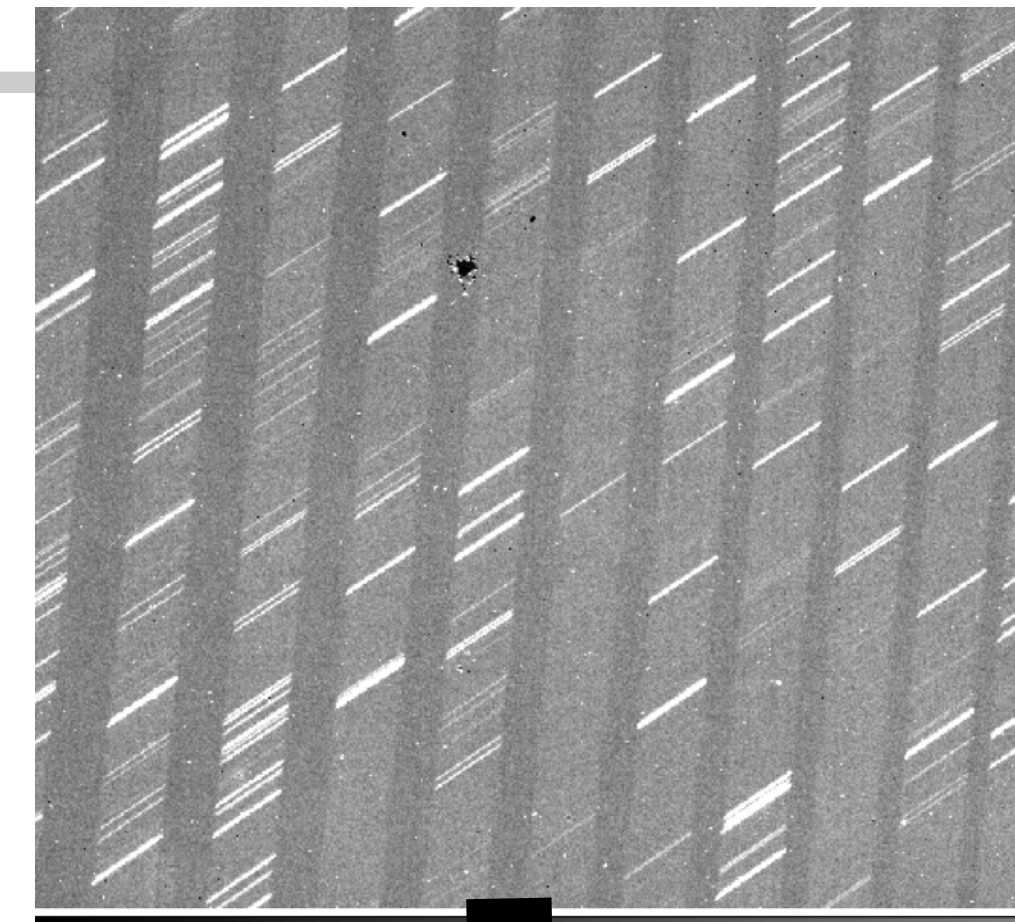
Magellan



Ikeda et al 2006

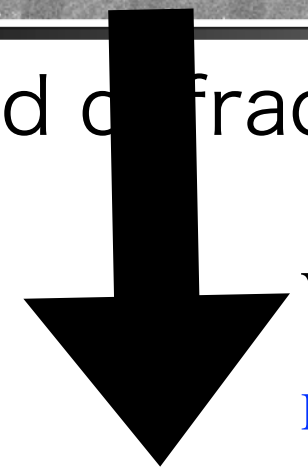


What we will obtain



1st diffraction

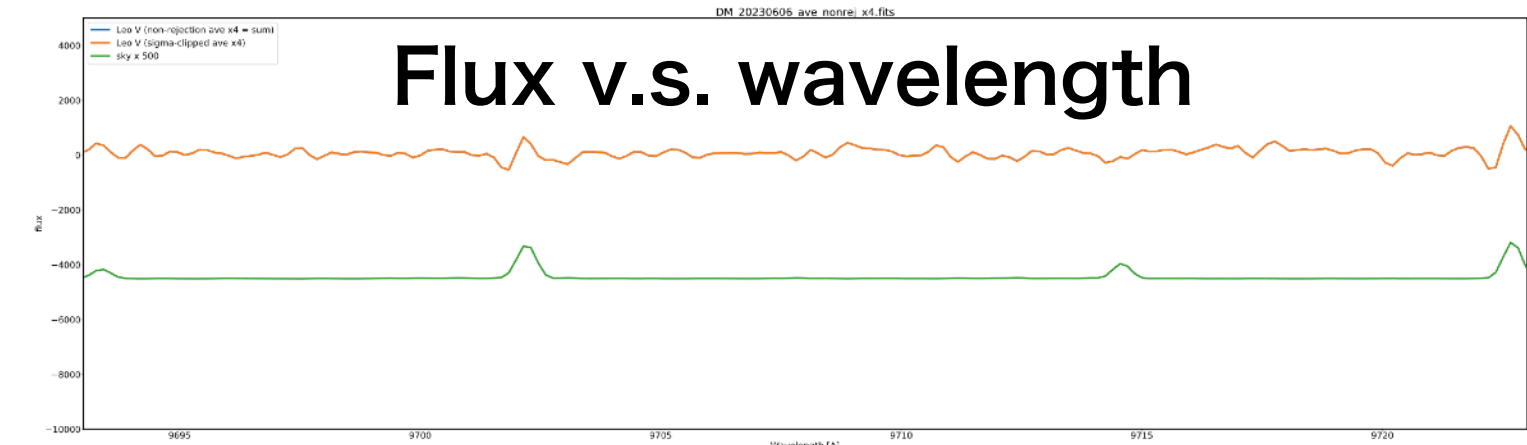
2nd diffraction



WARP

Hamano et al, 2024

Flux v.s. wavelength



What we have observed

Based on proposals “eV-Dark Matter search with WINERED”, Jun 2023, PI. WY Co-I. Ikeda, Bessho
“eV-Dark Matter search with WINERED”, Nov 2023, PI. WY Co-I. Ikeda, Bessho
WY, Ikeda, Bessho, Kobayashi+WINERED team, 2402.07976

Table. I. Observation logs. Here, Regions 1, 2, and 3 are for Leo V, Tucana II, and Tucana II, respectively. resolution. T_I denotes the total integration time. [Simbad](#), [Inger et al 0002110](#)

Object name	Object type	RA(J2000)	DEC(J2000)	Obs. date	J_m	R	T_I (sec)
Leo V	dSph	11:31:09.6	+02:13:12	2023.06.06	—	28,000	3600
Tucana II	dSph	22:51:55.1	-58:34:08	2023.11.02	—	28,000	4200
Sky region 1	—	11:31:56.97	+02:09:19	2023.06.06	—	28,000	1800
Sky region 2	—	22:51:06.5	-57:28:46	2023.11.02	—	28,000	1200
Sky region 3	—	22:38:08.1	-58:24:39	2023.11.02	—	28,000	1200
HD134936	A0V	15:14:41.4	-52:35:42	2023.06.06	9.44	28,000	90

What we have observed

Based on proposals “eV-Dark Matter search with WINERED”, Jun 2023, PI. WY Co-I. Ikeda, Bessho
“eV-Dark Matter search with WINERED”, Nov 2023, PI. WY Co-I. Ikeda, Bessho
WY, Ikeda, Bessho, Kobayashi+WINERED team, 2402.07976

Table. I. Observation logs. Here, Regions 1, 2, and 3 are for Leo V, Tucana II, and Tucana II, respectively. resolution. T_I denotes the total integration time. [Simbad](#), [Inger et al 0002110](#)

Target dSphs

Object name	Object type	RA(J2000)	DEC(J2000)	Obs. date	J_m	R	T_I (sec)
Leo V	dSph	11:31:09.6	+02:13:12	2023.06.06	—	28,000	3600
Tucana II	dSph	22:51:55.1	-58:34:08	2023.11.02	—	28,000	4200
Sky region 1	—	11:31:56.97	+02:09:19	2023.06.06	—	28,000	1800
Sky region 2	—	22:51:06.5	-57:28:46	2023.11.02	—	28,000	1200
Sky region 3	—	22:38:08.1	-58:24:39	2023.11.02	—	28,000	1200
HD134936	A0V	15:14:41.4	-52:35:42	2023.06.06	9.44	28,000	90

What we have observed

Based on proposals “eV-Dark Matter search with WINERED”, Jun 2023, PI. WY Co-I. Ikeda, Bessho
“eV-Dark Matter search with WINERED”, Nov 2023, PI. WY Co-I. Ikeda, Bessho
WY, Ikeda, Bessho, Kobayashi+WINERED team, 2402.07976

Table. I. Observation logs. Here, Regions 1, 2, and 3 are for Leo V, Tucana II, and Tucana II, respectively. resolution. T_I denotes the total integration time. [Simbad](#), [Inger et al 0002110](#)

Target dSphs

For background subtraction.

Object name	Object type	RA(J2000)	DEC(J2000)	Obs. date	J_m	R	T_I (sec)
Leo V	dSph	11:31:09.6	+02:13:12	2023.06.06	—	28,000	3600
Tucana II	dSph	22:51:55.1	-58:34:08	2023.11.02	—	28,000	4200
Sky region 1	—	11:31:56.97	+02:09:19	2023.06.06	—	28,000	1800
Sky region 2	—	22:51:06.5	-57:28:46	2023.11.02	—	28,000	1200
Sky region 3	—	22:38:08.1	-58:24:39	2023.11.02	—	28,000	1200
HD134936	A0V	15:14:41.4	-52:35:42	2023.06.06	9.44	28,000	90

What we have observed

Based on proposals “eV-Dark Matter search with WINERED”, Jun 2023, PI. WY Co-I. Ikeda, Bessho
“eV-Dark Matter search with WINERED”, Nov 2023, PI. WY Co-I. Ikeda, Bessho
WY, Ikeda, Bessho, Kobayashi+WINERED team, 2402.07976

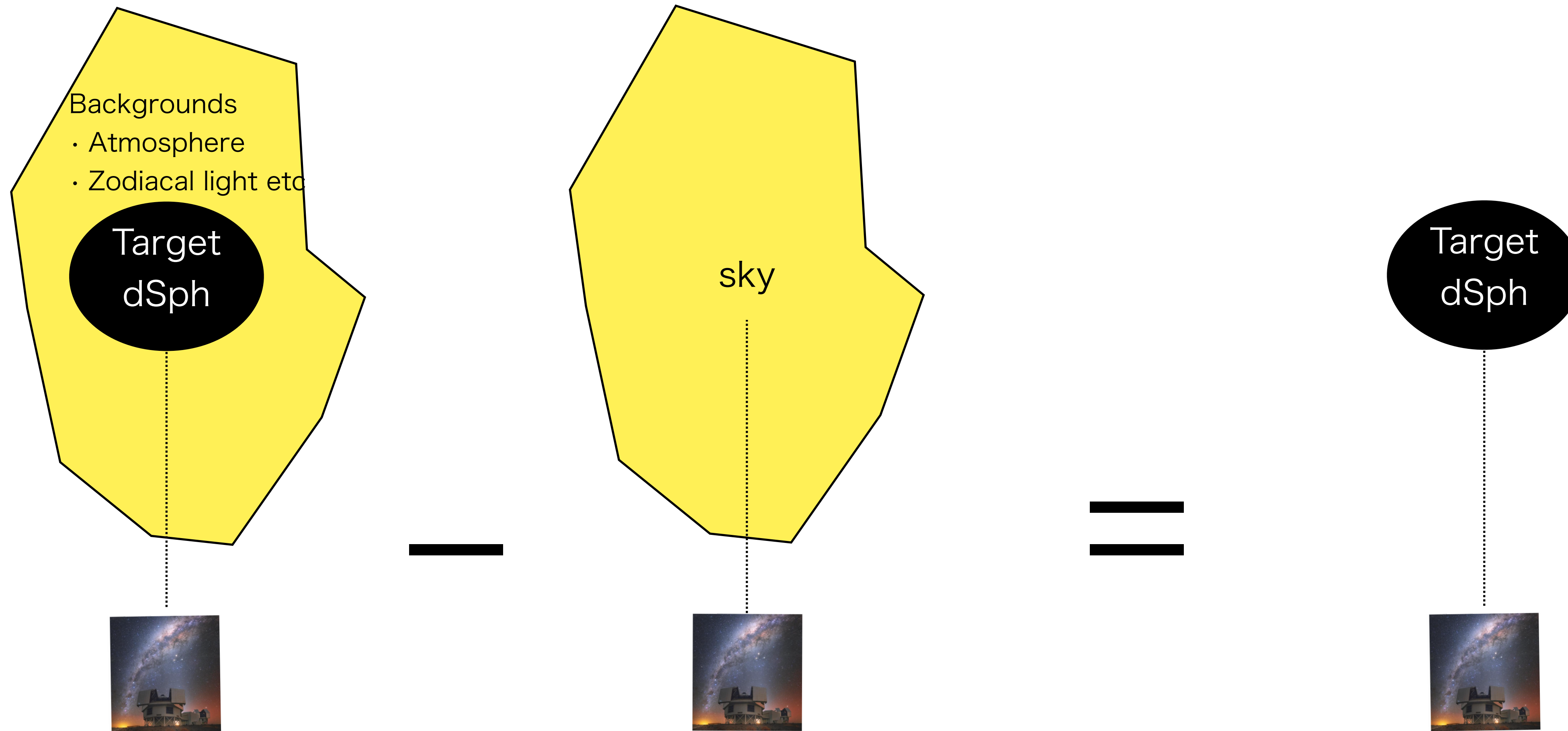
Table. I. Observation logs. Here, Regions 1, 2, and 3 are for Leo V, Tucana II, and Tucana II, respectively. resolution. T_I denotes the total integration time. [Simbad](#), [Inger et al 0002110](#)

	Object name	Object type	RA(J2000)	DEC(J2000)	Obs. date	J_m	R	T_I (sec)
Target dSphs	Leo V	dSph	11:31:09.6	+02:13:12	2023.06.06	—	28,000	3600
	Tucana II	dSph	22:51:55.1	-58:34:08	2023.11.02	—	28,000	4200
For background subtraction.	Sky region 1	—	11:31:56.97	+02:09:19	2023.06.06	—	28,000	1800
	Sky region 2	—	22:51:06.5	-57:28:46	2023.11.02	—	28,000	1200
	Sky region 3	—	22:38:08.1	-58:24:39	2023.11.02	—	28,000	1200
	HD134936	A0V	15:14:41.4	-52:35:42	2023.06.06	9.44	28,000	90

For flux calibration and measuring atmospheric transmittance.

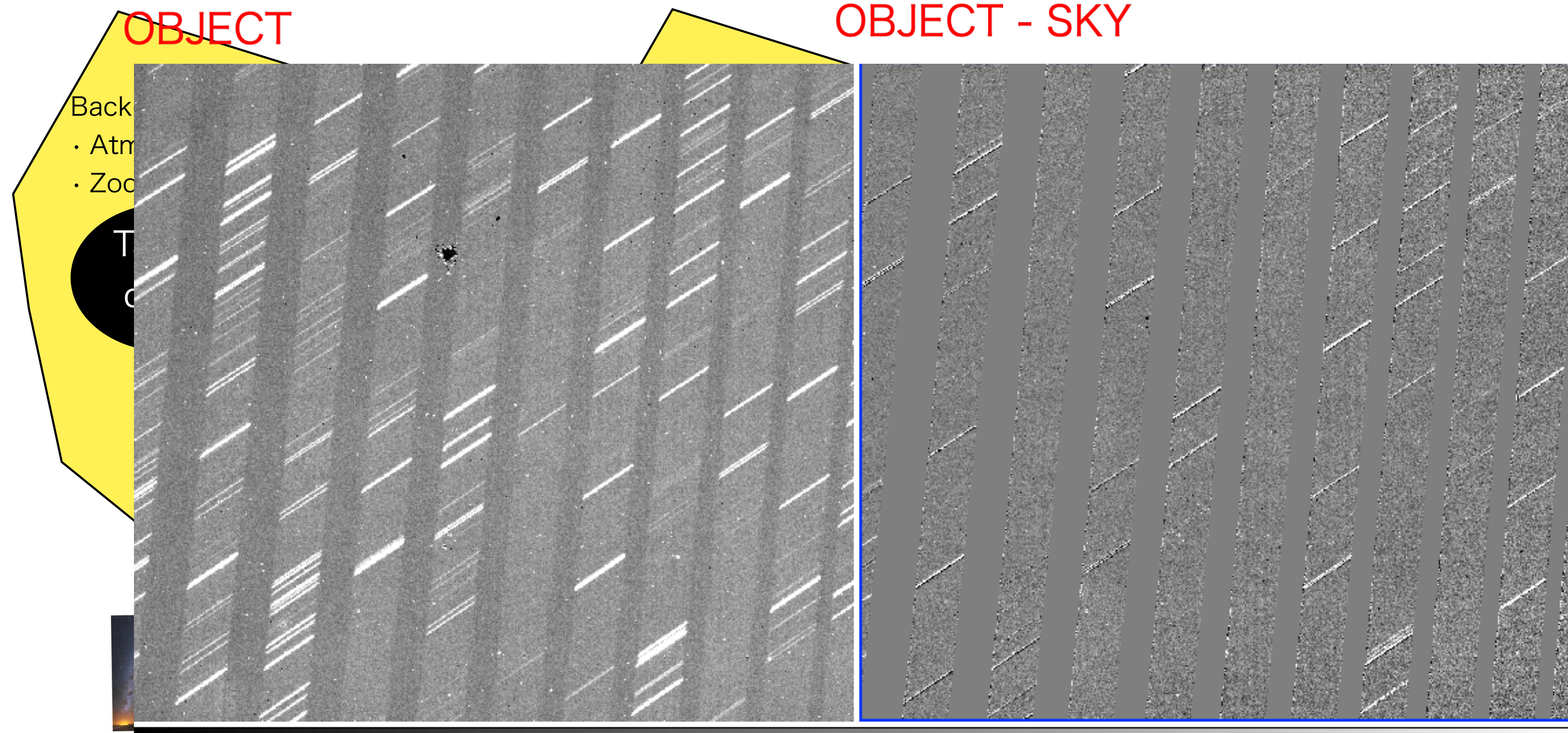
Object-Sky-Object Nodding Observation

WY, Ikeda, Bessho, Kobayashi+WINERED team, 2402.07976



Object-Sky-Object Nodding Observation

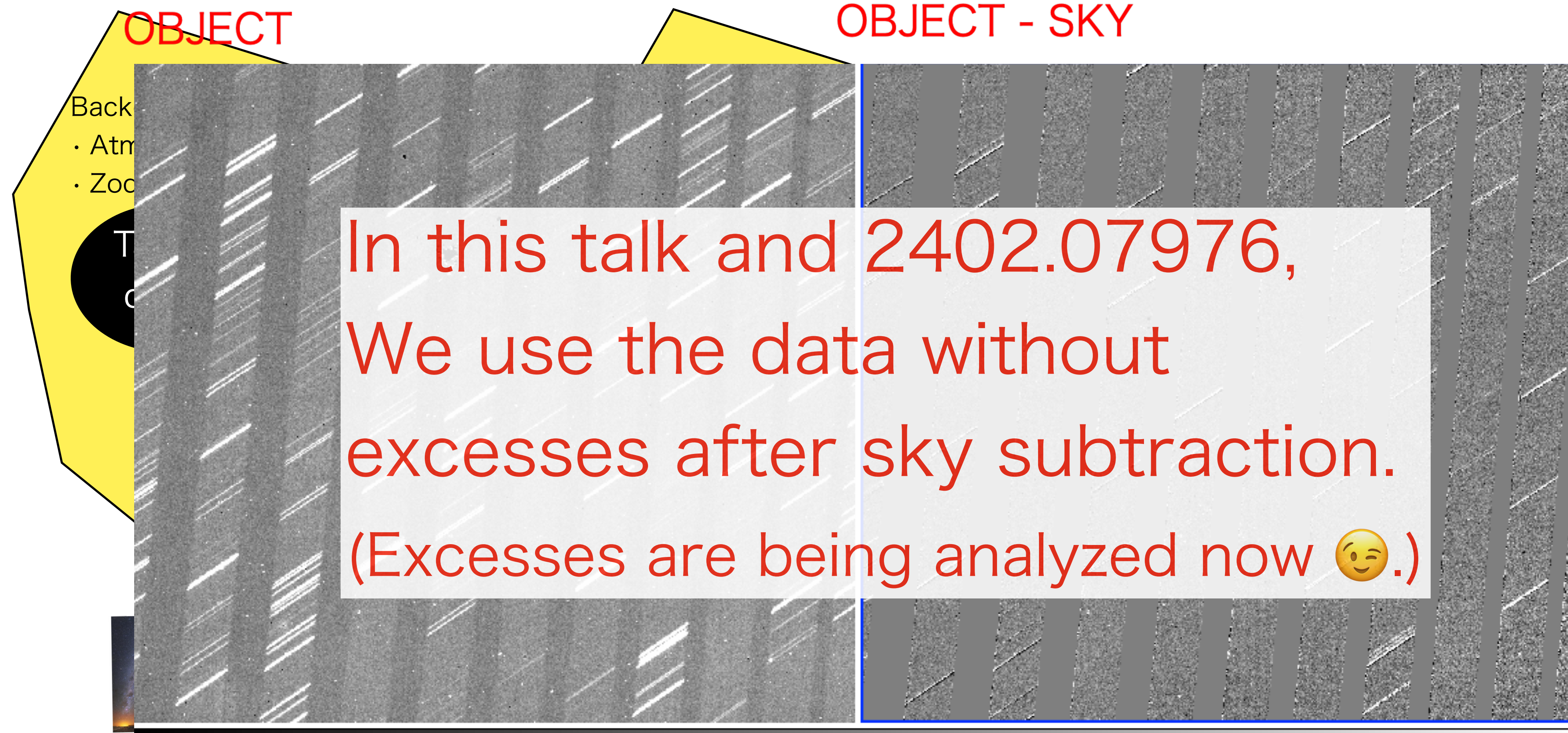
WY, Ikeda, Bessho, Kobayashi+WINERED team, 2402.07976



A tiny wavelength shift was found when we performed the first observation. We take this effect into account in the data analysis. In the second observation, we reduced each exposure time to suppress this effect.

Object-Sky-Object Nodding Observation

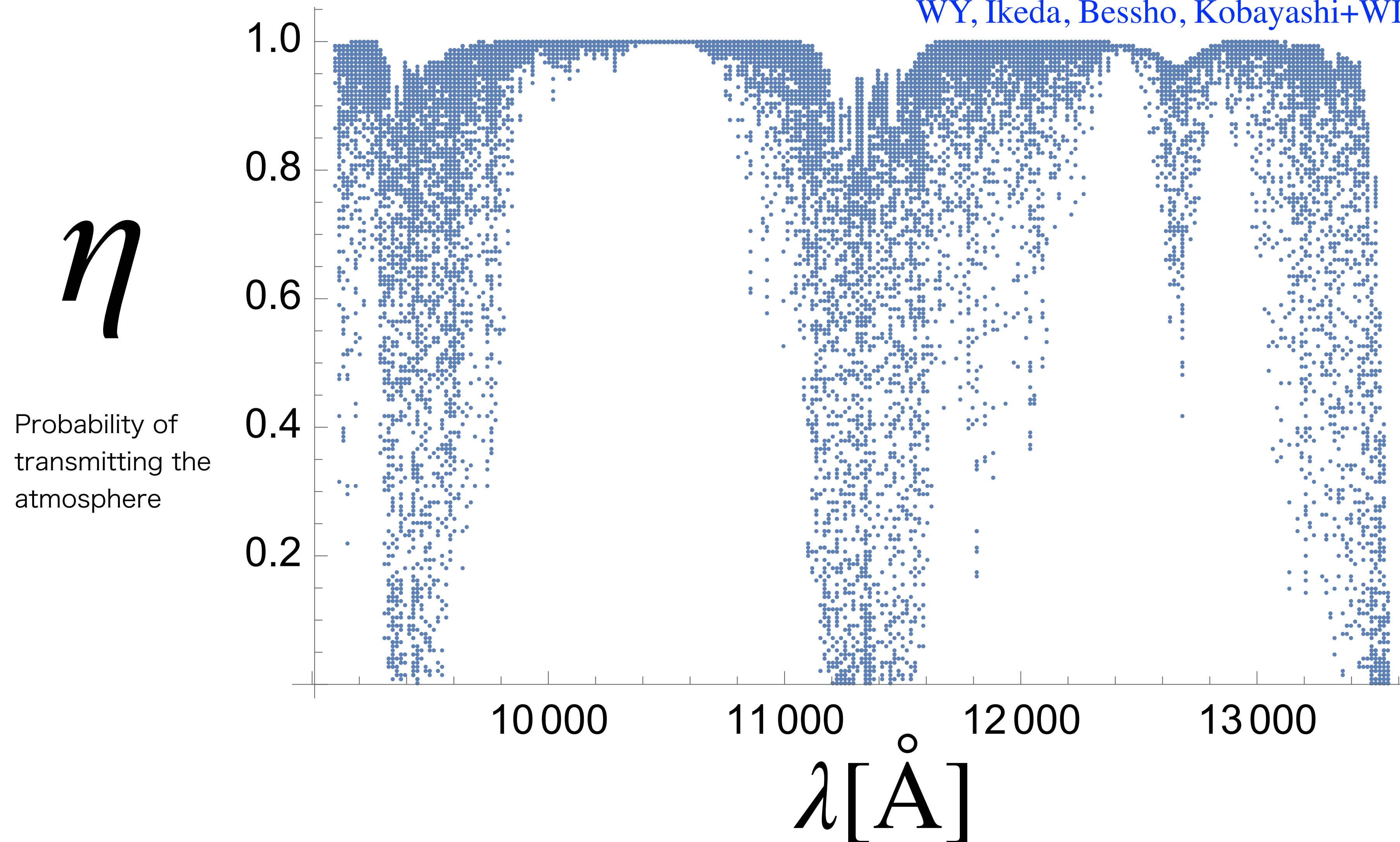
WY, Ikeda, Bessho, Kobayashi+WINERED team, 2402.07976



A tiny wavelength shift was found when we performed the first observation. We take this effect into account in the data analysis. In the second observation, we reduced each exposure time to suppress this effect.

Atmospheric transmittance, η , measured from standard star.

WY, Ikeda, Bessho, Kobayashi+WINERED team, 2402.07976



Analysis with Doppler Shift: Earth frame

WY, Ikeda, Bessho, Kobayashi+WINERED team, 2402.07976

Radial velocities of the dSphs are much larger than the resolution of WINERED

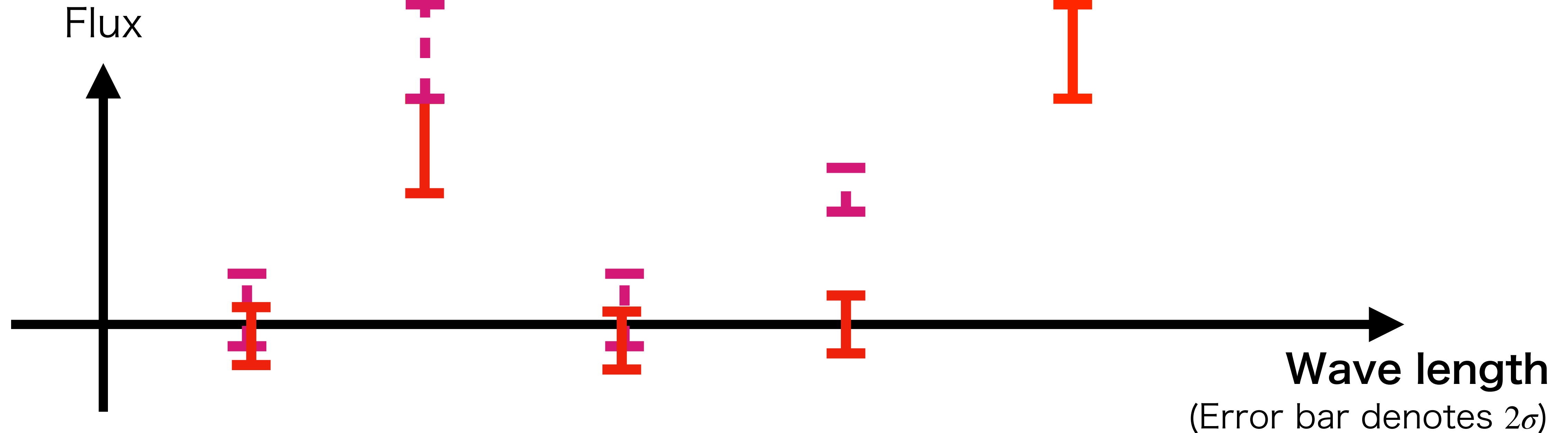
Simbad, Inger et al 0002110

$$v_{\text{LeoV}} \approx 173.3 \text{ km/s}, \text{ and } v_{\text{TucII}} \approx -129.1 \text{ km/s},$$

Leo V data



Tuc II data



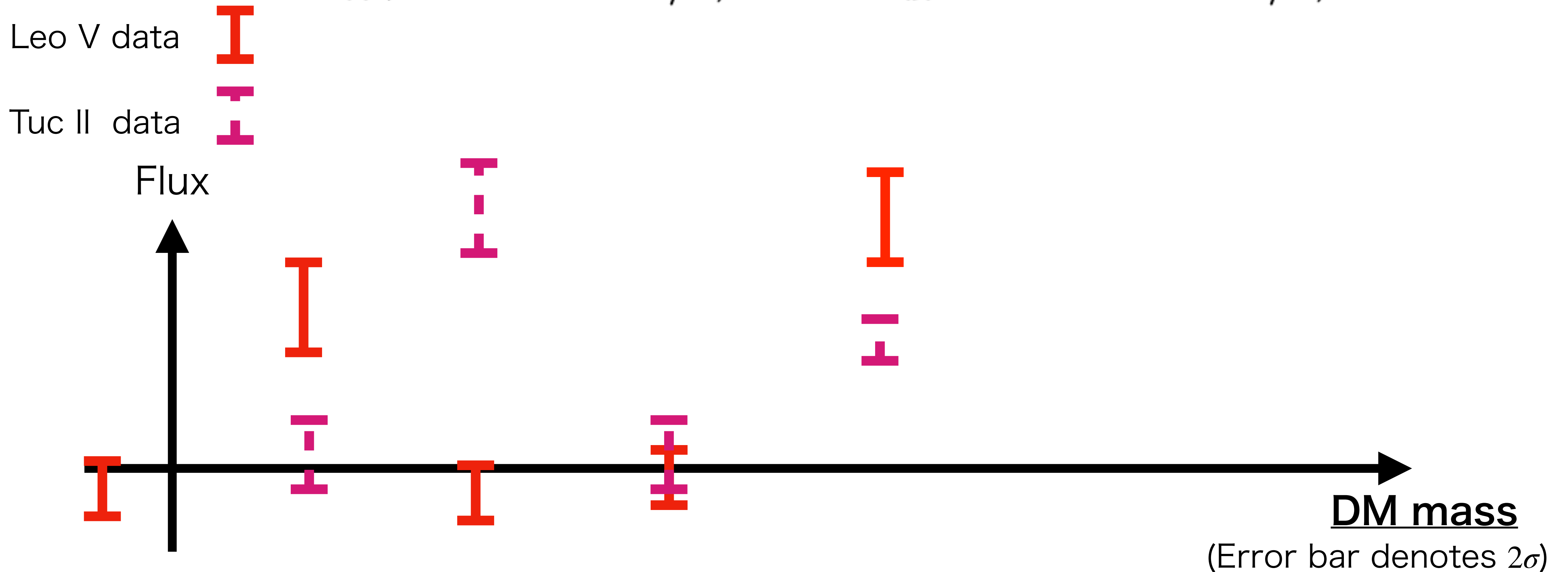
We move to dSphs' frames for DM limit.

WY, Ikeda, Bessho, Kobayashi+WINERED team, 2402.07976

Radial velocities of the dSphs are much larger than the resolution of WINERED

Simbad, Inger et al 0002110

$$v_{\text{LeoV}} \approx 173.3 \text{ km/s}, \text{ and } v_{\text{TucII}} \approx -129.1 \text{ km/s},$$



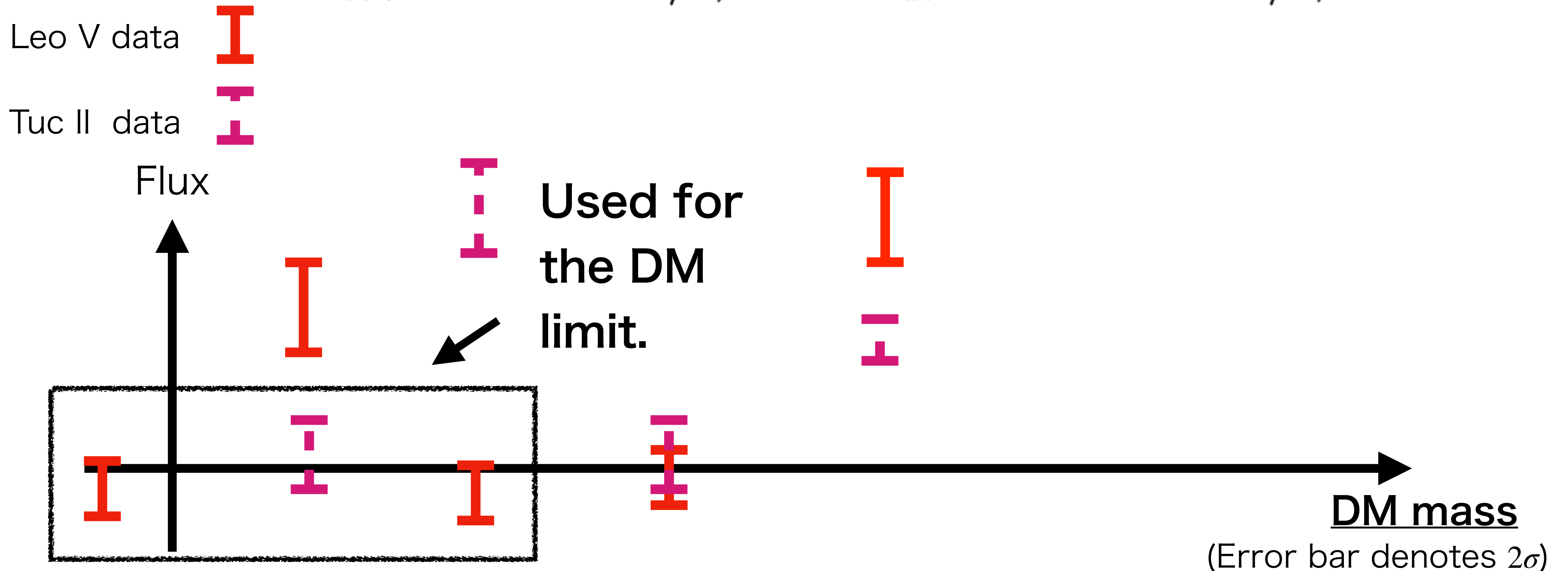
We move to dSphs' frames for DM limit.

WY, Ikeda, Bessho, Kobayashi+WINERED team, 2402.07976

Radial velocities of the dSphs are much larger than the resolution of WINERED

Simbad, Inger et al 0002110

$$v_{\text{LeoV}} \approx 173.3 \text{ km/s}, \text{ and } v_{\text{TucII}} \approx -129.1 \text{ km/s},$$



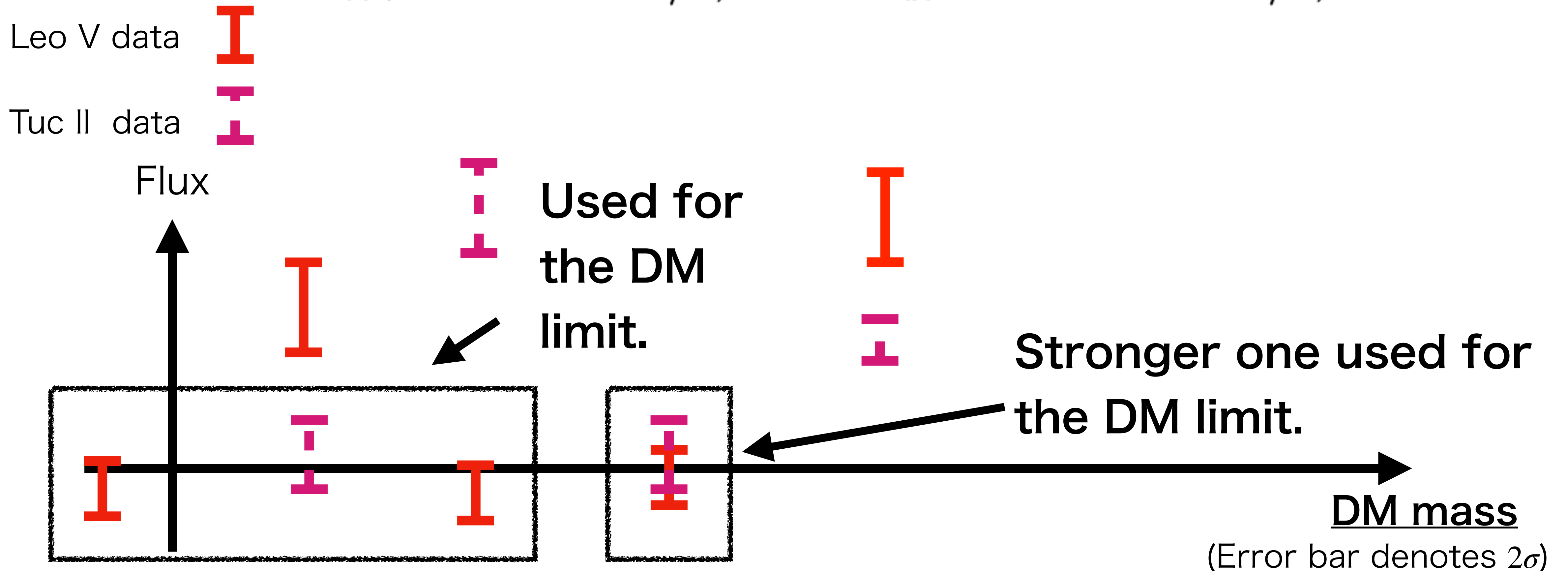
We move to dSphs' frames for DM limit.

WY, Ikeda, Bessho, Kobayashi+WINERED team, 2402.07976

Radial velocities of the dSphs are much larger than the resolution of WINERED

Simbad, Inger et al 0002110

$$v_{\text{LeoV}} \approx 173.3 \text{ km/s, and } v_{\text{TucII}} \approx -129.1 \text{ km/s,}$$



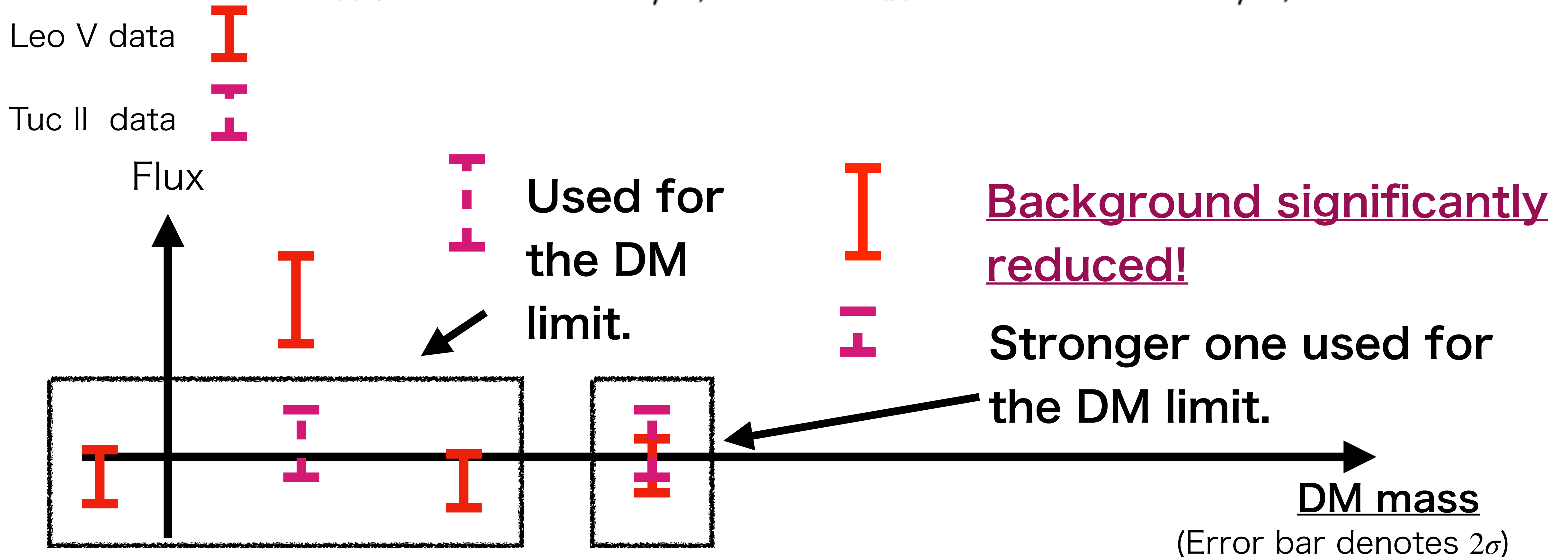
We move to dSphs' frames for DM limit.

WY, Ikeda, Bessho, Kobayashi+WINERED team, 2402.07976

Radial velocities of the dSphs are much larger than the resolution of WINERED

Simbad, Inger et al 0002110

$$v_{\text{LeoV}} \approx 173.3 \text{ km/s, and } v_{\text{TucII}} \approx -129.1 \text{ km/s,}$$



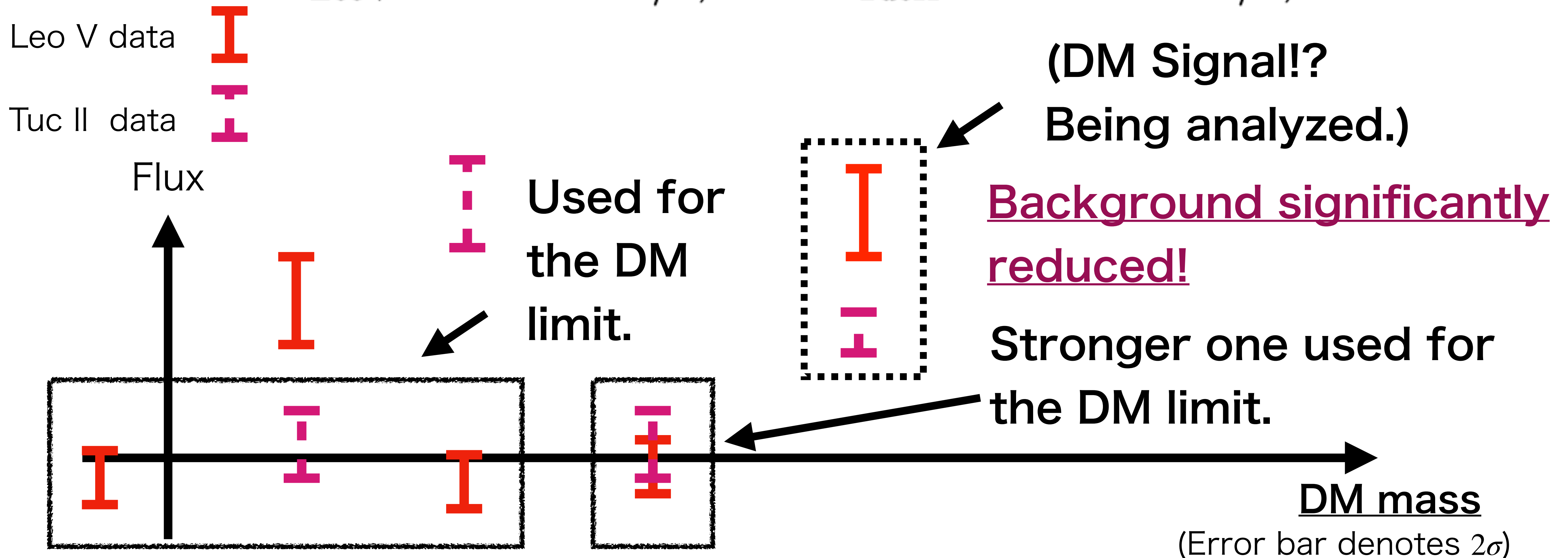
We move to dSphs' frames for DM limit.

WY, Ikeda, Bessho, Kobayashi+WINERED team, 2402.07976

Radial velocities of the dSphs are much larger than the resolution of WINERED

Simbad, Inger et al 0002110

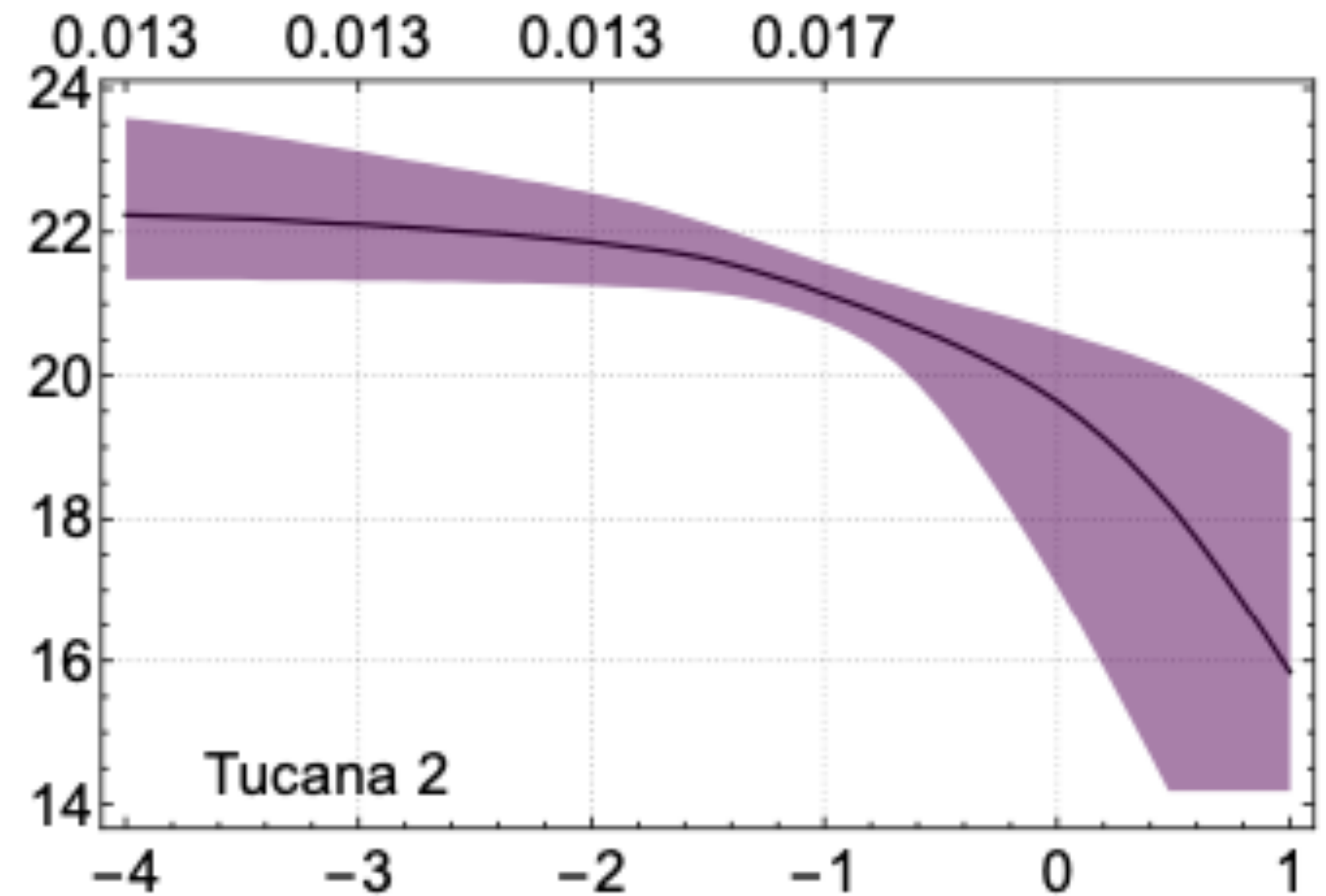
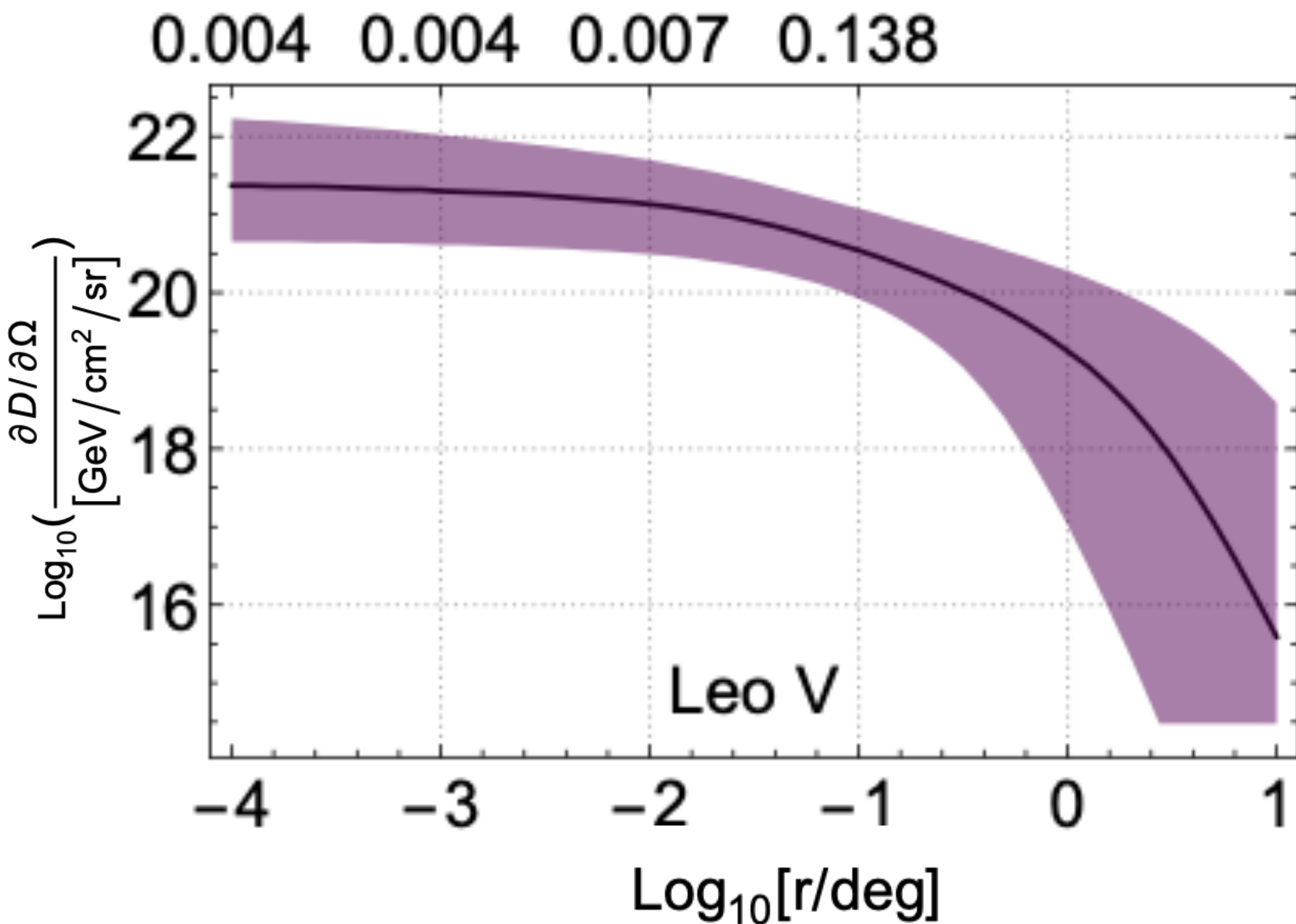
$$v_{\text{LeoV}} \approx 173.3 \text{ km/s, and } v_{\text{TucII}} \approx -129.1 \text{ km/s,}$$



We use differential D-factor of dSphs at around the center

This gives O(10) enhancement of flux compared with using typical value

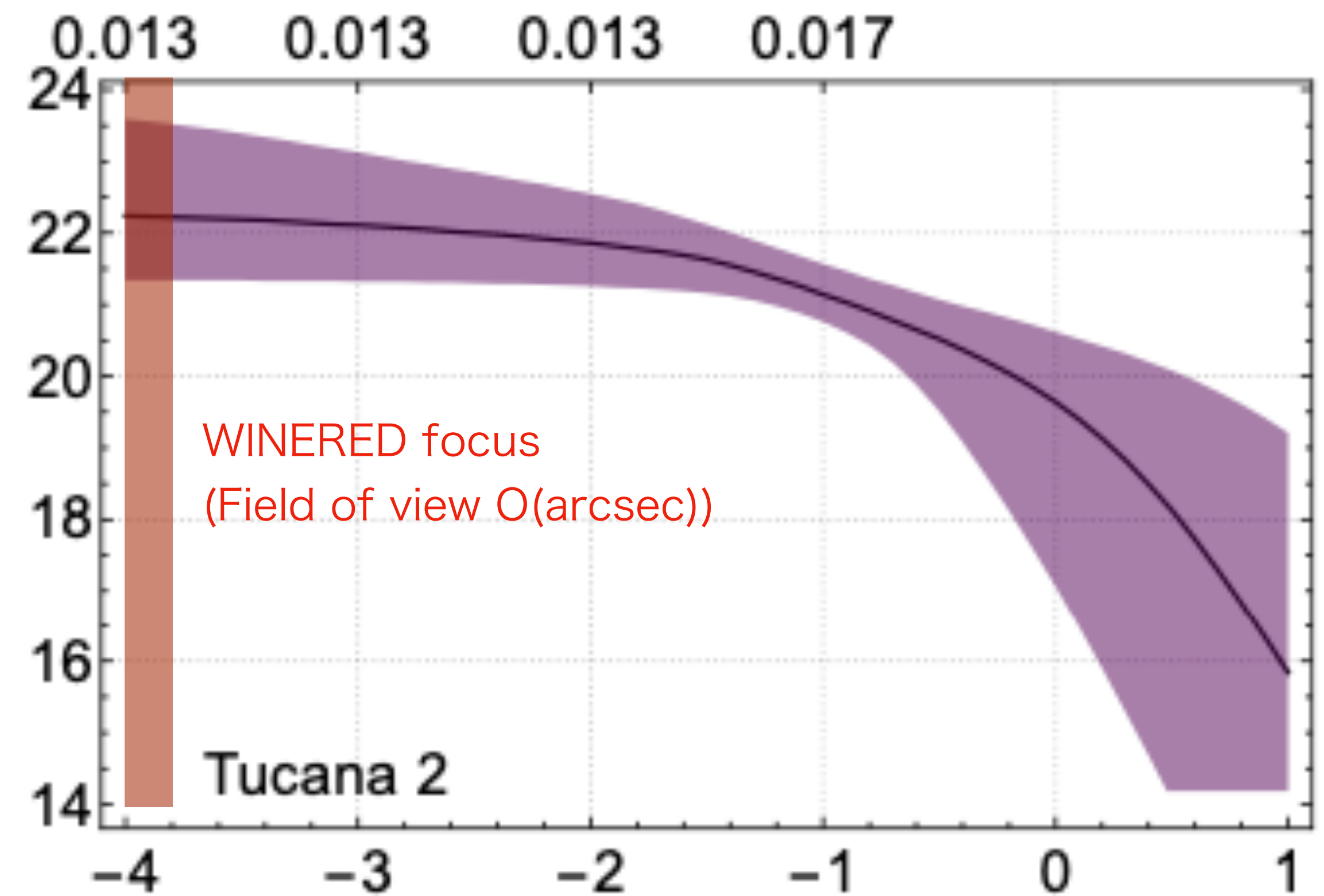
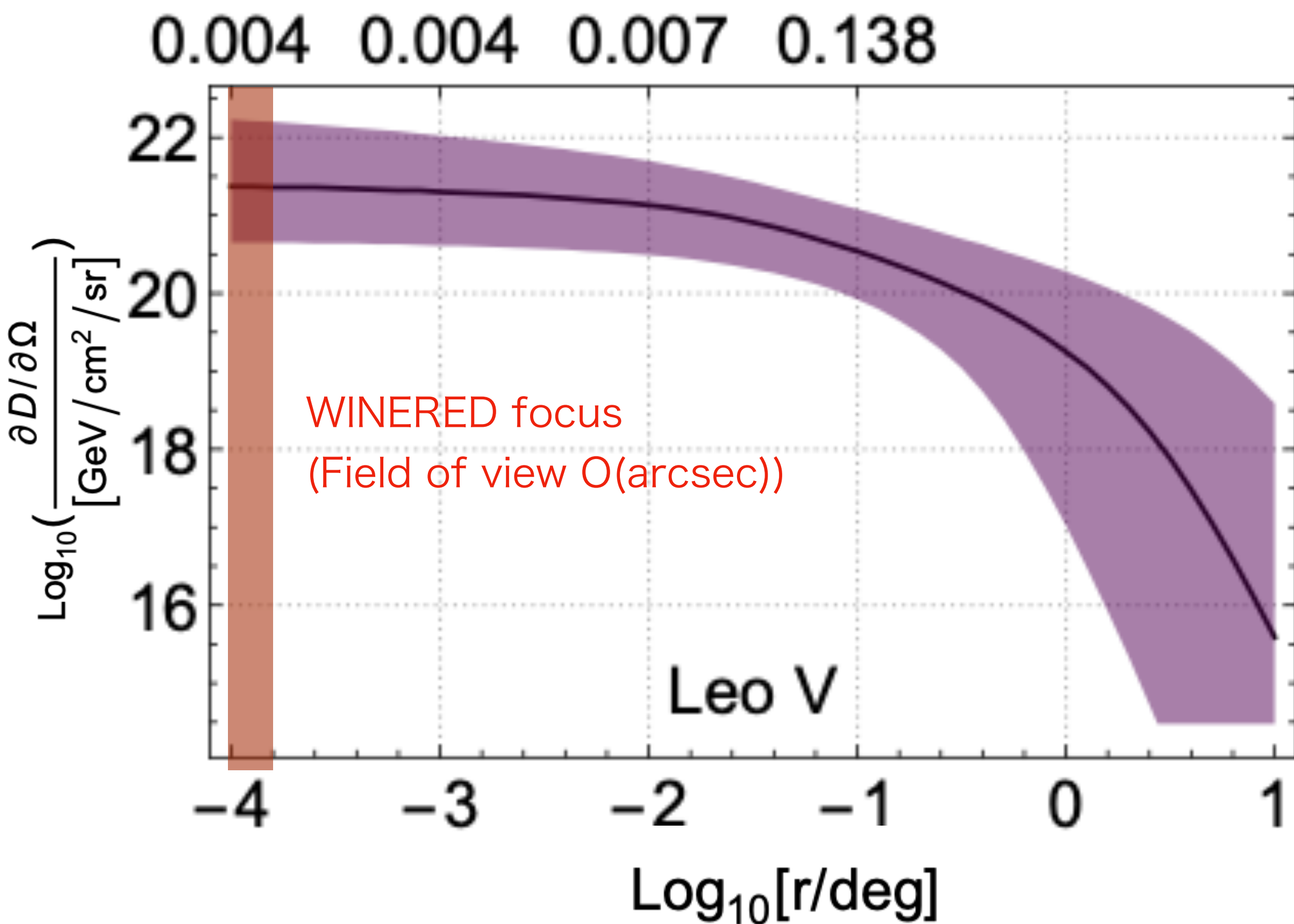
WY, Hayashi, 2305.13415
(See also Hayashi et al 2007.13780, 2206.02821)



We use differential D-factor of dSphs at around the center

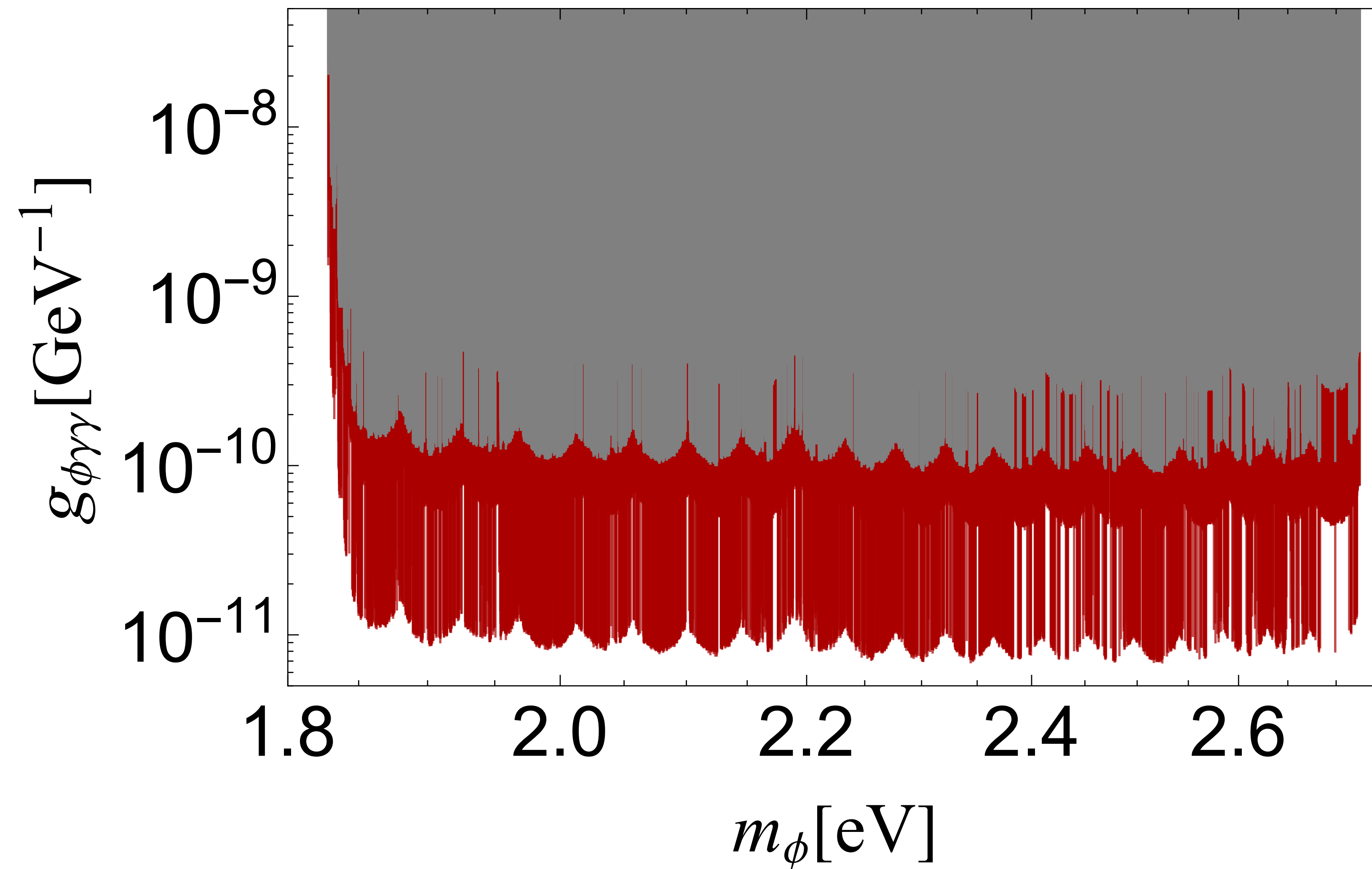
This gives O(10) enhancement of flux compared with using typical value

WY, Hayashi, 2305.13415
(See also Hayashi et al 2007.13780, 2206.02821)



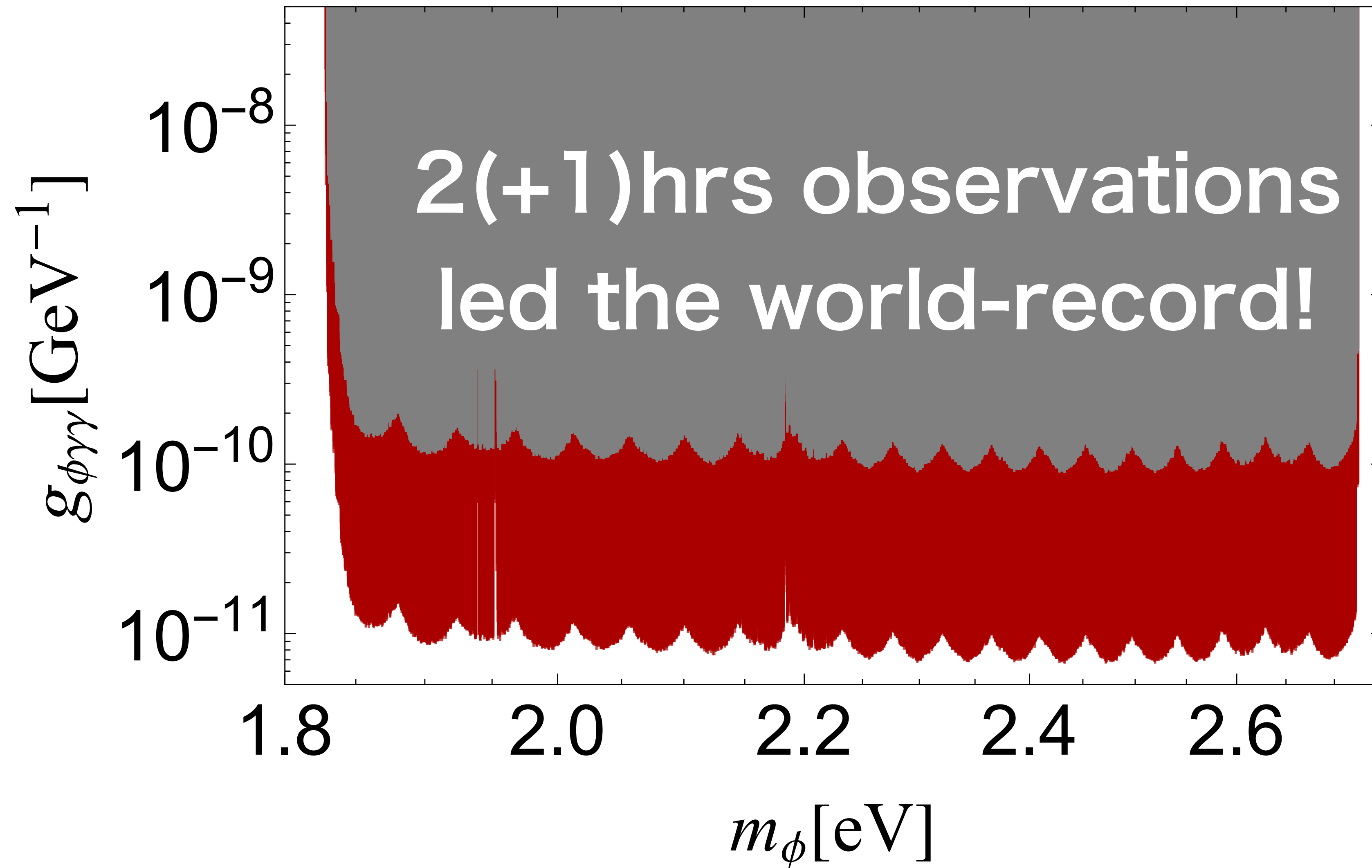
Result: before further data analysis (can be recast to generic spectra)

WY, Ikeda, Bessho, Kobayashi+WINERED team, 2402.07976



Result: subtracting continuous spectra (Only apply to line spectra)

WY, Ikeda, Bessho, Kobayashi+WINERED team, 2402.07976



Conclusions: eV axion DM

- eV dark matter may be interesting because various hints coincide.
 - It can be very efficiently searched for by using state-of-the-art infrared spectrographs.
Bessho, Ikeda, WY, 2208.05975
WY, Hayashi 2305.13415
 - Performing just 2(+1)hours observations we set one of the strongest bounds in the world.
WY, Ikeda, Bessho, Kobayashi
+WINERED team, 2402.07976
 - Some excesses coincide after Doppler analysis.
Further analysis/observation is planned.
- stay tuned!

Back up slides

DM profiles

Hayashi et al 2020, 2022

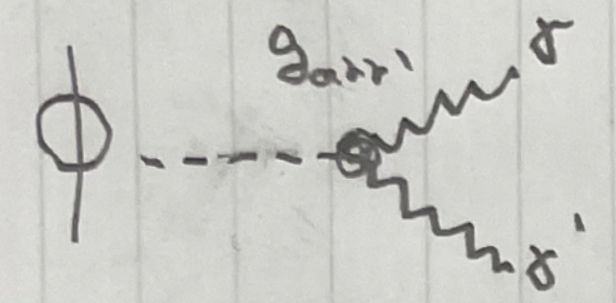
Einasto, and Burkert profiles. The generalized Hernquist profile in the cylindrical coordinates is expressed as

$$\rho_{\text{DM}}(m) = \rho_0 \left(\frac{m}{b_{\text{halo}}} \right)^{-\gamma} \left[1 + \left(\frac{m}{b_{\text{halo}}} \right)^\alpha \right]^{-\frac{\beta-\gamma}{\alpha}},$$
$$m^2 = R^2 + z^2/Q^2, \quad (7)$$

where ρ_0 and b_{halo} are the scale density and radius, respectively; α is the sharpness parameter of the transition from the inner slope γ to the outer slope β ; and Q is a constant axial ratio of a DM halo. These $(Q, \rho_0, b_{\text{halo}}, \alpha, \beta, \gamma)$ are the

Reheating for g_{arr}

Decay



$$f_{\gamma'} \propto \rho \frac{8\pi^2 V_{\phi} n_{\phi}}{H P_{\gamma'}^3}$$

bose enhancement

$$P_{\gamma'} \approx \frac{m_{\phi}}{2} - \frac{m_{th}}{2m_{\phi}}$$

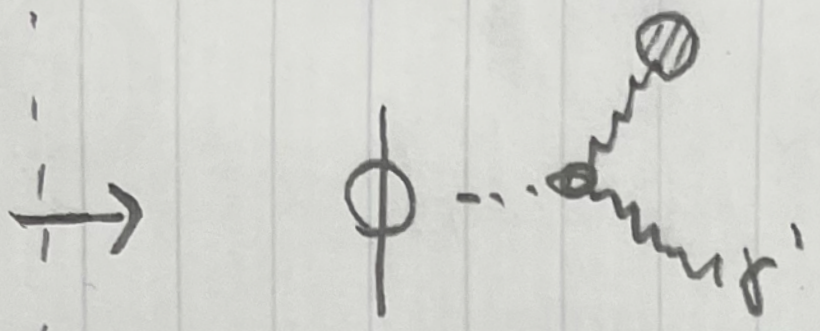
[Moroi, WY, 2011.09475]

$$m_{th} \uparrow P_{\gamma'} \downarrow \log f_{\gamma'} \uparrow$$

• Significant Production of γ'

• Even if $m_{\phi} < m_{th}$ stimulated decay is expected to proceed due to dissipation effect,

Equilibration



$$f_{\phi} \propto -f_{th} [f_{\phi} - f_{\gamma'}]$$

$$f_{th}^{(1)} f_{th}^{(2)} [f_{\phi} - f_{\gamma'}]$$

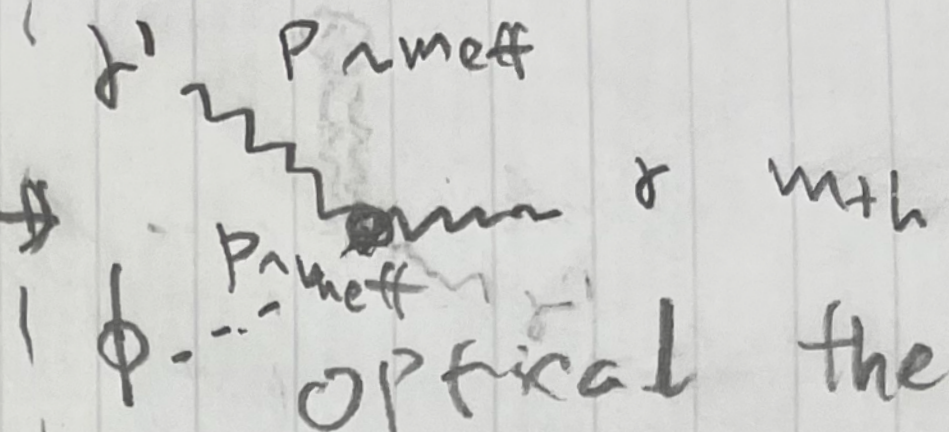
$$\left(\begin{array}{l} P_{\phi} \sim P_{\gamma'} \sim m_{eff} \ll T \\ f_{th}^{(1)} \sim f_{th}^{(2)} \end{array} \right)$$

$$\Rightarrow f_{\phi} \sim f_{\gamma'}$$

$$\Rightarrow n_{\phi} \sim n_{\gamma'}$$

[e.g. W.Y. 2301.08735]

Annihilation



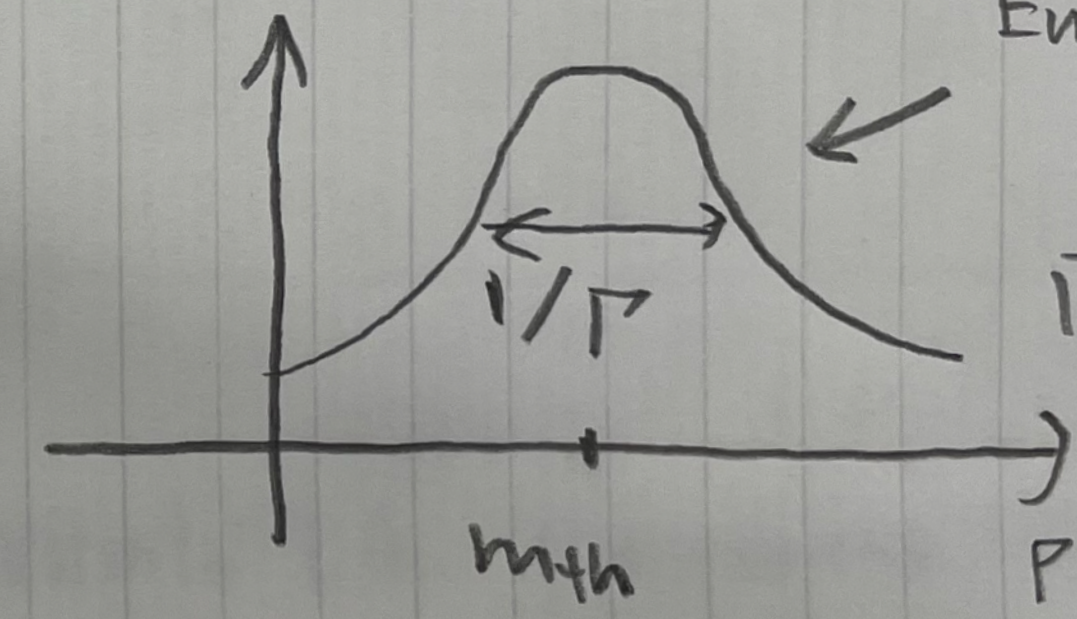
optical theorem

$$\sigma \sim \frac{1}{E_{cm} P_{cm}} \text{Im} [M_{\gamma'\phi \rightarrow \gamma'\phi}]$$

$$\sim \frac{1}{E_{cm}^2} \text{Im} \left[\frac{P_{\phi} g_{\phi\gamma\gamma'} P_{\phi}}{P^2 - m_{th}^2 + im_{th}\Gamma} \right]$$

Breit-Wigner

$$m_{th} \text{Im} \left[\frac{1}{P^2 - m_{th}^2 + im_{th}\Gamma} \right]$$



Energy conservation violation.

$$\Gamma \sim \frac{1}{2} g^2 \Gamma$$

[mean free path of photon in plasma]

$$\Rightarrow \sigma \sim g_{\phi\gamma\gamma'}^2 \frac{\Gamma}{m_{th}} \sim g_{\gamma\gamma'}^2$$

Axion abundance

Things will not change if axion is produced from misalignment. In both cases, we have $m_\phi \sim H$.

Axion abundance
Annihilation stops when
 $n_\phi \sigma \sim H \sim m_\phi$ ①

later comoving number conserves

$$\frac{n_\phi}{s} m_\phi \sim 0.1 \text{ eV}$$

for DM

$$\boxed{m_\phi \sim H \text{ inf} \sim H \text{ (instant reheating)} \quad \text{--- ②}$$

$$s \sim k^3 \sim m_\phi^2 M_{pl}^2$$

$$\Rightarrow \text{①②} \quad \frac{n_\phi m_\phi}{s} \sim \frac{m_\phi^{\frac{1}{2}}}{\sigma M_{pl}^{\frac{3}{2}}} \sim 0.1 \text{ eV} \left(\frac{g_{\phi\gamma\gamma'}}{10^{10} \text{ GeV}} \right)^{-2} \left(\frac{m_\phi}{\text{eV}} \right)^{\frac{1}{2}}$$

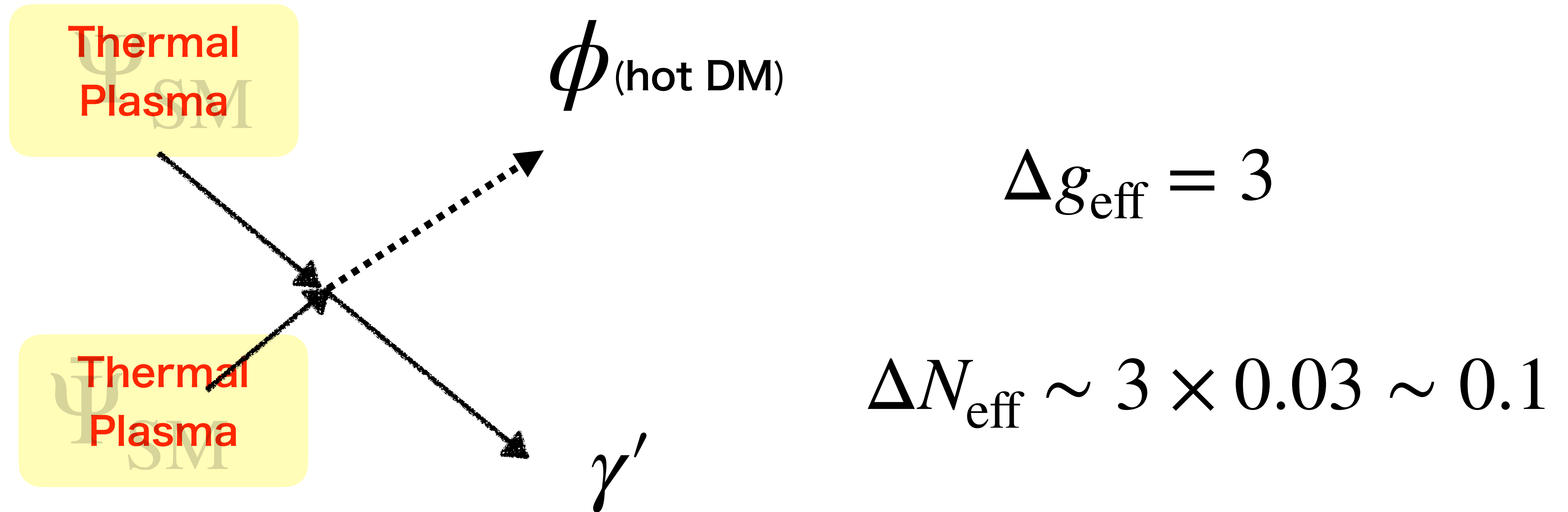
• many $O(1)$ factors

• $\sigma \equiv \frac{c g_{\phi\gamma\gamma'}^2 g_\gamma}{(4\pi)^3}$, using realistic parameters

$$\Omega_\phi = \frac{0.2}{C} \left(\frac{m_\phi}{2.5 \text{ eV}} \right)^{1/2} \left(\frac{g_{\phi\gamma\gamma'}}{\sqrt{2} \times 1.5 \times 10^{-10} \text{ GeV}} \right)^{-2}$$

Prediction

Thermal production of hot DM/dark radiation



2. DM=inflaton=ALP

Axion inflation

The slow-roll flat direction is stable under radiative corrections if ϕ is an axion featuring a discrete shift symmetry:

$$\phi \rightarrow \phi + 2\pi f_\phi$$

$$\rightarrow V_{\text{inf}}(\phi) = V_{\text{inf}}(\phi + 2\pi f_\phi)$$

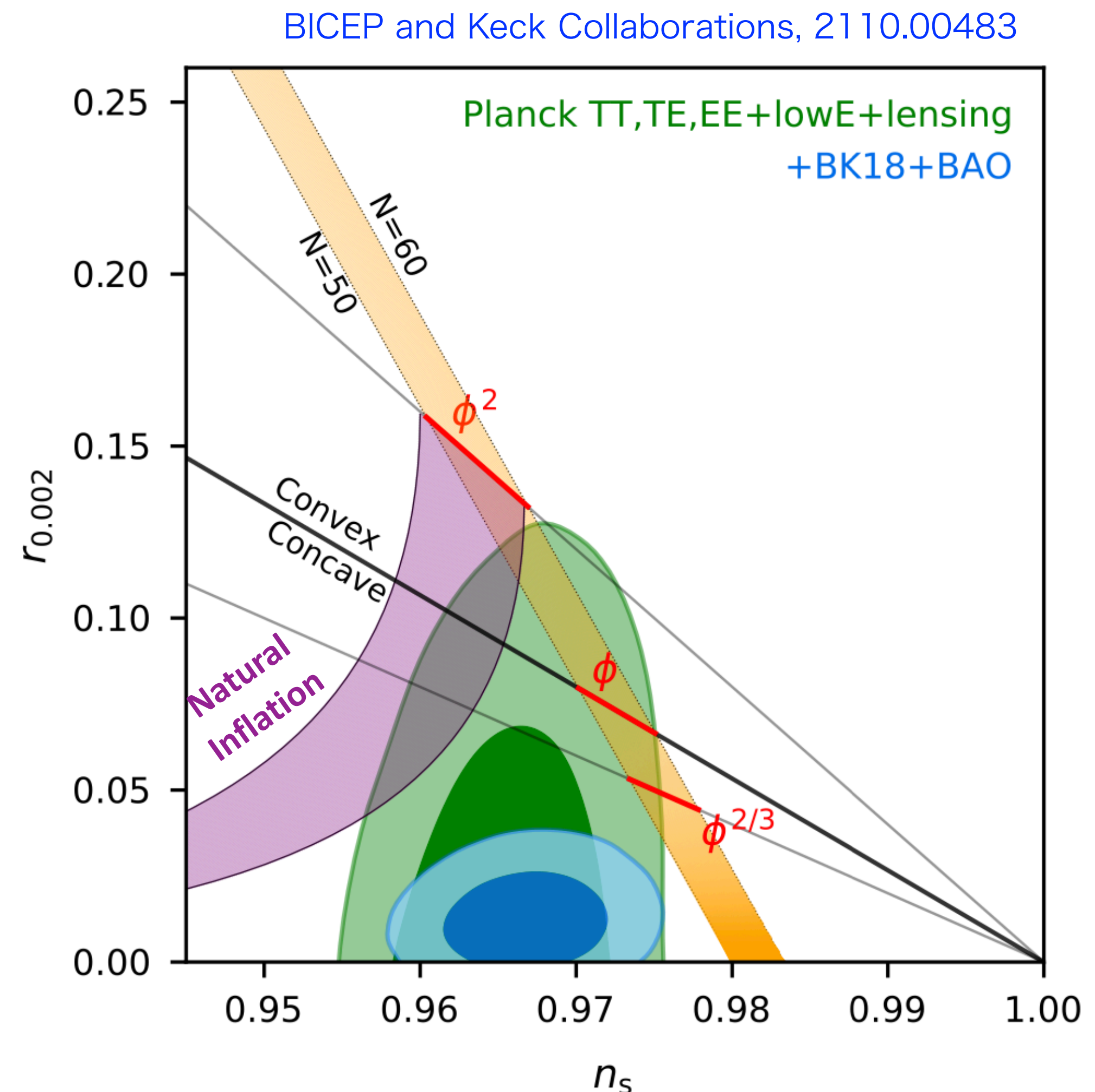
Realization of axion inflation:

Natural inflation: single cosine

Freese, Frieman, Olinto '90

$$V_{\text{inf}} = \Lambda^4 (1 - \cos(\phi/f_\phi))$$

$f_\phi > M_{\text{pl}}$ and excluded due to too high scale for inflation...



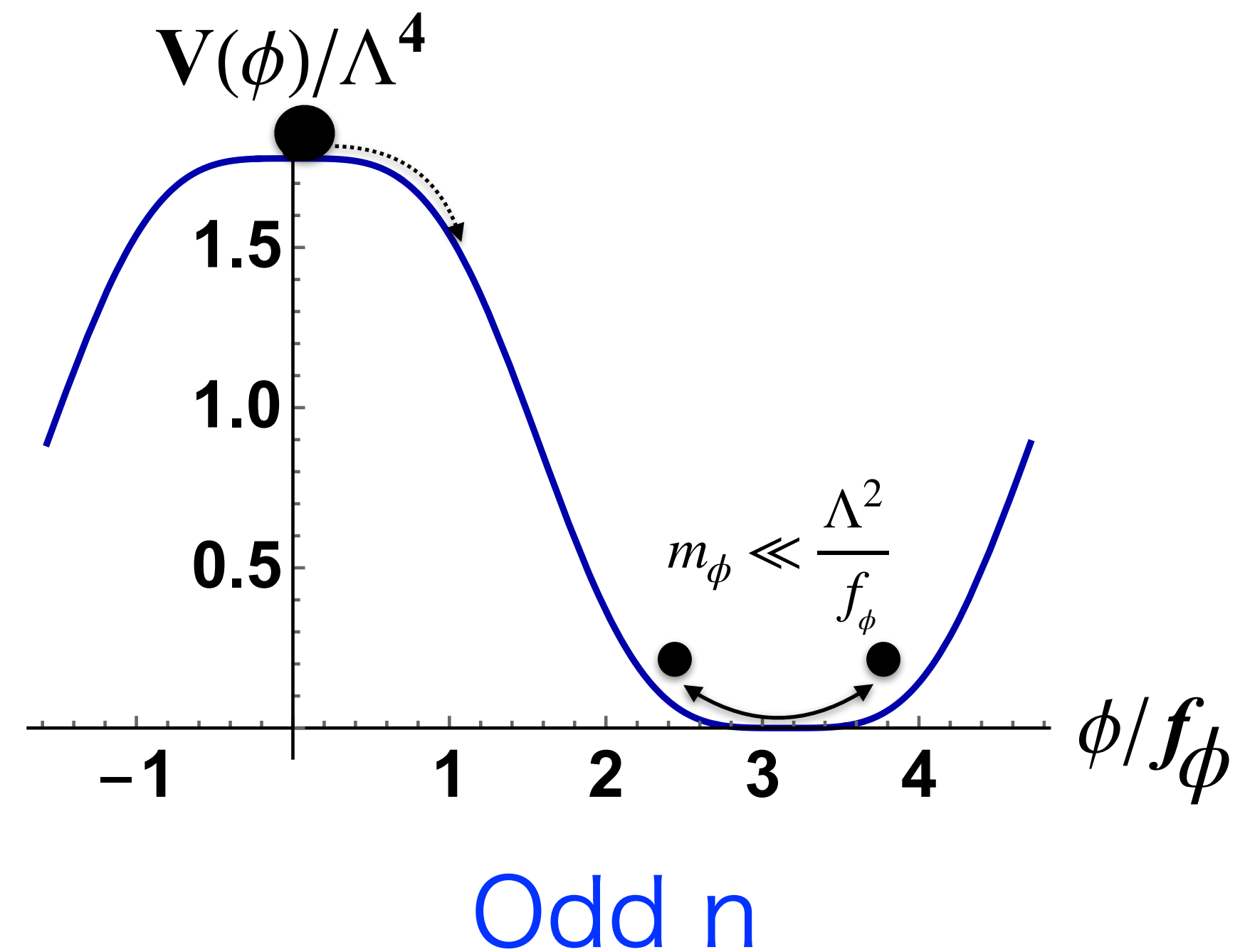
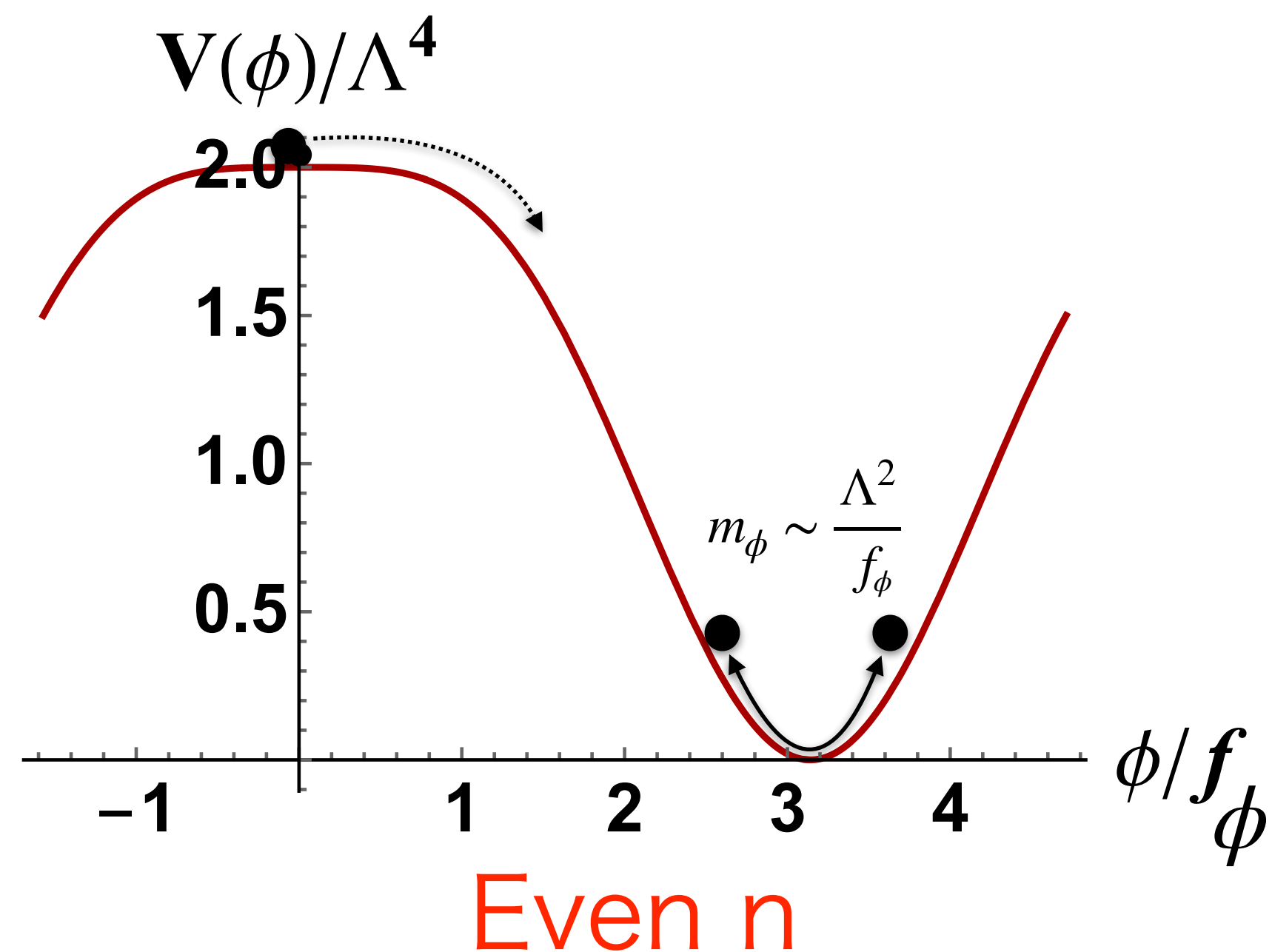
Multi-natural inflation: V_{inf} from 2 or more cos terms

Czerny, Takahashi 1401.5212; Czerny, Higaki, Takahashi 1403.0410, 1403.5883; Daido, Takahashi, and WY 1702.03284; 1710.11107; Takahashi and WY, 1903.00462;

In multi-natural inflation, CMB data can be well explained with $f_\phi \ll M_{\text{pl}}$.

$$V_{\text{inf}}(\phi) = \Lambda^4 \left(\cos \left(\frac{\phi}{f_\phi} + \theta \right) - \frac{\kappa}{n^2} \cos \left(\frac{n\phi}{f_\phi} \right) \right) + \text{const}$$

The inflaton masses depend on the parity of n .



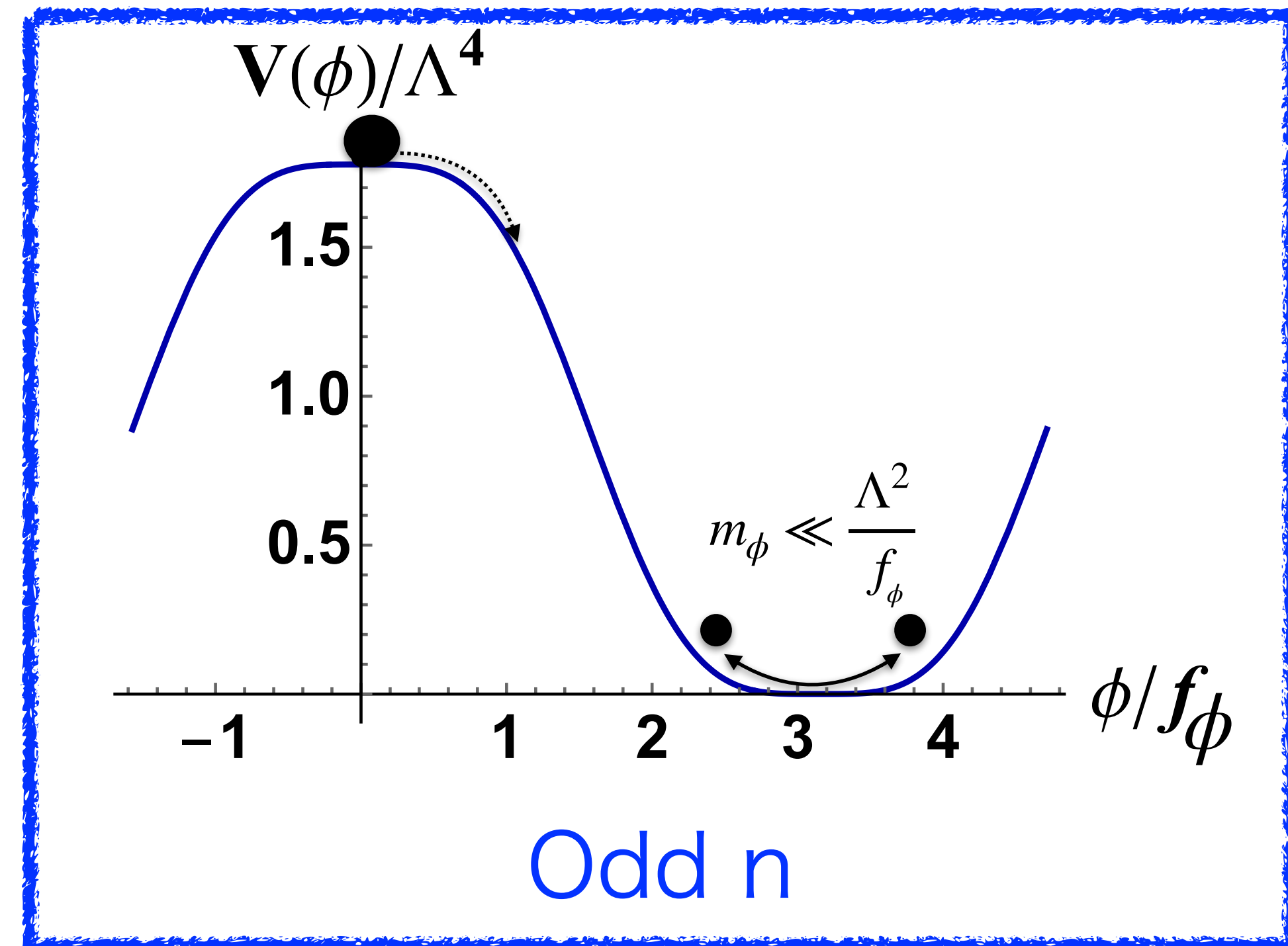
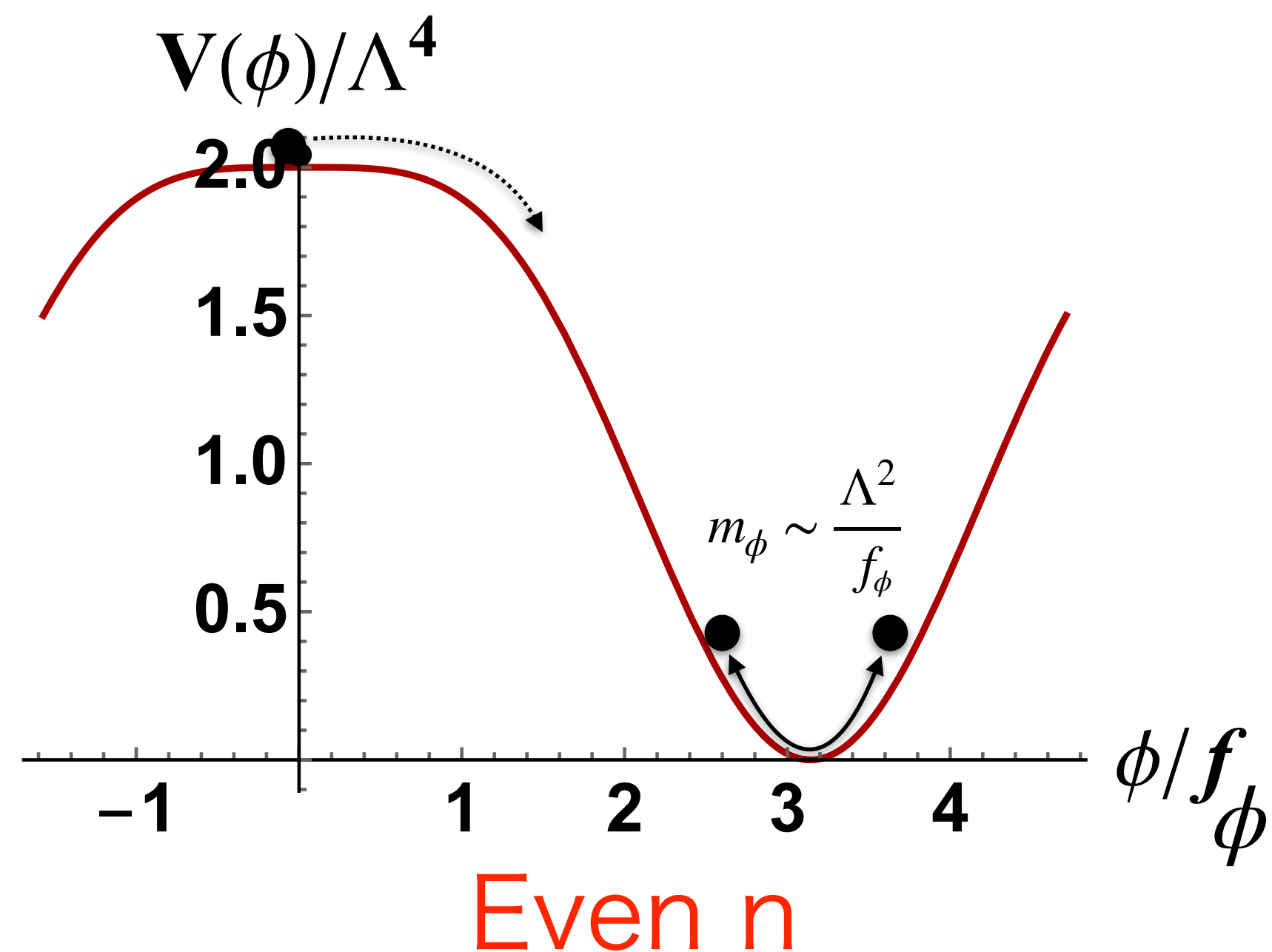
Multi-natural inflation: V_{inf} from 2 or more cos terms

Czerny, Takahashi 1401.5212; Czerny, Higaki, Takahashi 1403.0410, 1403.5883; Daido, Takahashi, and WY 1702.03284; 1710.11107; Takahashi and WY, 1903.00462;

In multi-natural inflation, CMB data can be well explained with $f_\phi \ll M_{\text{pl}}$.

$$V_{\text{inf}}(\phi) = \Lambda^4 \left(\cos \left(\frac{\phi}{f_\phi} + \theta \right) - \frac{\kappa}{n^2} \cos \left(\frac{n\phi}{f_\phi} \right) \right) + \text{const}$$

The inflaton masses depend on the parity of n .

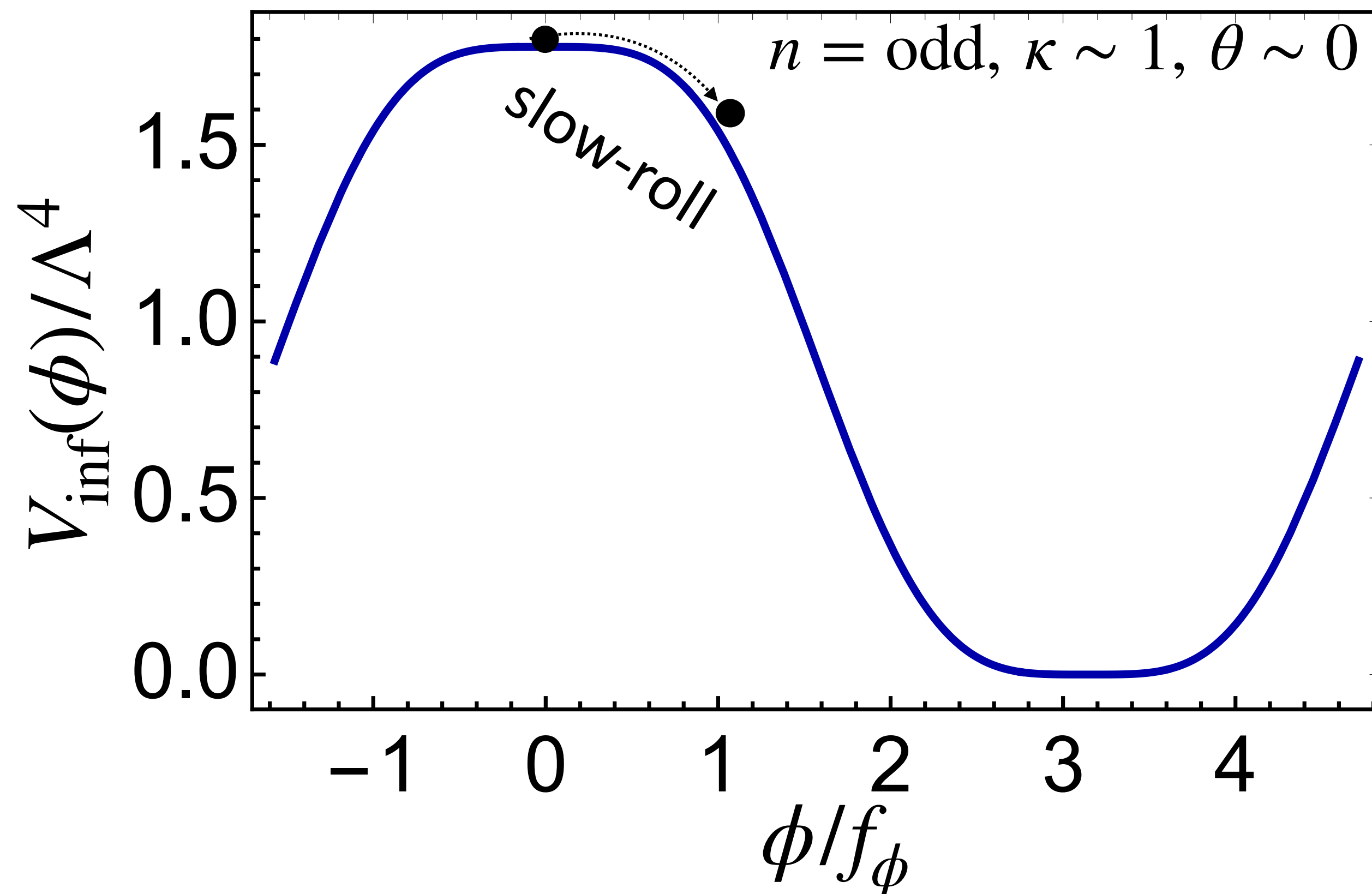


Axion Hilltop inflation

In multi-natural inflation, CMB data can be well explained with $f_\phi \ll M_{\text{pl}}$.

$$V_{\text{inf}}(\phi) = \Lambda^4 \left(\cos \left(\frac{\phi}{f_\phi} + \theta \right) - \frac{\kappa}{n^2} \cos \left(\frac{n\phi}{f_\phi} \right) \right) + \text{const}$$
$$\simeq V_0 - \lambda\phi^4 - \Lambda^4\theta \frac{\phi}{f_\phi} + \dots$$

- Almost quartic hilltop inflation.

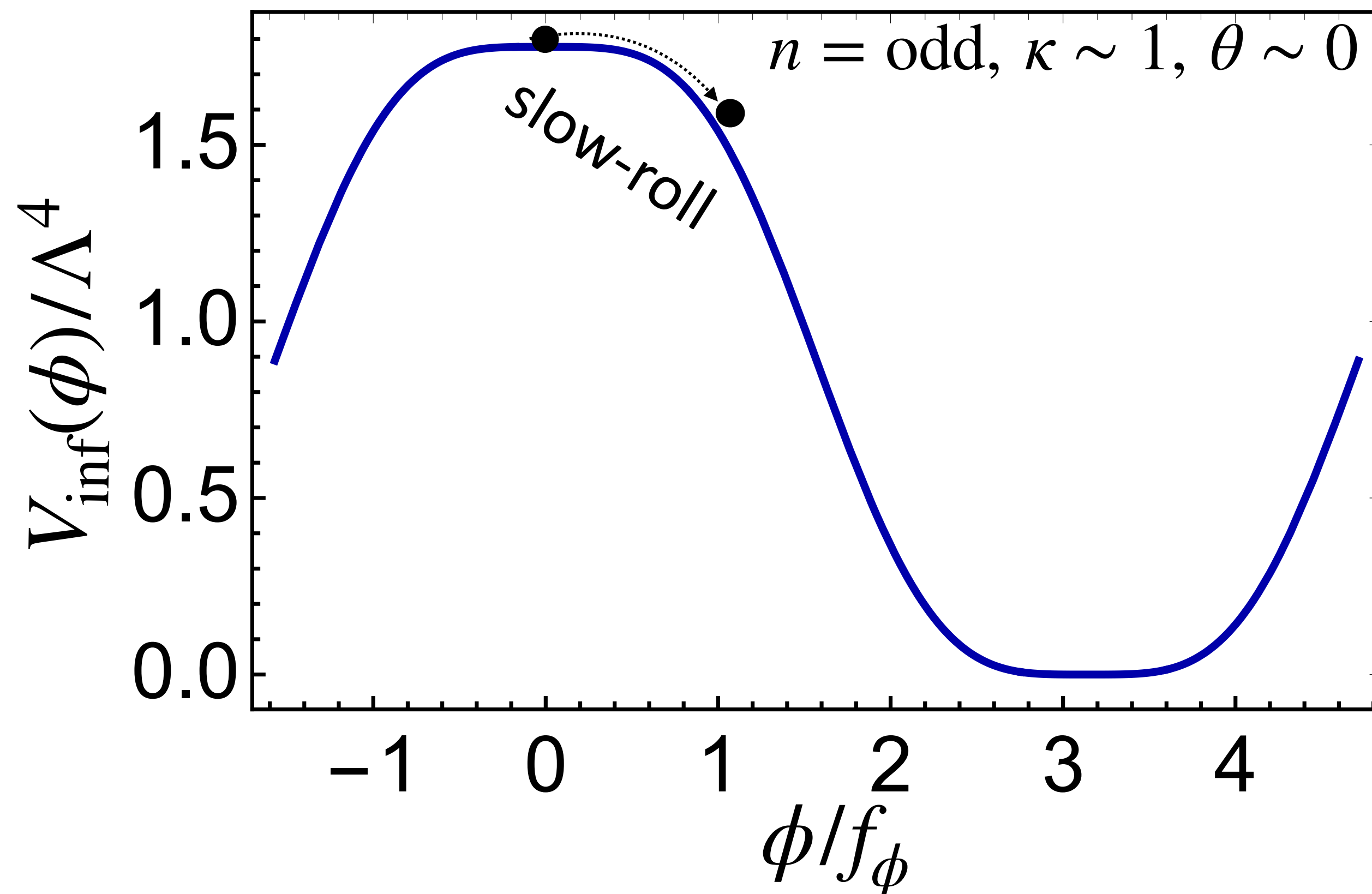


- n_s corrected from non-vanishing θ
- Upside-down symmetry when $n = \text{odd}$

Axion Hilltop inflation

In multi-natural inflation, CMB data can be well explained with $f_\phi \ll M_{\text{pl}}$.

$$V_{\text{inf}}(\phi) = \Lambda^4 \left(\cos \left(\frac{\phi}{f_\phi} + \theta \right) - \frac{\kappa}{n^2} \cos \left(\frac{n\phi}{f_\phi} \right) \right) + \text{const}$$
$$\simeq V_0 - \lambda \phi^4 - \Lambda^4 \theta \frac{\phi}{f_\phi} + \dots$$



- Almost quartic hilltop inflation.

CMB normalization:

$$\lambda \sim \Lambda^4/f_\phi^4 \sim 10^{-12}$$

- n_s corrected from non-vanishing θ
- Upside-down symmetry when $n = \text{odd}$

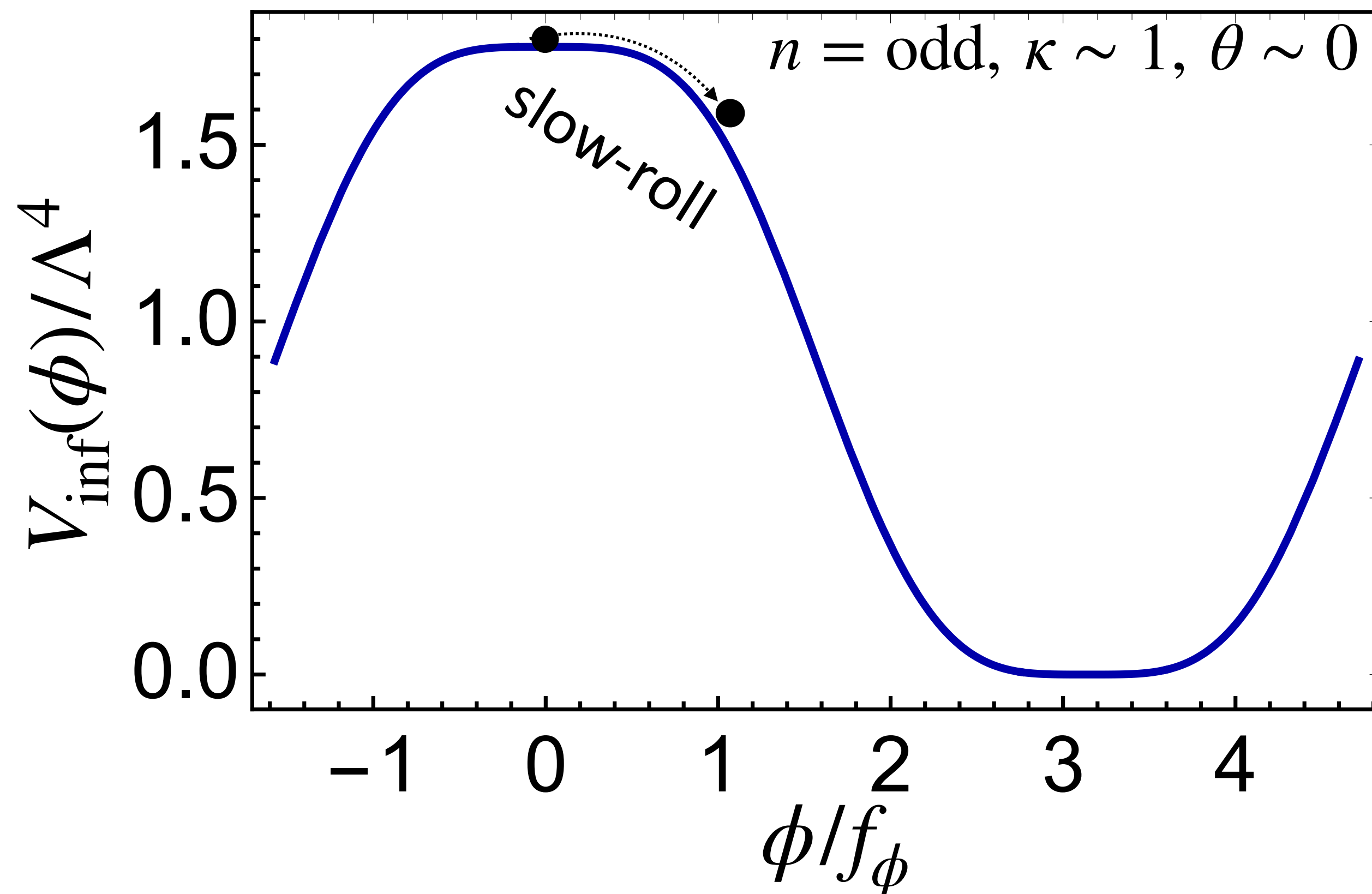
Axion Hilltop inflation

In multi-natural inflation, CMB data can be well explained with $f_\phi \ll M_{\text{pl}}$.

$$V_{\text{inf}}(\phi) = \Lambda^4 \left(\cos \left(\frac{\phi}{f_\phi} + \theta \right) - \frac{\kappa}{n^2} \cos \left(\frac{n\phi}{f_\phi} \right) \right) + \text{const}$$

$$\simeq V_0 - \lambda \phi^4 - \Lambda^4 \theta \frac{\phi}{f_\phi} + \dots$$

A linear term can give better fit of n_s .
Takahashi, 1308.4212



- Almost quartic hilltop inflation.

CMB normalization:

$$\lambda \sim \Lambda^4/f_\phi^4 \sim 10^{-12}$$

- n_s corrected from non-vanishing θ

$$n_s \approx 1 + 2V''_{\text{inf}}/3H_{\text{inf}}^2 \approx 0.97$$

$$V''_{\text{inf}}|_{\text{hilltop}} \approx -O(0.1 - 1)H_{\text{inf}}^2$$

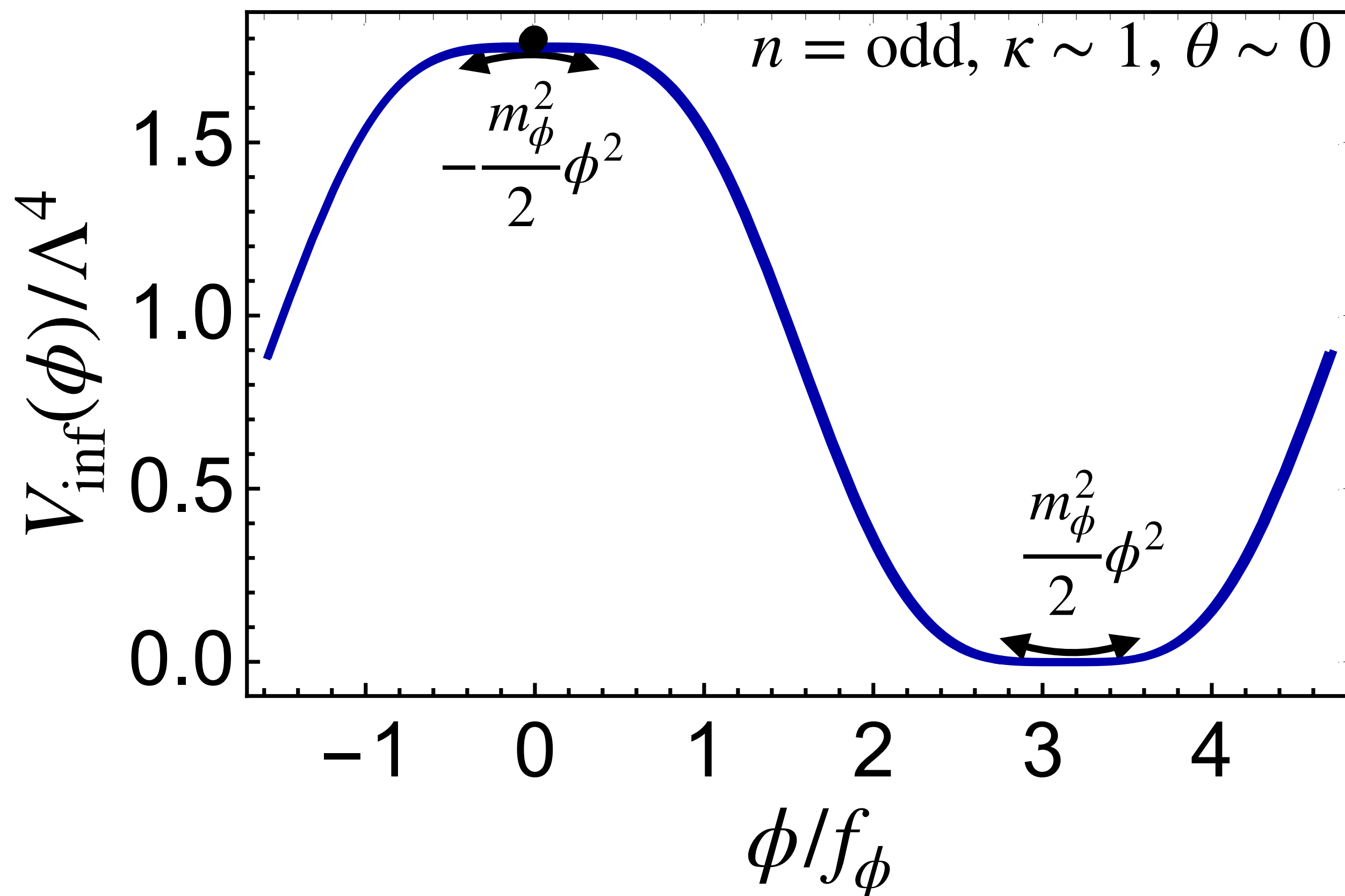
- Upside-down symmetry when $n = \text{odd}$

Upside-down symmetry in axion hilltop inflation

Daido, Takahashi, WY 1702.03284, 1710.11107; Takahashi and WY, 1903.00462;

UV model for hilltop condition: e.g. Croon and Sanz 1411.7809; Higaki, Takahashi 1501.02354;

$$V_{\text{inf}}(\phi) = \Lambda^4 \left(\cos \left(\frac{\phi}{f_\phi} + \theta \right) - \frac{\kappa}{n^2} \cos \left(\frac{n\phi}{f_\phi} \right) \right) + \text{const}$$
$$\simeq V_0 - \lambda \phi^4 - \Lambda^4 \theta \frac{\phi}{f_\phi} + \dots$$



- Almost quartic hilltop inflation.

CMB normalization:

$$\lambda \sim \Lambda^4/f_\phi^4 \sim 10^{-12}$$

- n_s corrected from non-vanishing θ

$$n_s \approx 1 + 2V''_{\text{inf}}/3H_{\text{inf}}^2 \approx 0.97$$

$$V'''_{\text{inf}}|_{\text{hilltop}} \approx -O(0.1 - 1)H_{\text{inf}}^2$$

- Upside-down symmetry when $n = \text{odd}$

(Note $H_{\text{inf}} \sim \Lambda^2/M_{\text{pl}}$)

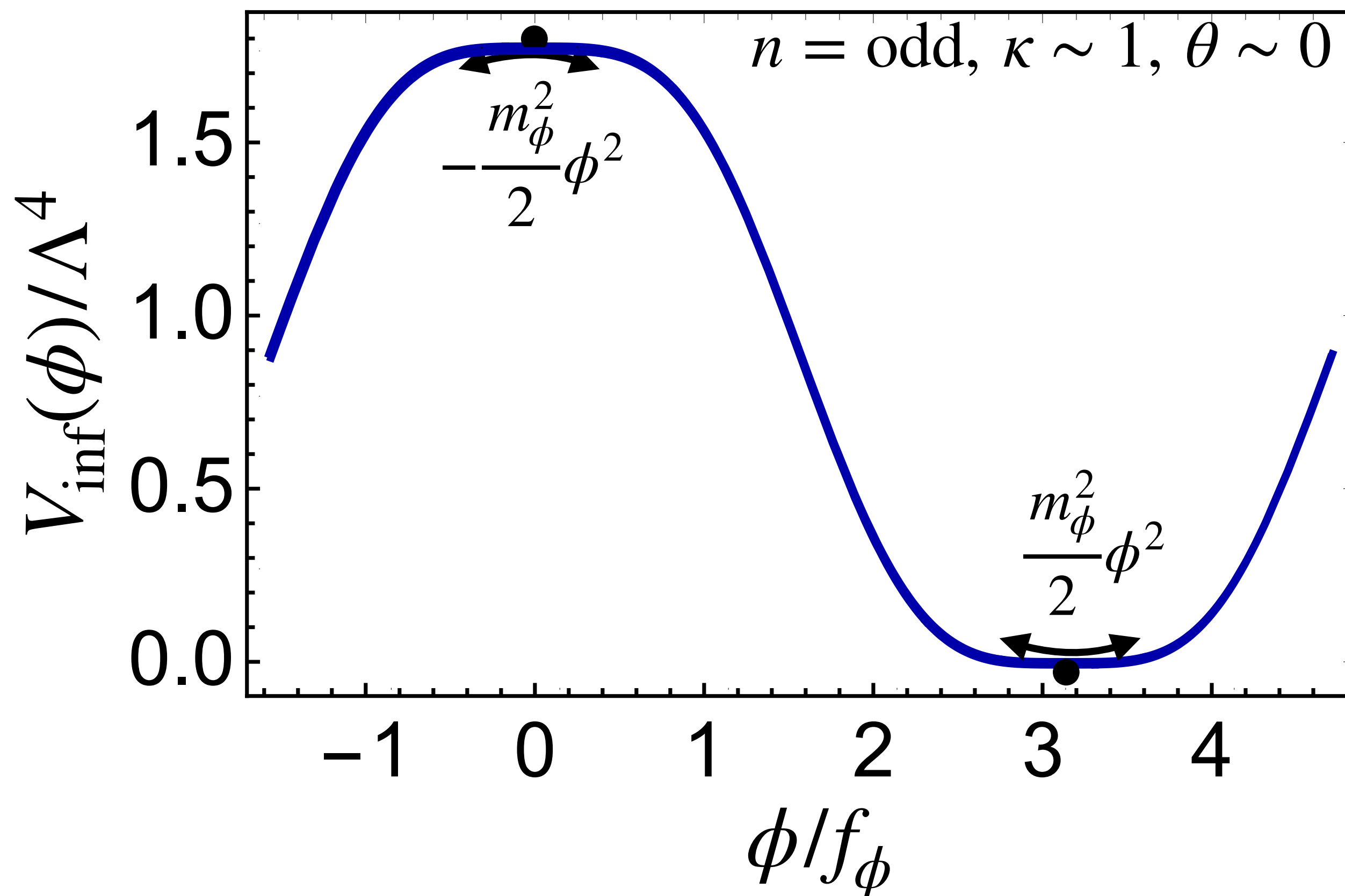
Upside-down symmetry in axion hilltop inflation

Daido, Takahashi, WY 1702.03284, 1710.11107; Takahashi and WY, 1903.00462;

UV model for hilltop condition: e.g. Croon and Sanz 1411.7809; Higaki, Takahashi 1501.02354;

$$V_{\text{inf}}(\phi) = \Lambda^4 \left(\cos\left(\frac{\phi}{f_\phi} + \theta\right) - \frac{\kappa}{n^2} \cos\left(\frac{n\phi}{f_\phi}\right) \right) + \text{const}$$

$$\simeq V_0 - \lambda\phi^4 - \Lambda^4\theta\frac{\phi}{f_\phi} + \dots$$



- Almost quartic hilltop inflation.

CMB normalization:

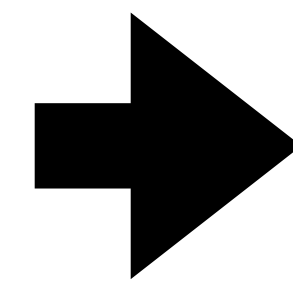
$$\lambda \sim \Lambda^4/f_\phi^4 \sim 10^{-12}$$

- n_s corrected from non-vanishing θ

$$n_s \approx 1 + 2V''_{\text{inf}}/3H_{\text{inf}}^2 \approx 0.97$$

$$V''_{\text{inf}}|_{\text{hilltop}} \approx -O(0.1 - 1)H_{\text{inf}}^2$$

- Upside-down symmetry when $n = \text{odd}$



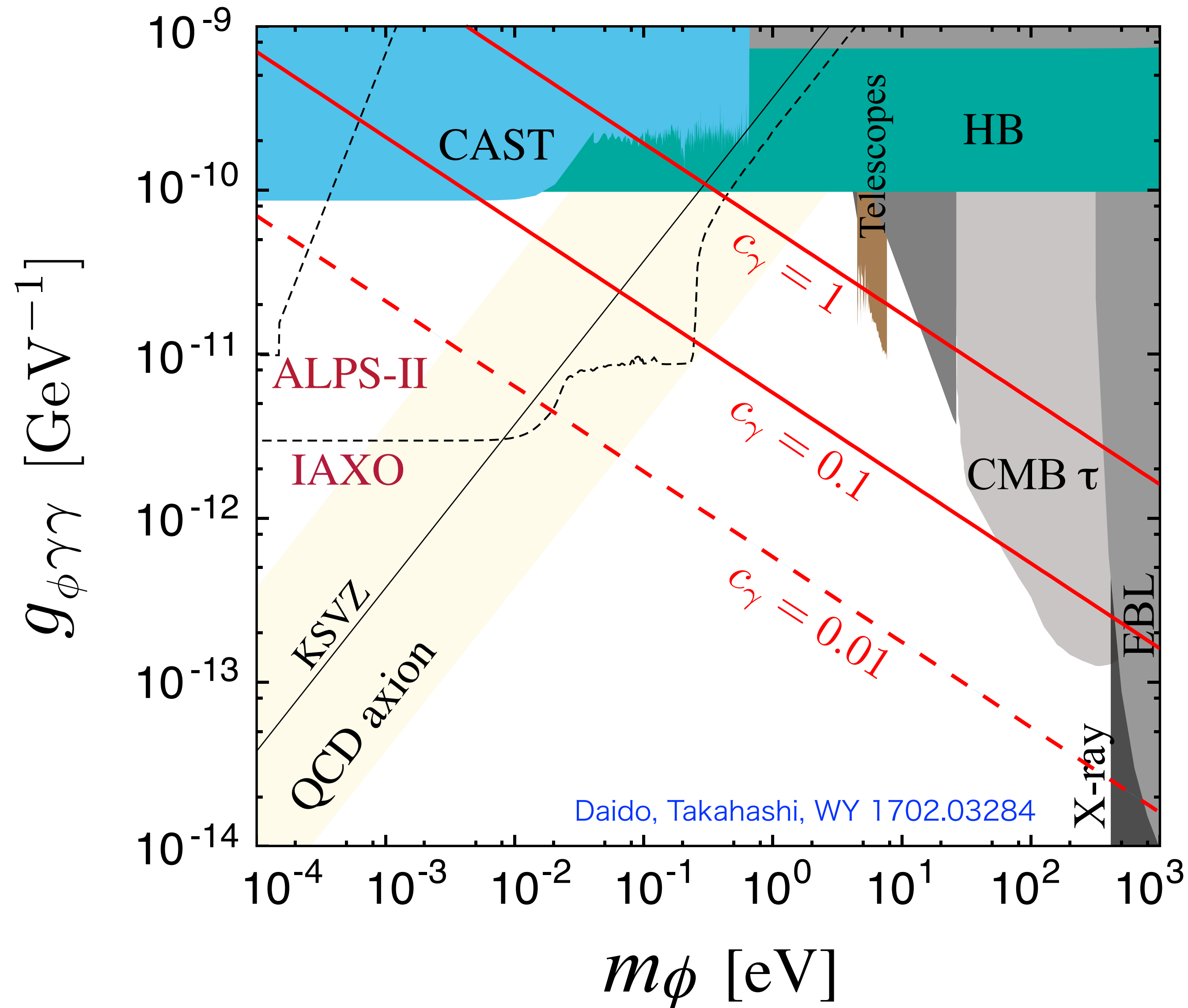
$$\lambda(\text{self-coupling}) \sim 10^{-12}$$

$$m_\phi = O(0.1 - 1)H_{\text{inf}} \sim 10^{-6} \frac{f_\phi^2}{M_{\text{pl}}}$$

(Note $H_{\text{inf}} \sim \Lambda^2/M_{\text{pl}}$)

ALP(axion coupled to photon)=inflaton

$$\mathcal{L} = \frac{g_{\phi\gamma\gamma}}{4} \phi F_{\mu\nu} \tilde{F}^{\mu\nu} \quad g_{\phi\gamma\gamma} = \frac{c_\gamma \alpha}{\pi f}$$

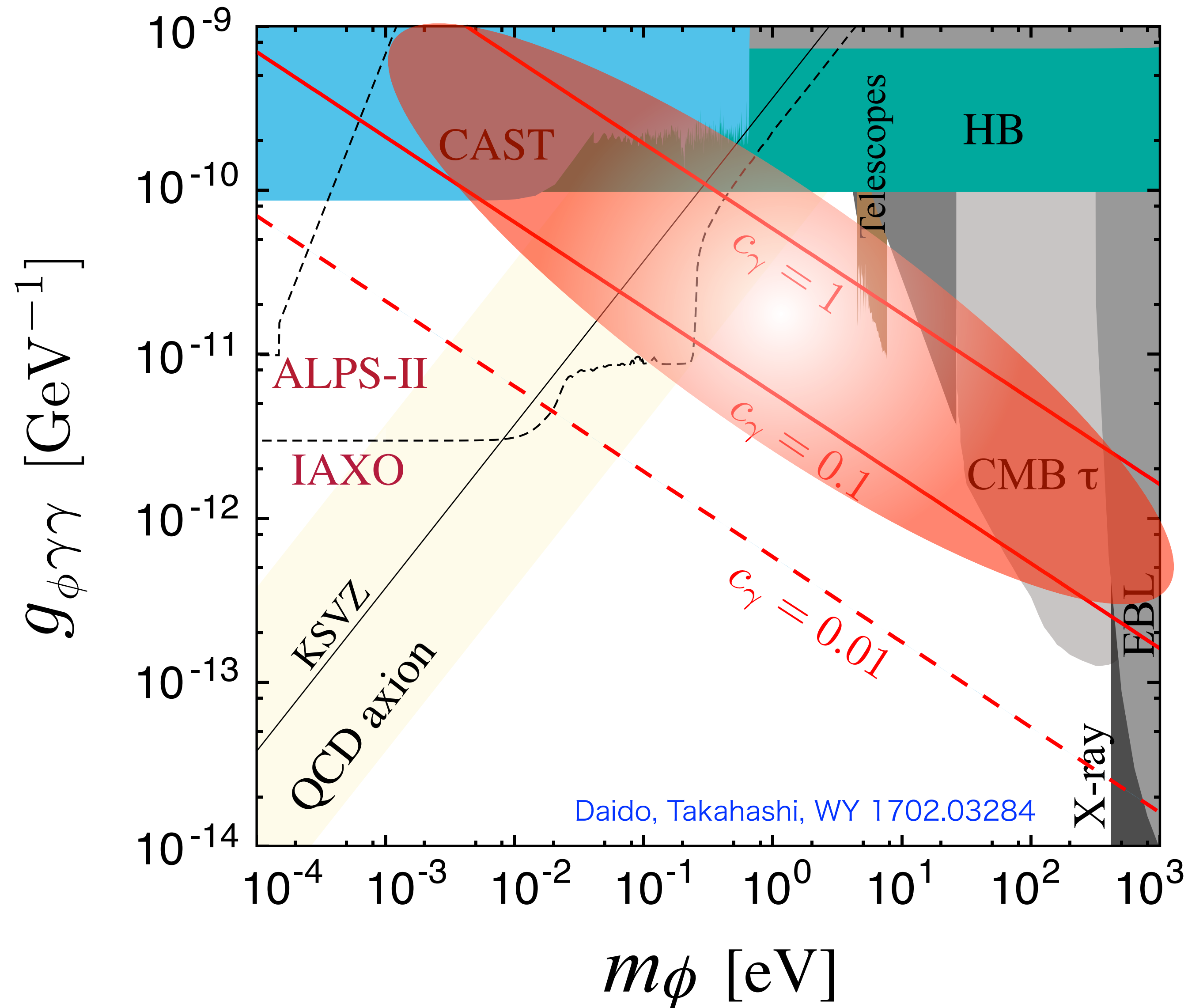


$$m_\phi = O(0.1 - 1)H_{\text{inf}} \sim 10^{-6} \frac{f_\phi^2}{M_{\text{pl}}}$$

→ sub-eV or eV-scale ALP DM candidate.

ALP(axion coupled to photon)=inflaton

$$\mathcal{L} = \frac{g_{\phi\gamma\gamma}}{4} \phi F_{\mu\nu} \tilde{F}^{\mu\nu} \quad g_{\phi\gamma\gamma} = \frac{c_\gamma \alpha}{\pi f}$$



$$m_\phi = O(0.1 - 1)H_{\text{inf}} \sim 10^{-6} \frac{f_\phi^2}{M_{\text{pl}}}$$

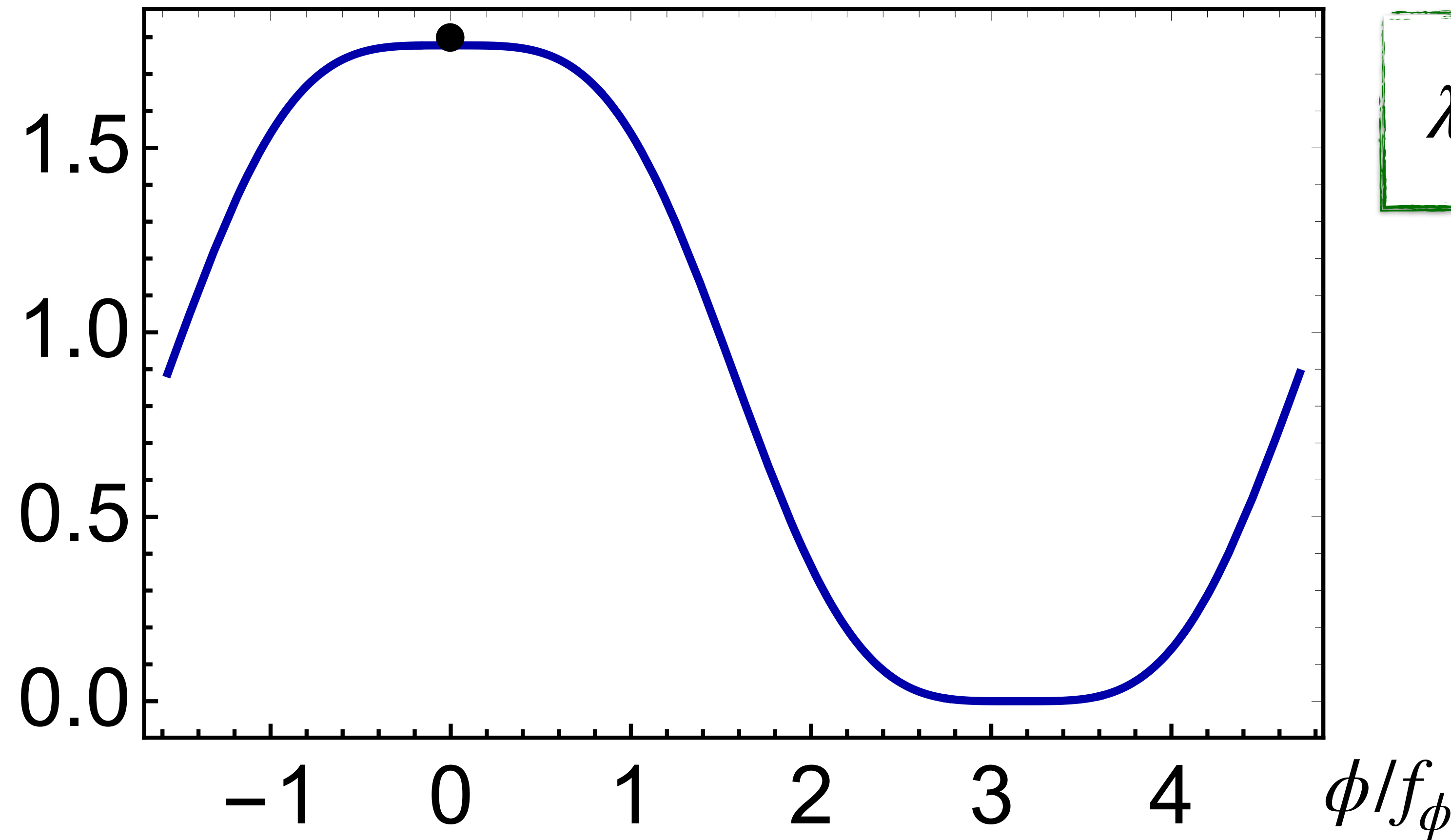
Successful
inflation

→ sub-eV or eV-scale
ALP DM candidate.

Inflaton decays due to large effective mass

Just after inflation, ϕ acquires an effective mass

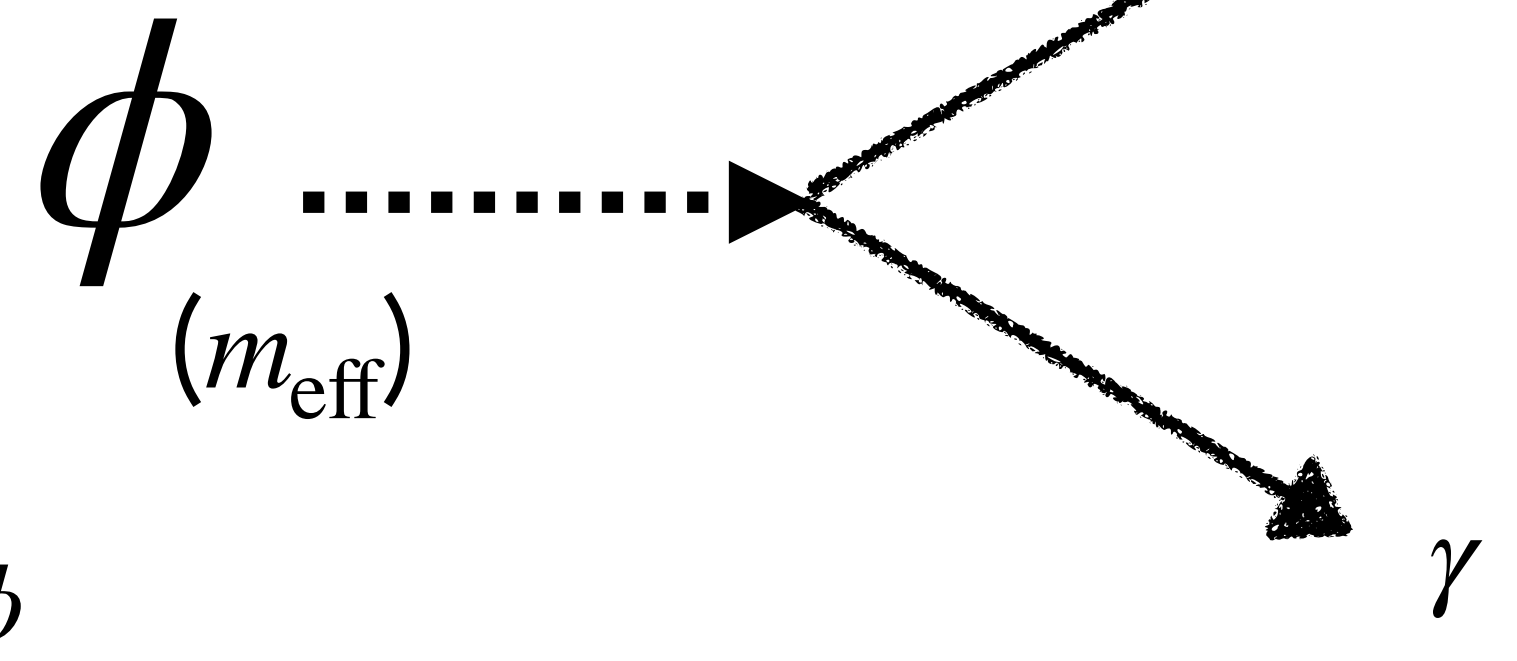
$$m_{\text{eff}} \sim \sqrt{\lambda} \phi_{\text{amp}} \sim 10 \text{ GeV} \left(\frac{\phi_{\text{amp}}}{10^7 \text{ GeV}} \right).$$



$$\lambda(\text{self-coupling}) \sim 10^{-12}$$

$$\Gamma_{\phi \rightarrow \gamma\gamma} |_{\text{reheating}}$$

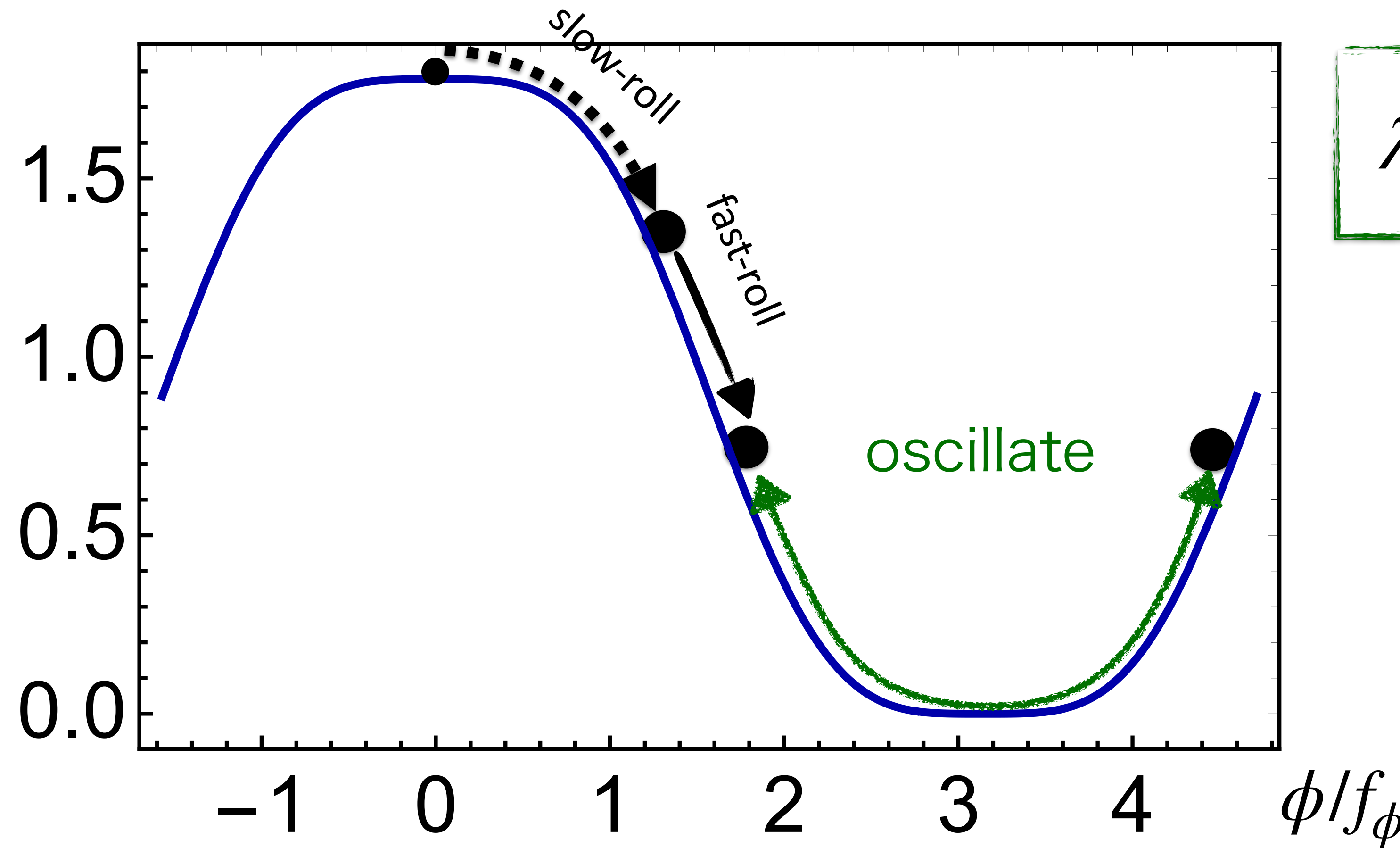
$$\left(\sim 10^{33} \left(\frac{10^7 \text{ GeV}}{f_\phi} \right)^3 \Gamma_{\phi \rightarrow \gamma\gamma} |_{\text{vacuum}} \right)$$



Inflaton decays due to large effective mass

Just after inflation, ϕ acquires an effective mass

$$m_{\text{eff}} \sim \sqrt{\lambda} \phi_{\text{amp}} \sim 10 \text{ GeV} \left(\frac{\phi_{\text{amp}}}{10^7 \text{ GeV}} \right).$$



$$\lambda(\text{self-coupling}) \sim 10^{-12}$$

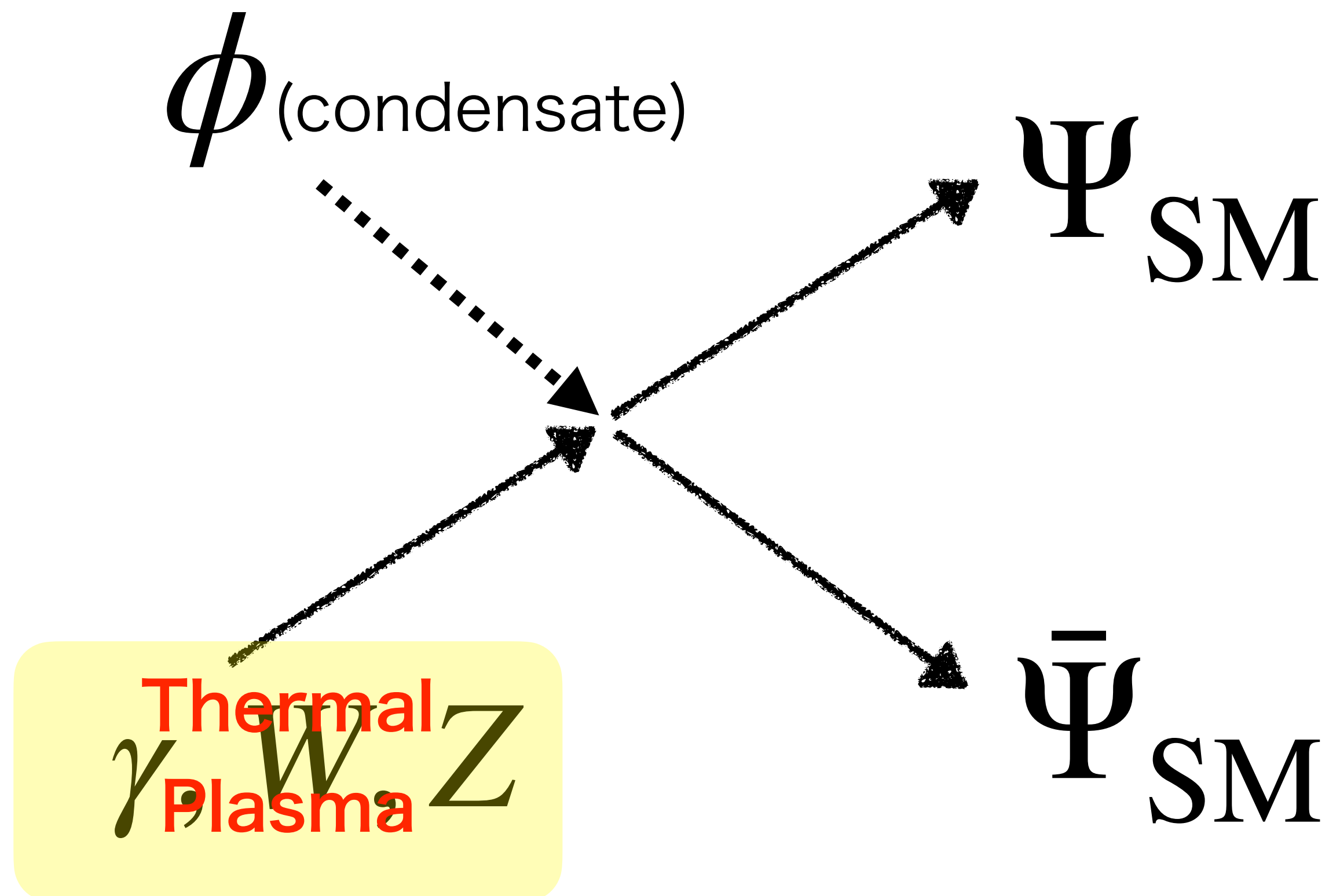
$$\Gamma_{\phi \rightarrow \gamma\gamma} \Big|_{\text{reheating}} \left(\sim 10^{33} \left(\frac{10^7 \text{ GeV}}{f_\phi} \right)^3 \Gamma_{\phi \rightarrow \gamma\gamma} \Big|_{\text{vacuum}} \right)$$

The diagram illustrates the decay of the inflaton ϕ into two photons γ . A horizontal dashed arrow labeled ϕ (m_{eff}) points to a vertex. From this vertex, two diagonal arrows point downwards and outwards, labeled γ .

Cold ALP DM from incomplete reheating.

Reheating proceeds due to thermal scattering when $eT \gtrsim m_{\text{eff}}$.

Dissipation effect for reheating

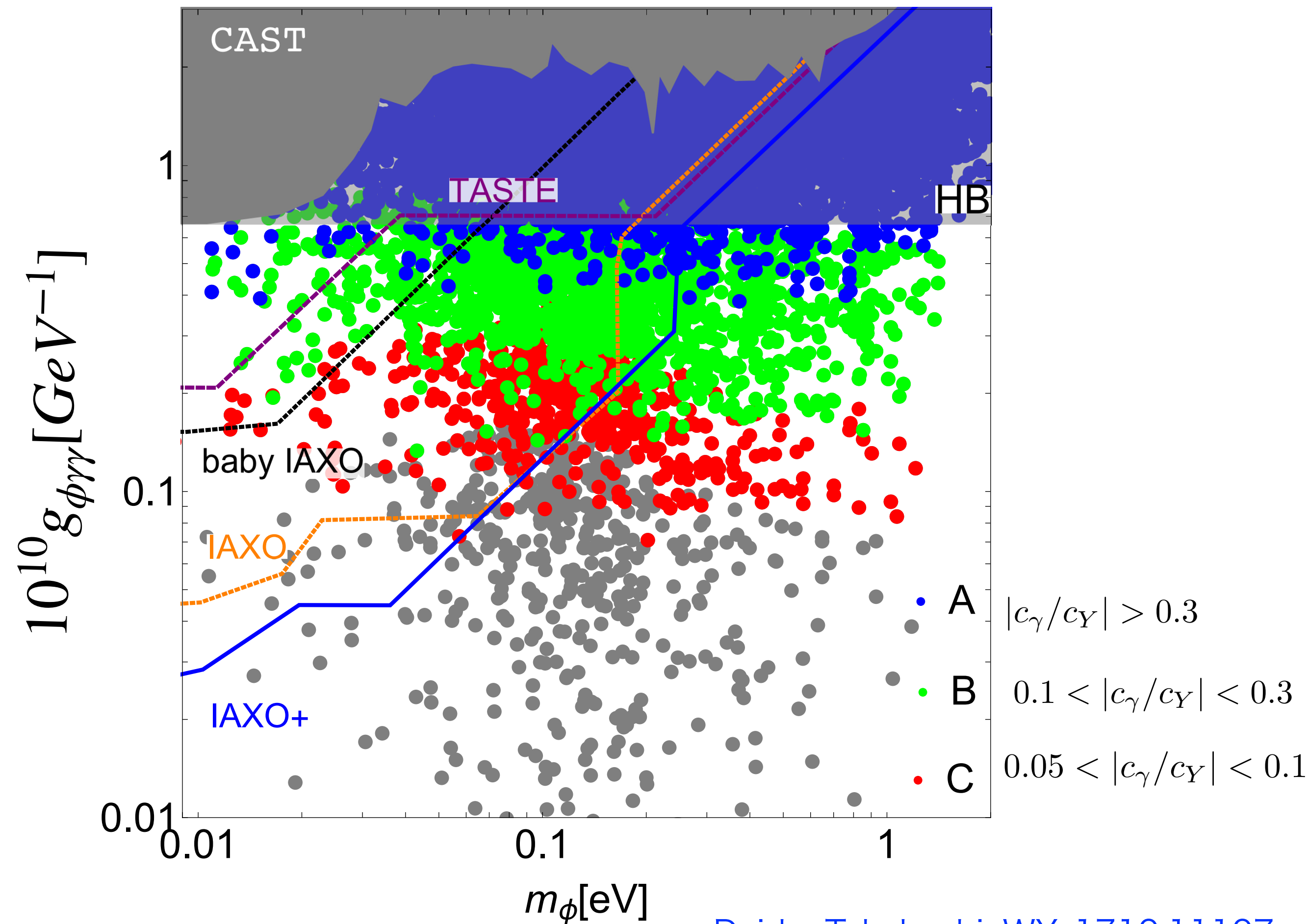


$$\Gamma_{\text{dis},\gamma} = C \frac{c_\gamma^2 \alpha^2 T^3}{8\pi^2 f^2} \frac{m_{\text{eff}}^2}{e^4 T^2}$$

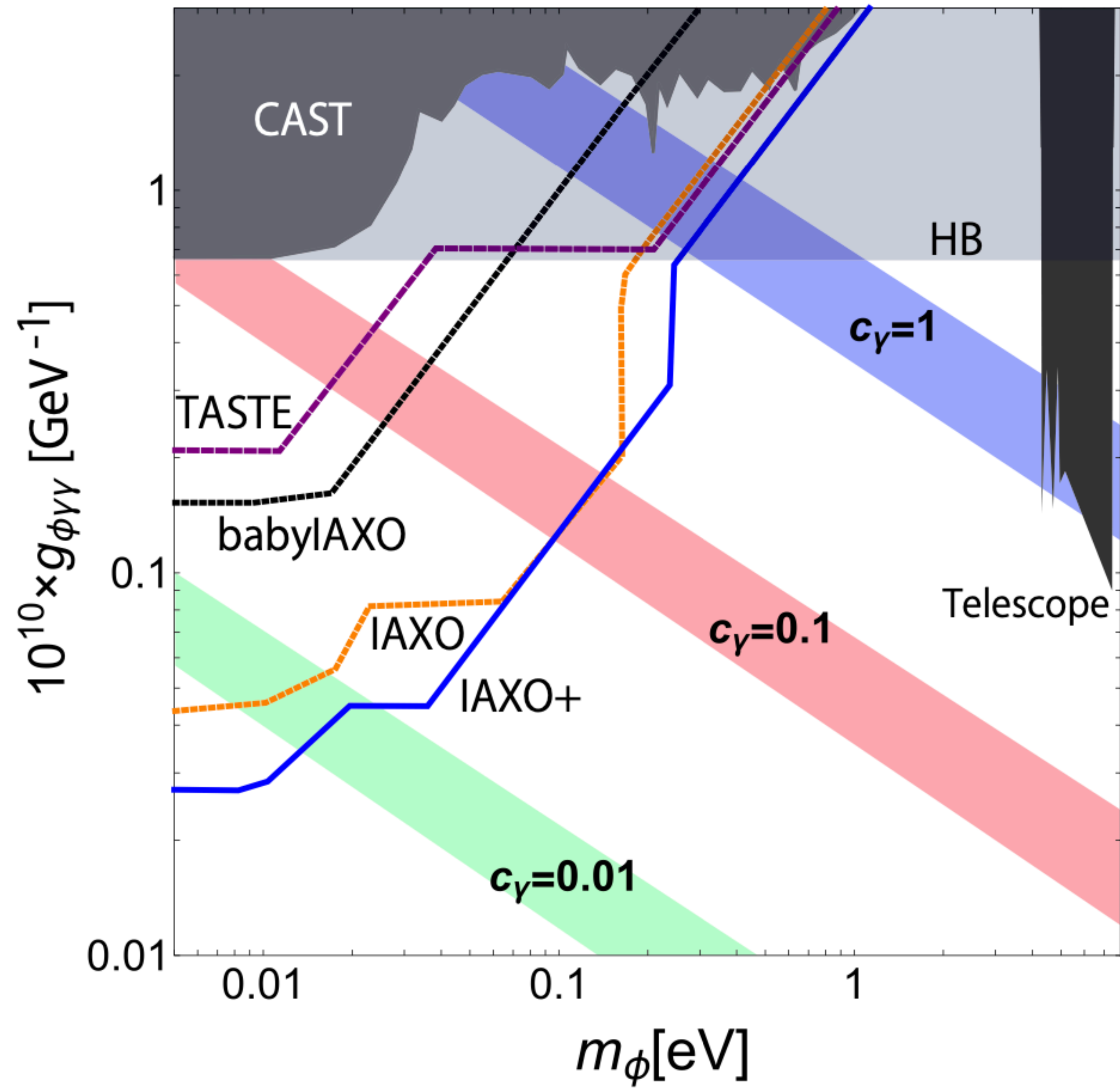
Moroi, Mukaida, Nakayama and Takimoto, 1407.7465;

C=O(10) to take account of self-resonance, Lozanov, and Amin, 1710.06851;

Imposing $\Omega_\phi^{(\text{remnant})} h^2 \sim \Omega_{\text{DM}} h^2$ we obtain

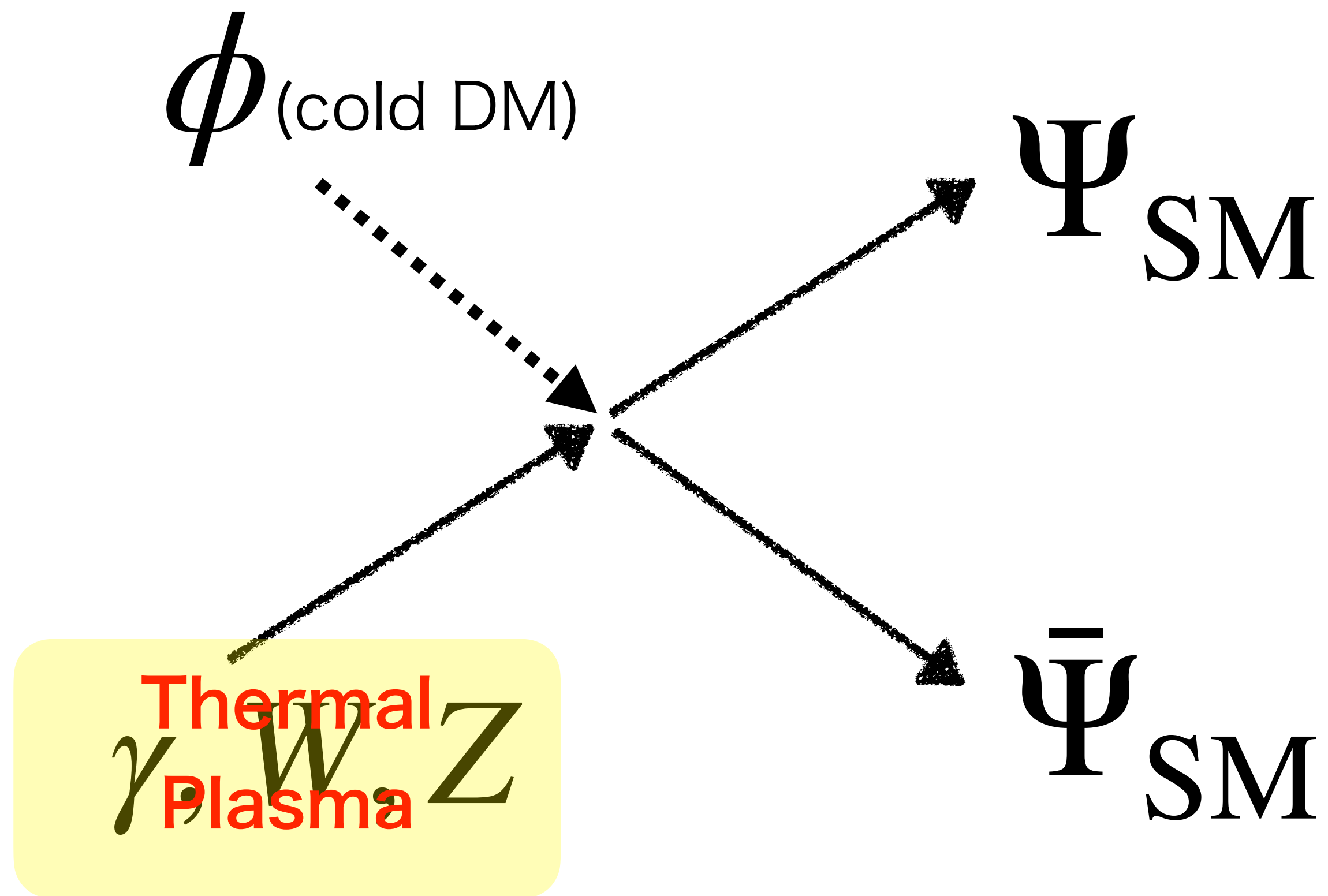


Daido, Takahashi, WY, 1710.11107

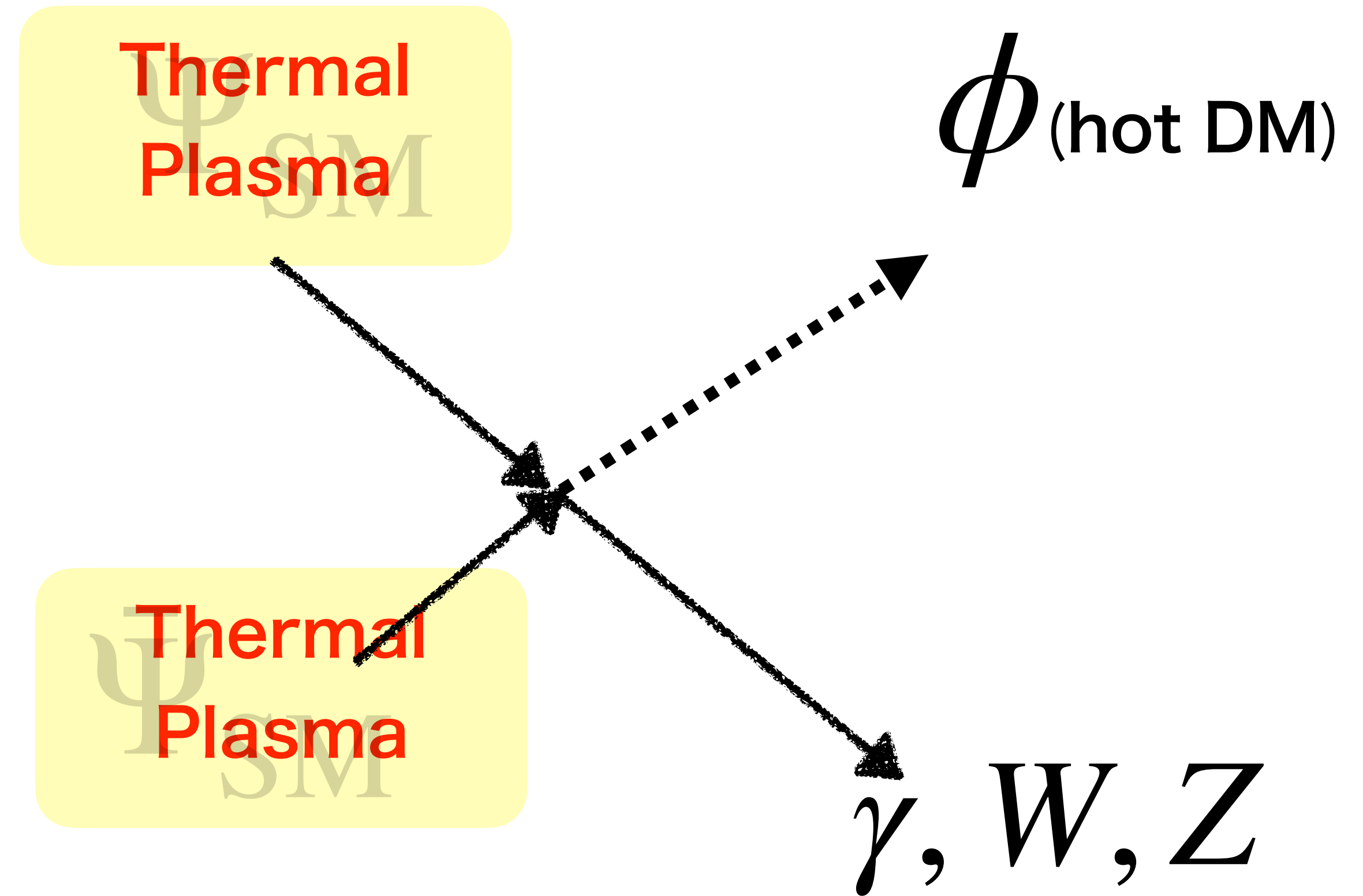


Successful reheating means two typical momenta of DM.

Dissipation effect for reheating

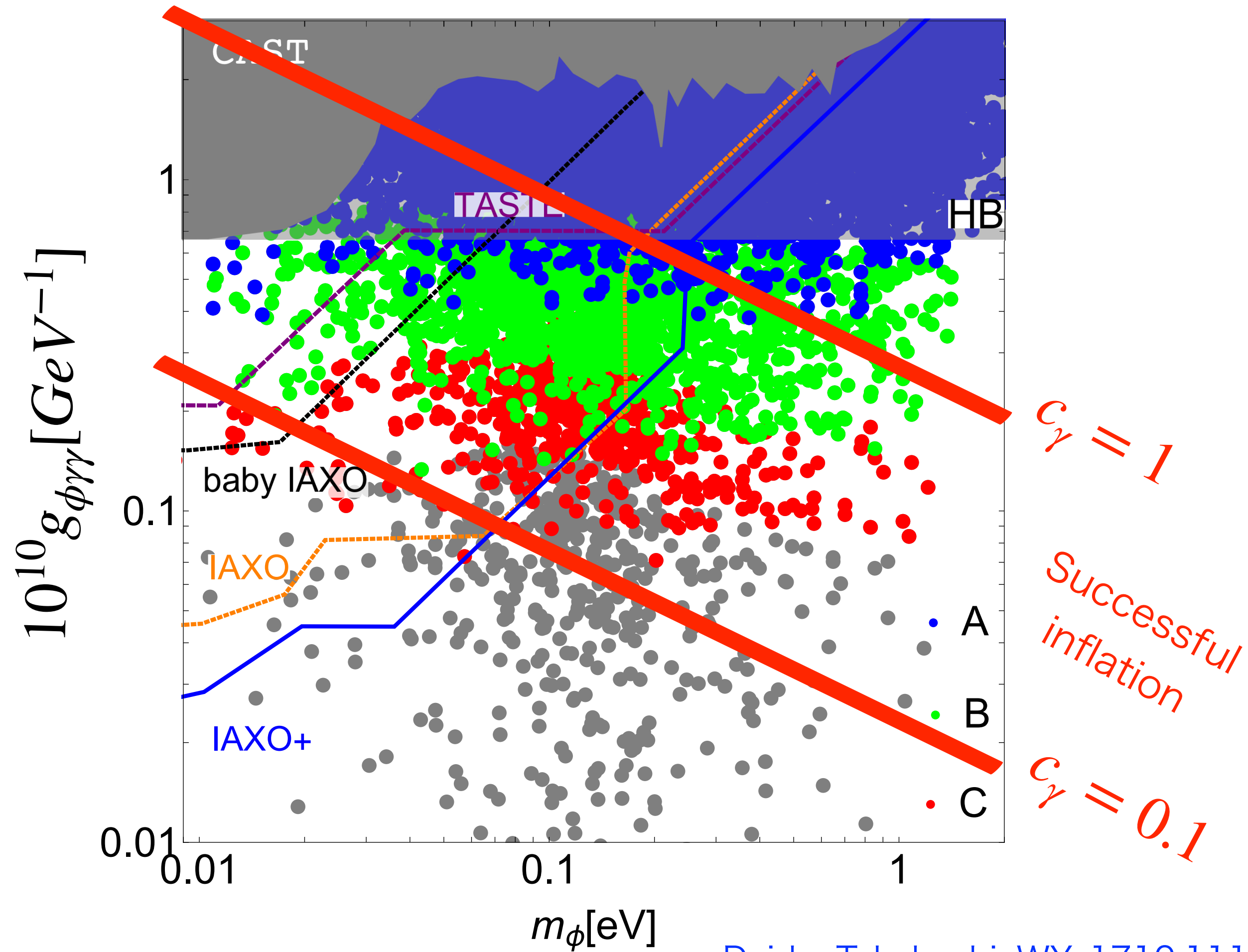


Thermal production of hot DM



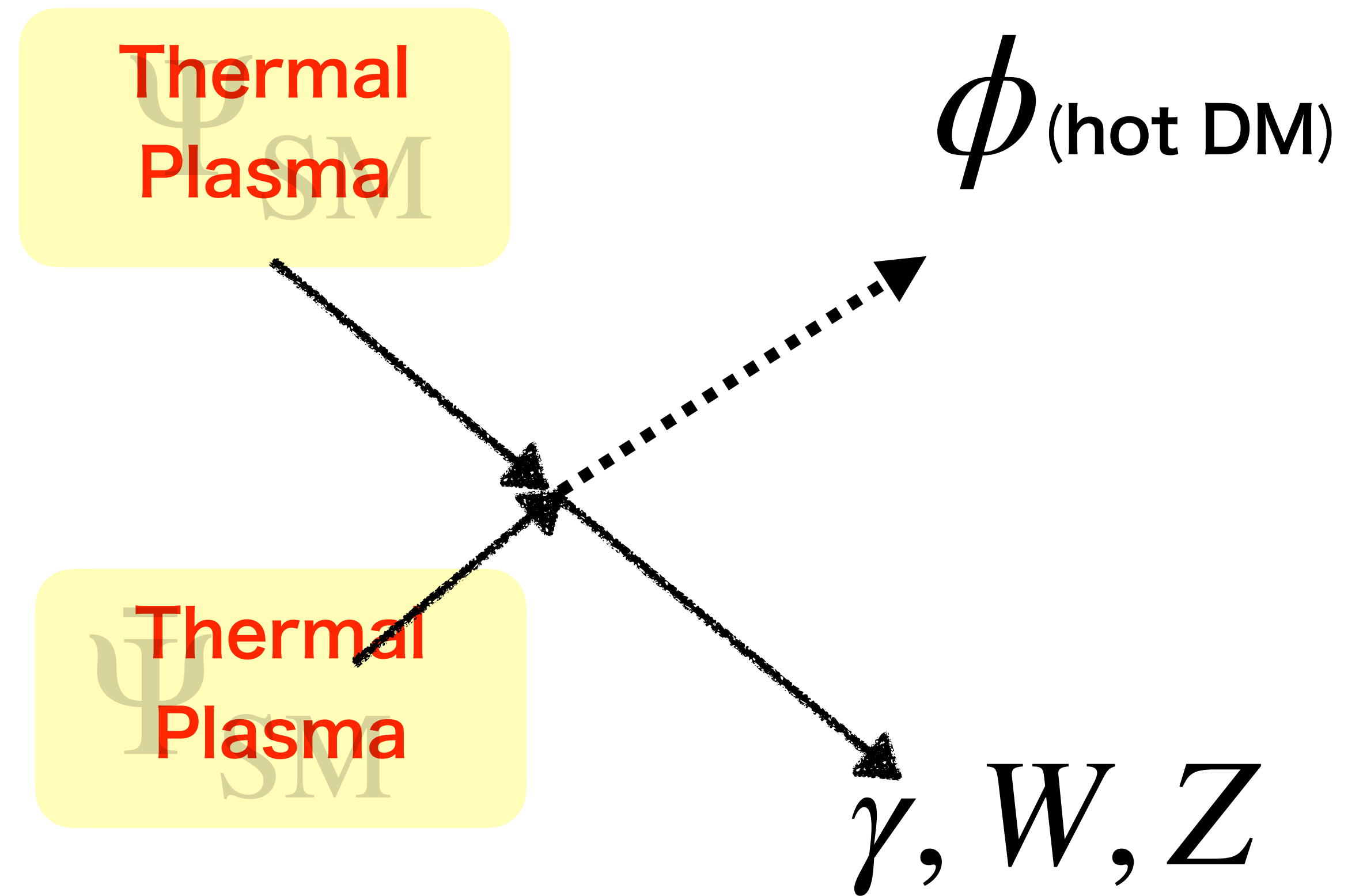
DM components: Cold ALP condensate + hot ALP with $\Delta N_{\text{eff}} \sim 0.03$

Hot DM bound: $m_\phi \lesssim 1 \text{ eV}$

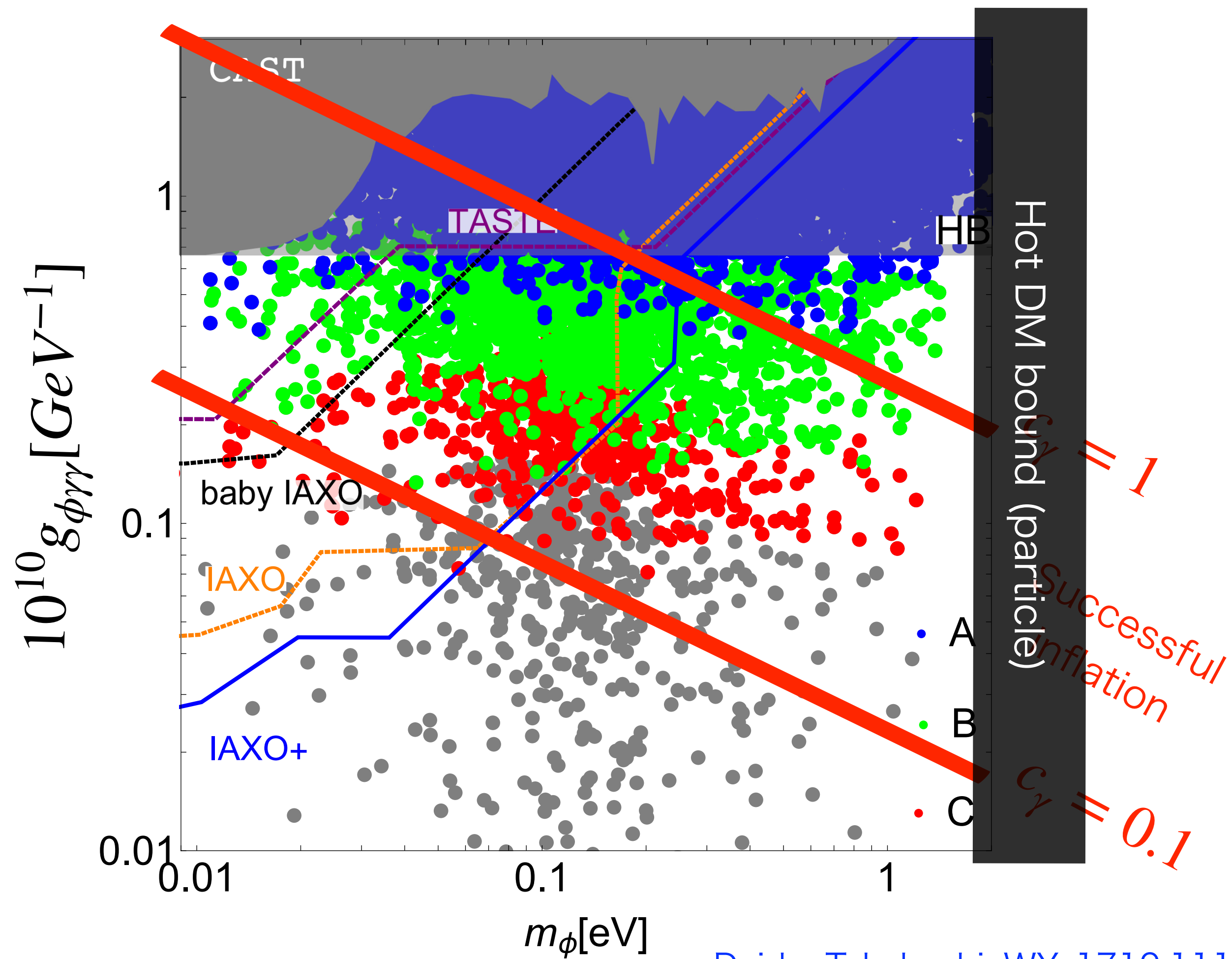


Daido, Takahashi, WY, 1710.11107

Thermal production of hot DM

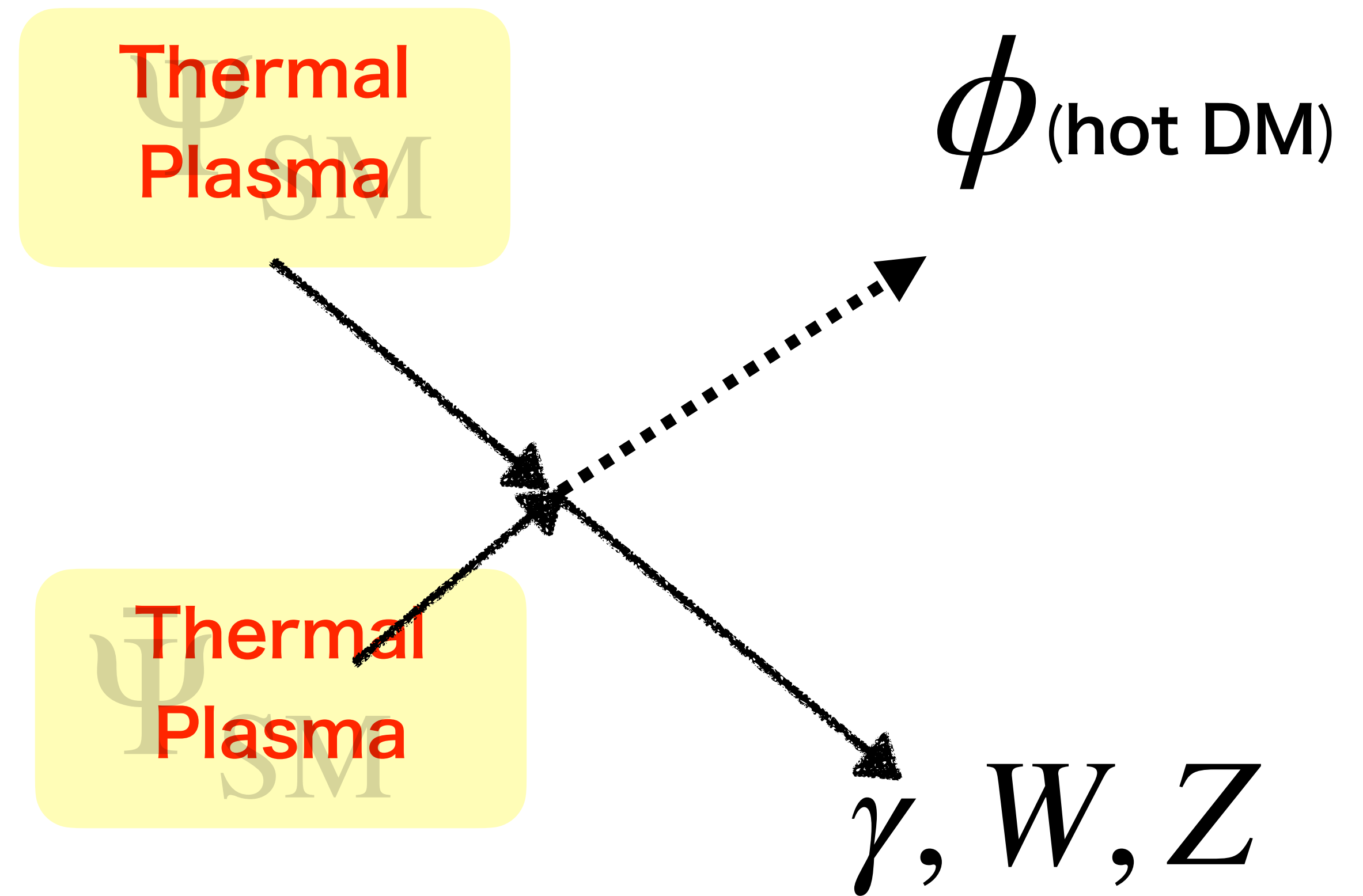


Hot DM bound: $m_\phi \lesssim 1 \text{ eV}$

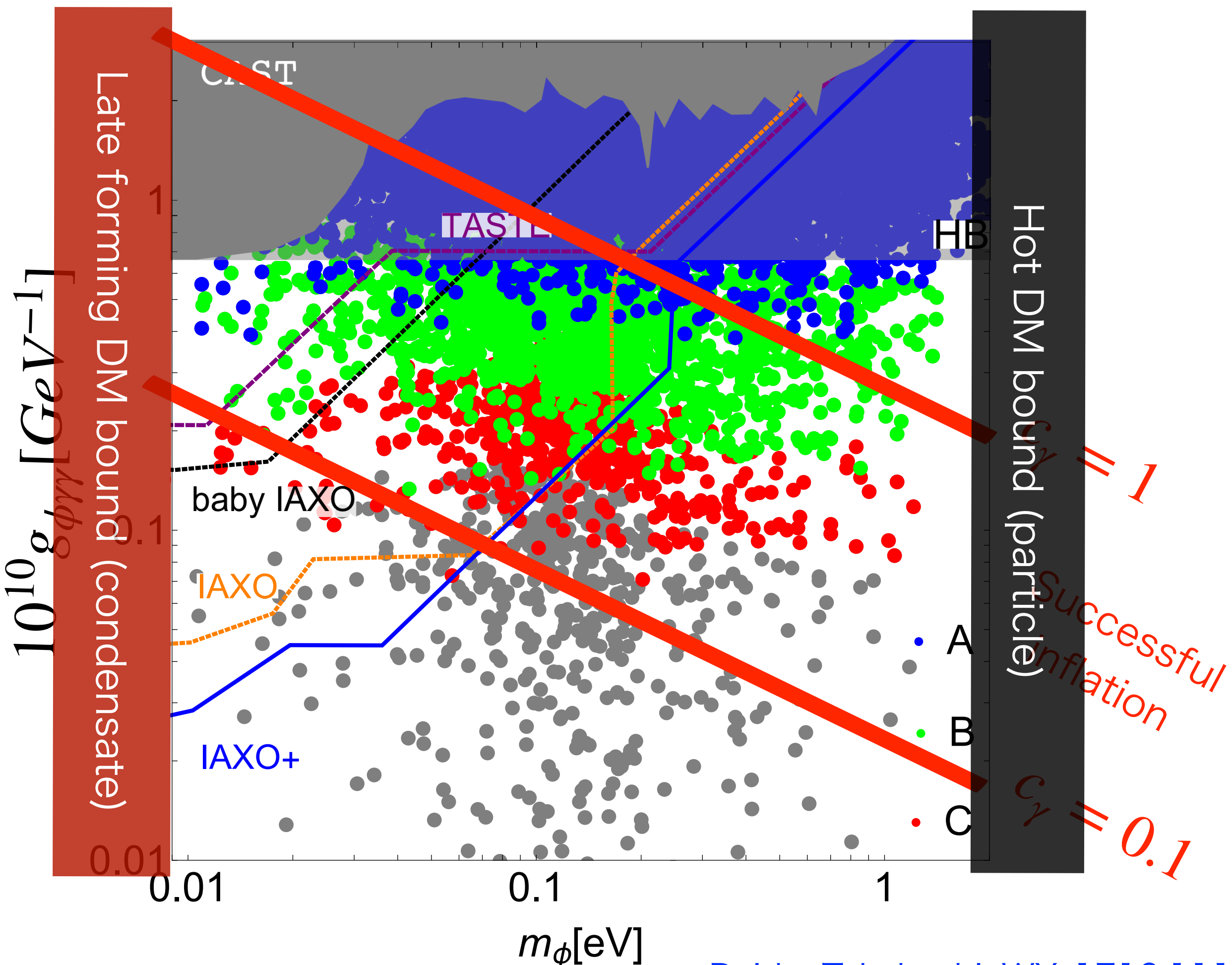


Daido, Takahashi, WY, 1710.11107

Thermal production of hot DM

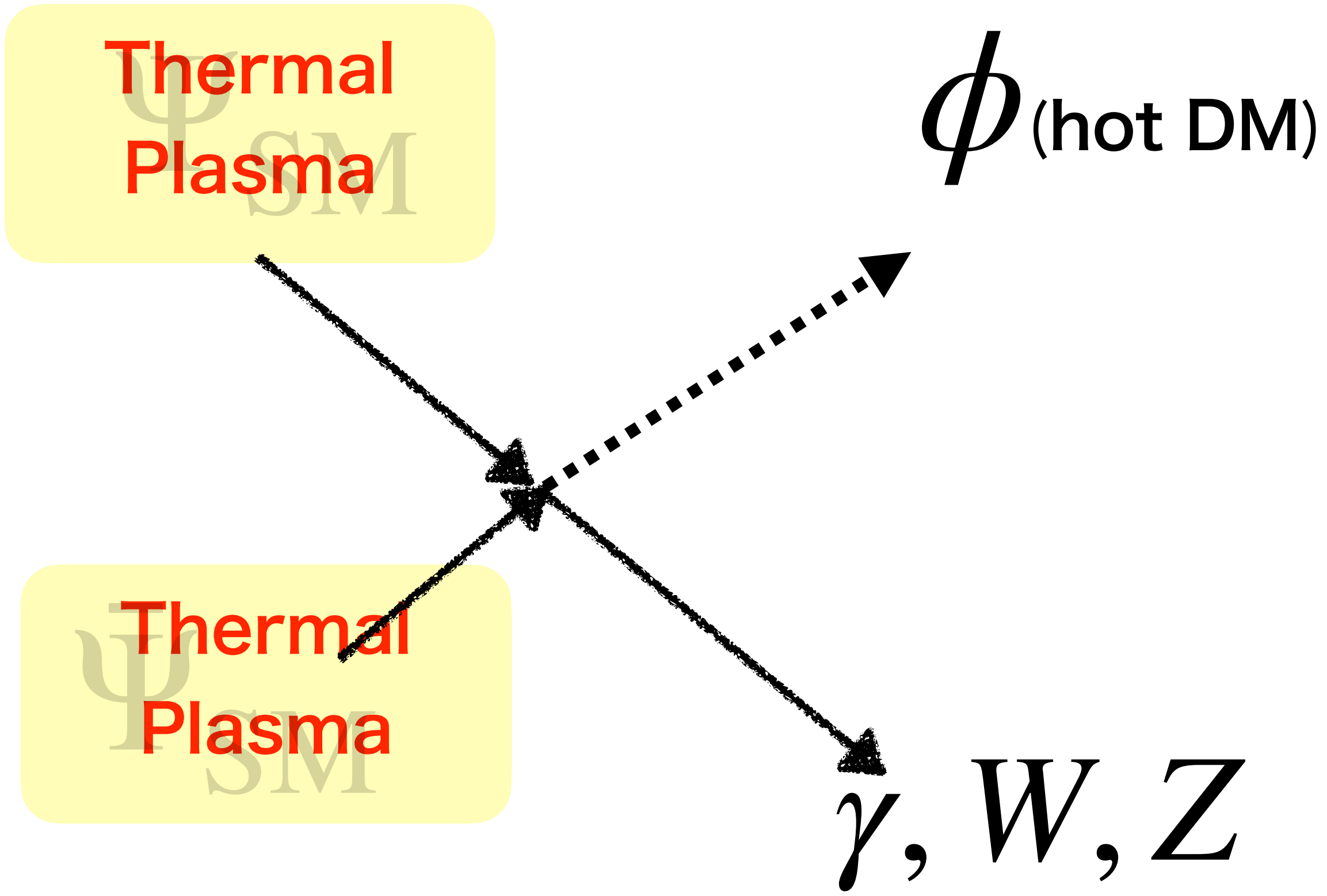


Hot DM bound: $m_\phi \lesssim 1 \text{ eV}$



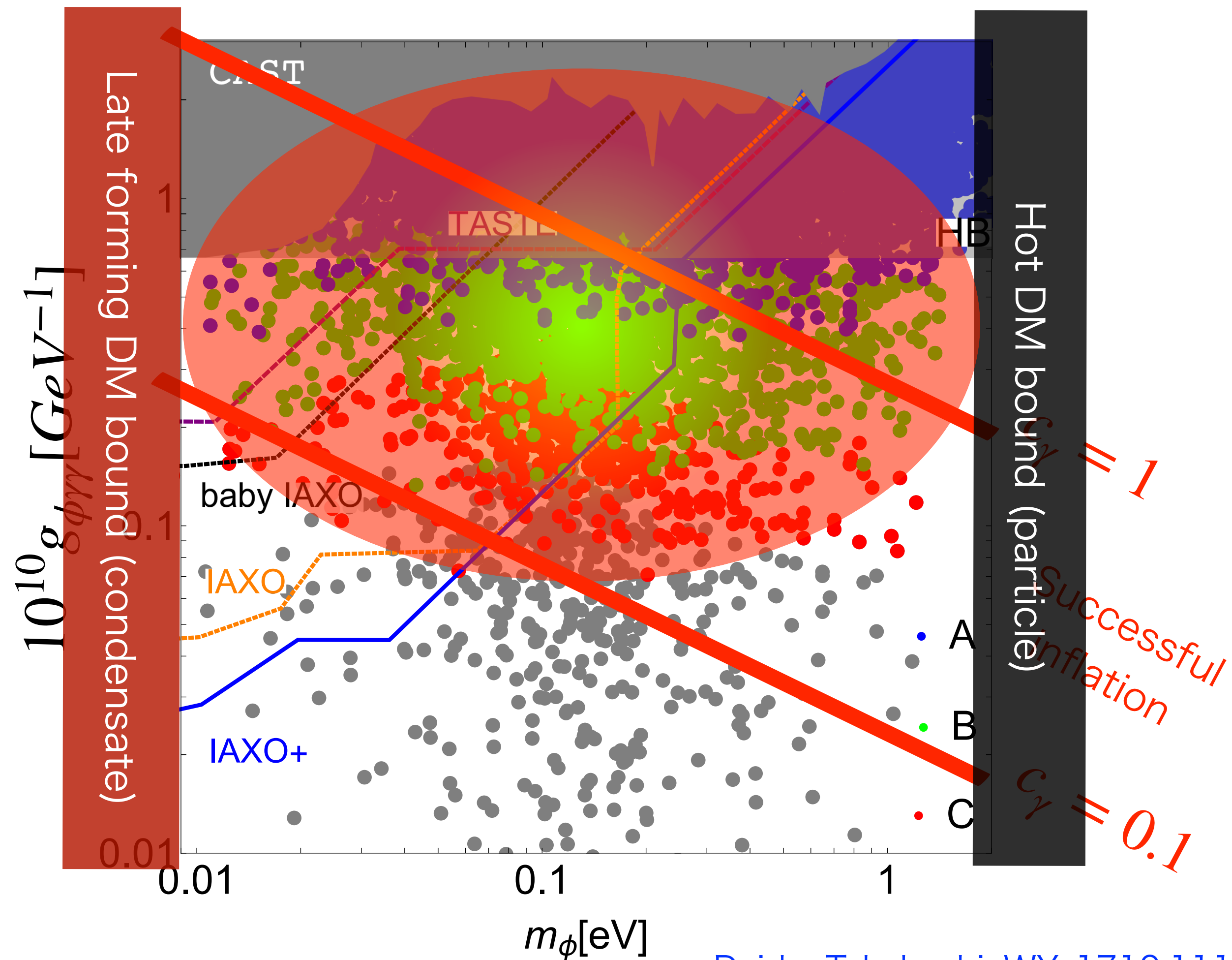
Daido, Takahashi, WY, 1710.11107

Thermal production of hot DM

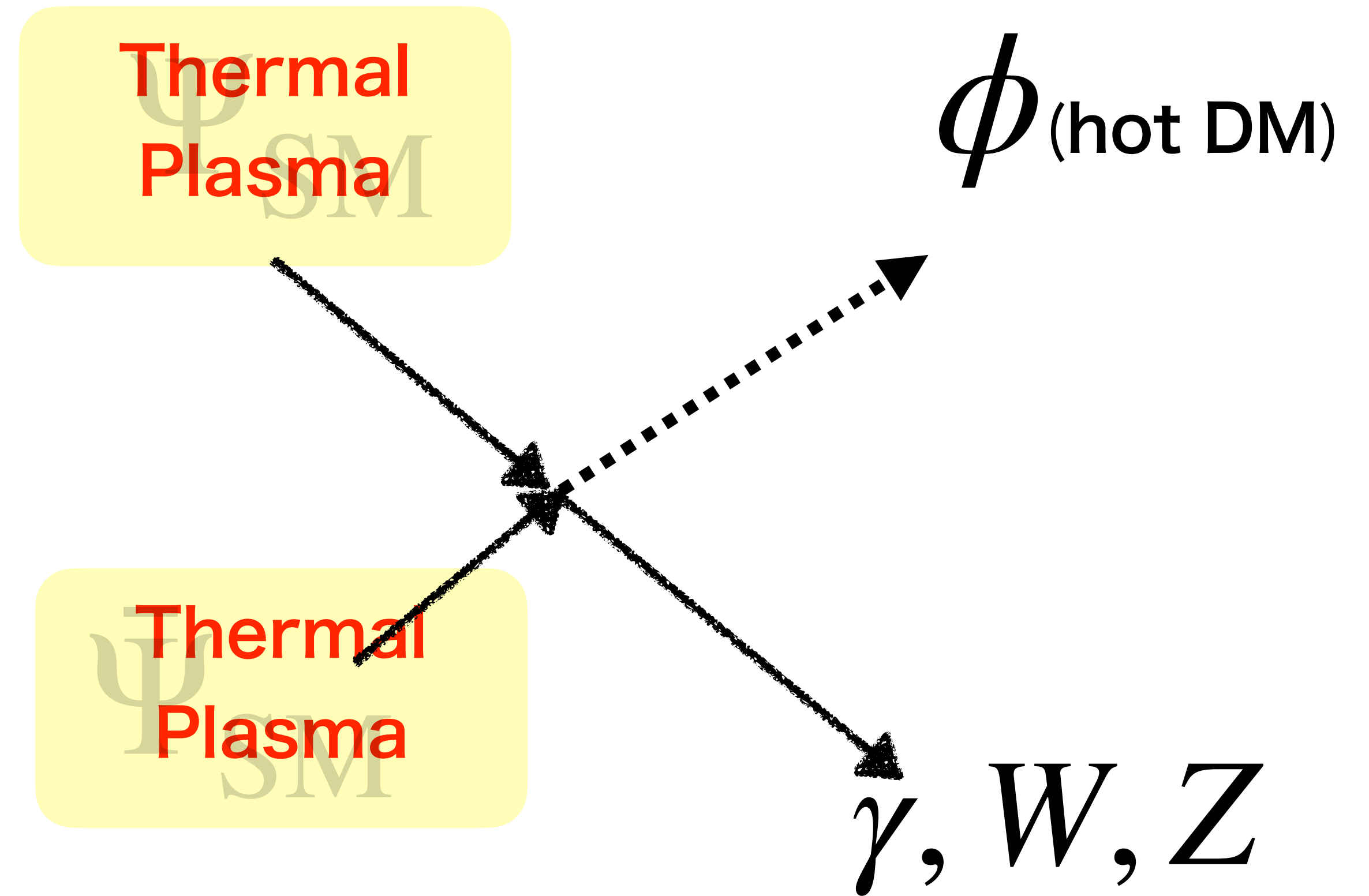


Hot DM bound: $m_\phi \lesssim 1 \text{ eV}$

Several independent conditions point to the region!



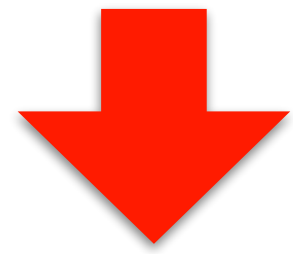
Thermal production of hot DM



“The ALP miracle”.

Daido, Takahashi, WY 1702.03284,1710.11107

Inflaton = DM = ALP



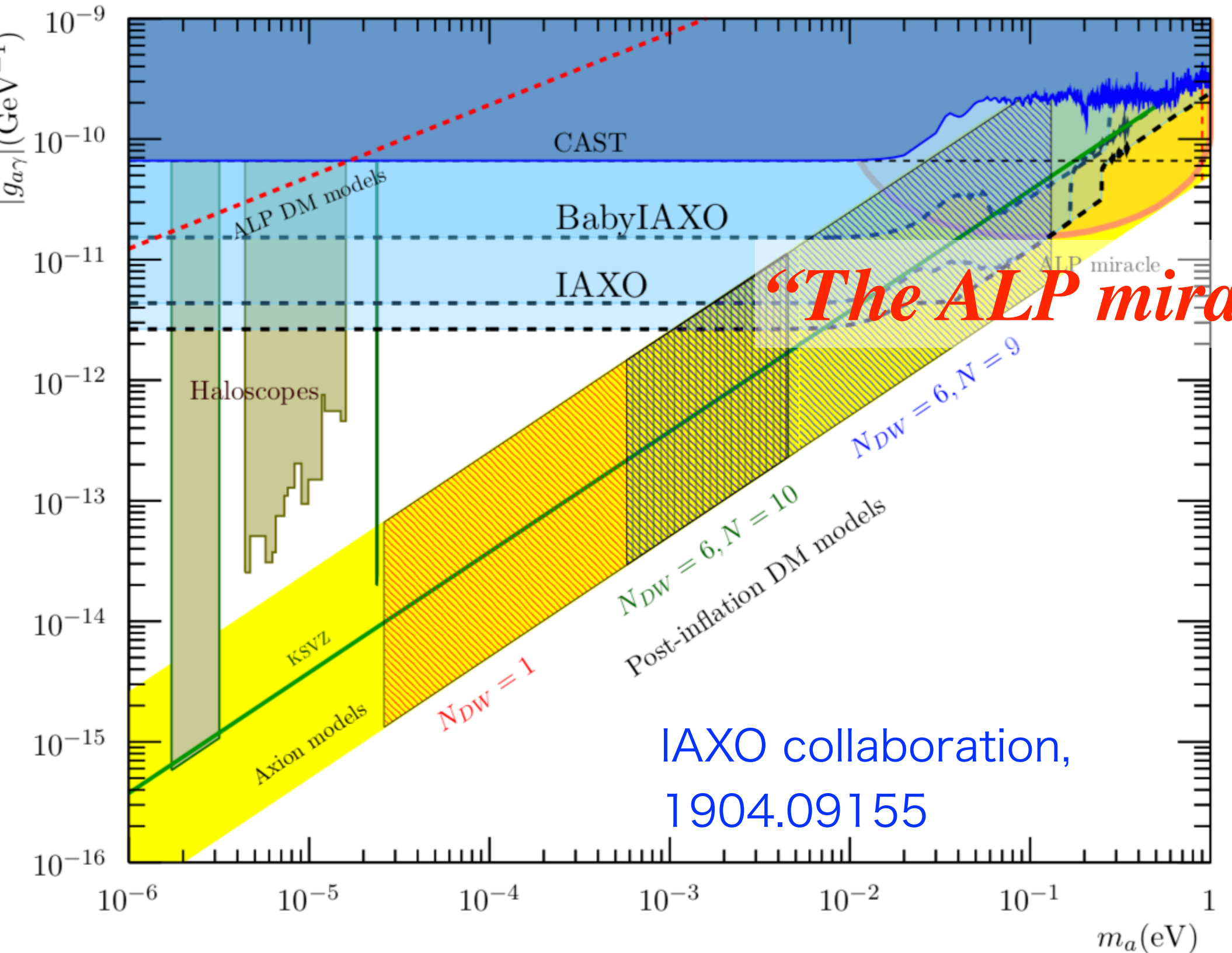
$$0.01 \text{ eV} \lesssim m_\phi \lesssim 1 \text{ eV}$$

$$g_{\phi\gamma\gamma} \gtrsim 10^{-11} \text{ GeV}^{-1}$$

significantly overlapping with future reach of axion helioscopes, IAXO/TASTE.

- $\Delta N_{\text{eff}} \approx 0.03$ probed in the future CMB and BAO experiments.
- Overlapping with cooling hint of HB stars.
- O(1) eV ALP with $g_{\phi\gamma\gamma} \sim 10^{-10} \text{ GeV}^{-1}$ is hinted by EBL analysis

Ayala, Dominguez, Giannotti, Mirizzi and Straniero, 1406.6053, DESY- PROC-2015-02

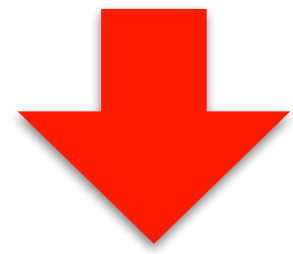


Korochkin et al, 1911.13291

“The ALP miracle”.

Daido, Takahashi, WY 1702.03284,1710.11107

Inflaton = DM = ALP



$$0.01 \text{ eV} \lesssim m_\phi \lesssim 1 \text{ eV}$$

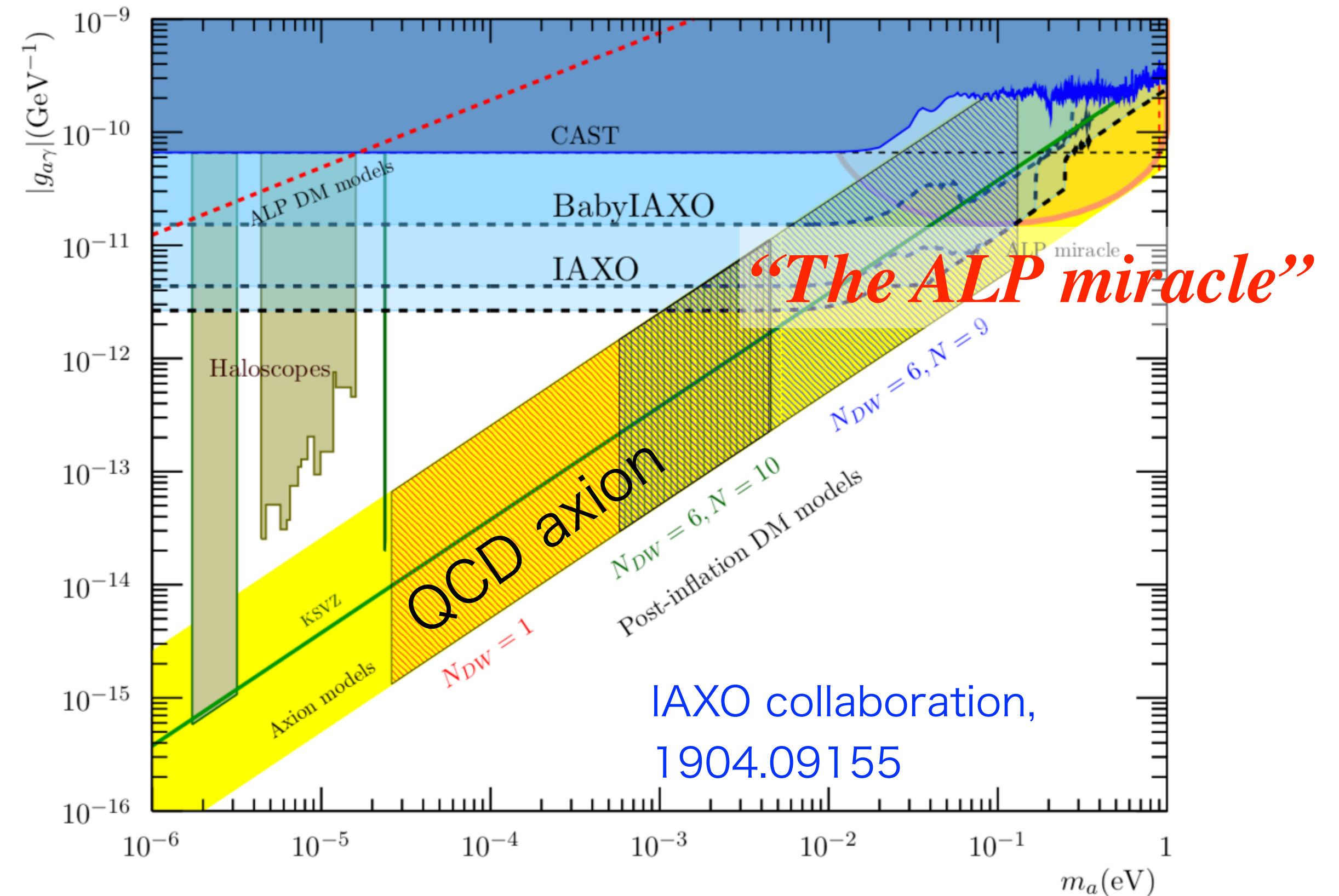
$$g_{\phi\gamma\gamma} \gtrsim 10^{-11} \text{ GeV}^{-1}$$

significantly overlapping with future reach of axion helioscopes, IAXO/TASTE.

- $\Delta N_{\text{eff}} \approx 0.03$ probed in the future CMB and BAO experiments.
- Overlapping with cooling hint of HB stars.
- O(1) eV ALP with $g_{\phi\gamma\gamma} \sim 10^{-10} \text{ GeV}^{-1}$ is hinted by EBL analysis

Ayala, Dominguez, Giannotti, Mirizzi and Straniero, 1406.6053, DESY- PROC-2015-02

Korochkin et al,1911.13291

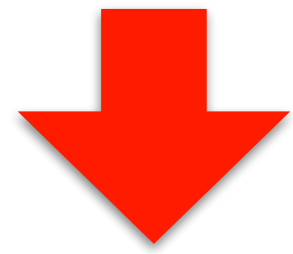


★ Is the ALP relevant to the strong CP problem?

“The ALP miracle”.

Daido, Takahashi, WY 1702.03284, 1710.11107

Inflaton = DM = ALP



$$0.01 \text{ eV} \lesssim m_\phi \lesssim 1 \text{ eV}$$

$$g_{\phi\gamma\gamma} \gtrsim 10^{-11} \text{ GeV}^{-1}$$

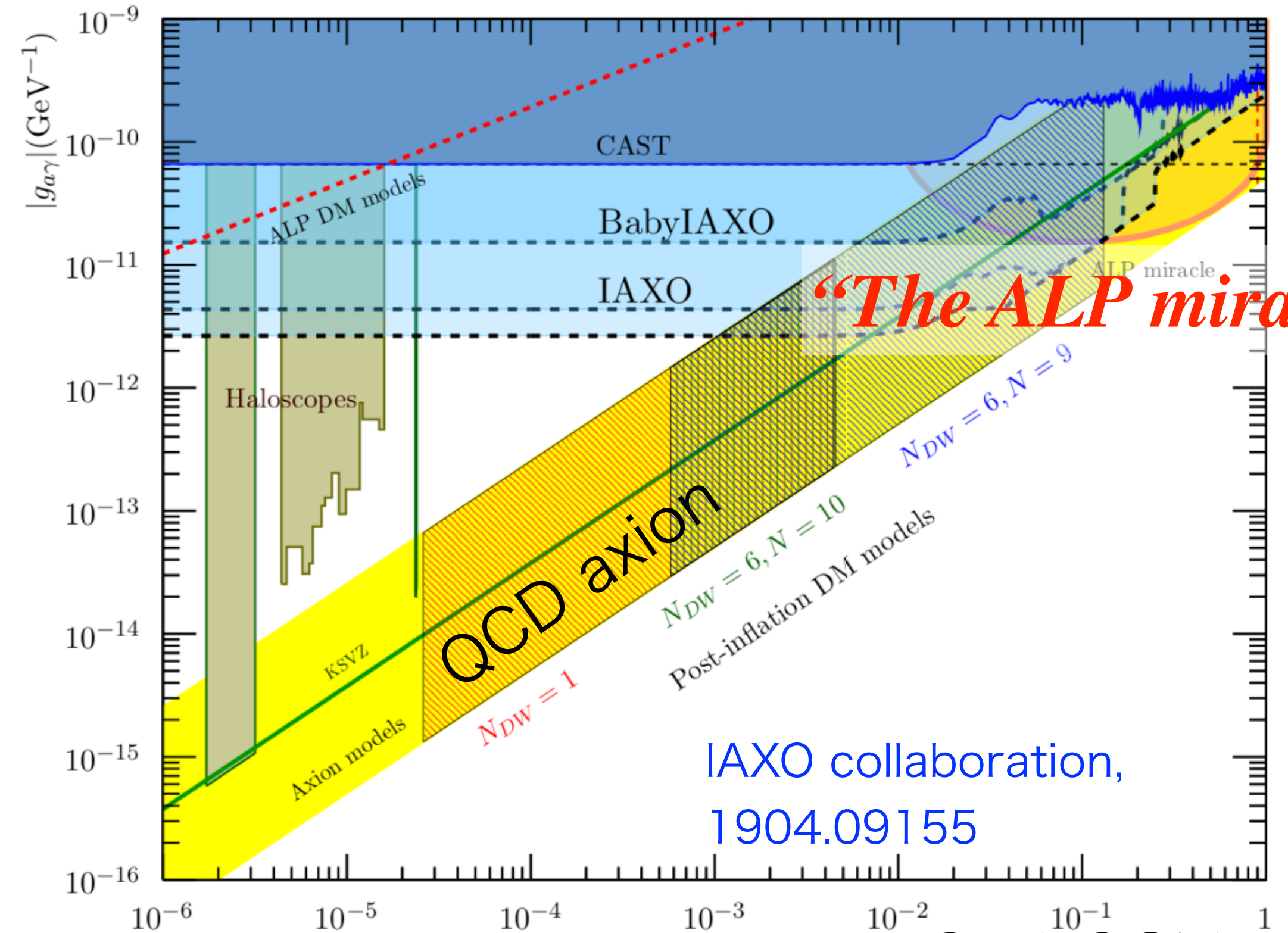
significantly overlapping with future reach of axion helioscopes, IAXO/TASTE.

- $\Delta N_{\text{eff}} \approx 0.03$ probed in the future CMB and BAO experiments.
- Overlapping with cooling hint of HB stars.
- O(1) eV ALP with $g_{\phi\gamma\gamma} \sim 10^{-10} \text{ GeV}^{-1}$ is hinted by EBL analysis

Ayala, Dominguez, Giannotti, Mirizzi and Straniero, 1406.6053, DESY-PROC-2015-02

Korochkin et al, 1911.13291

★ Is the ALP relevant to the strong CP problem?



“The ALP miracle”

SN1987A,
NS bounds:

$$f_\phi > 10^{8-9} \text{ GeV}$$

ALP miracle:

$$f_\phi \sim 10^7 \text{ GeV}$$

Comparison of usual hot DM and burst production in $\chi_1 \leftrightarrow \phi\chi_2$ system

WY 2301.08735

Hot DM paradigm (-1984):

Burst production of DM

$$\cdot \left(\frac{T}{M_1}\right)^3 \Gamma_{\chi_1 \rightarrow \chi_2 \phi}^{(\text{proper})} > \frac{M_1}{T} \Gamma_{\chi_1 \rightarrow \chi_2 \phi}^{(\text{proper})} > H \text{ for } T > M_1$$

$\cdot n_\phi \sim T^3$ from **thermal equilibrium**

\Rightarrow **eV mass** for DM abundance

\cdot Comoving momentum is

$$p_{\text{com}} \sim a_{\text{prod}} T_{\text{prod}}$$

\Rightarrow **hot**

$$\cdot \left(\frac{T}{M_1}\right)^3 \Gamma_{\chi_1 \rightarrow \chi_2 \phi}^{(\text{proper})} > H > \frac{M_1}{T} \Gamma_{\chi_1 \rightarrow \chi_2 \phi}^{(\text{proper})} @ \text{ a period}$$

$\cdot n_\phi \sim T^3$ from **quasi-equilibrium** of

bose-enhancement dynamics

\Rightarrow **eV mass** for DM abundance

\cdot Comoving momentum is

$$p_{\text{com}} \sim a_{\text{prod}} M_1^2 / T_{\text{prod}}$$

\Rightarrow **cold**

Stage 3: Saturation (quasi-equilibrium)

The burst production stops due to the inverse decay when $f_{\chi_2}[p_{\chi_2} \sim T] \sim f_{\chi_1}[p_{\chi_1} \approx p_{\chi_2}]$, c.f. thermal equilibrium.

With $f_\phi[p \sim p_\phi^{\text{burst}}] \gg 1, f_{\chi_2}[p_{\chi_2} \sim T] \sim 1$

$$C^\phi = \frac{1}{2E_\phi g_\phi} \sum \int d\Pi_{\chi_1} d\Pi_{\chi_2}$$

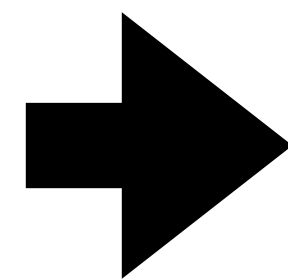
$$(2\pi)^4 \delta^4(p_{\chi_1} - p_\phi - p_{\chi_2}) \times |\mathcal{M}_{\chi_1 \rightarrow \chi_2 \phi}|^2$$

$$\times S(f_{\chi_1}[p_{\chi_1}], f_{\chi_2}[p_{\chi_2}], f_\phi[p_\phi])$$

$$S \equiv f_{\chi_1}[p_{\chi_1} \sim T](1 \pm f_{\chi_2}[p_{\chi_2} \sim T])(1 \mp f_\phi[p_\phi \sim p_\phi^{\text{burst}}])$$

$$-(1 \pm f_{\chi_1}[p_{\chi_1} \sim T])f_\phi[p_\phi \sim p_\phi^{\text{burst}}]f_{\chi_2}[p_{\chi_2} \sim T]$$

$$\sim (f_{\chi_1}[p_{\chi_1} \sim T] - f_{\chi_2}[p_{\chi_2} \sim T])f_\phi[p_\phi \sim p_\phi^{\text{burst}}]$$



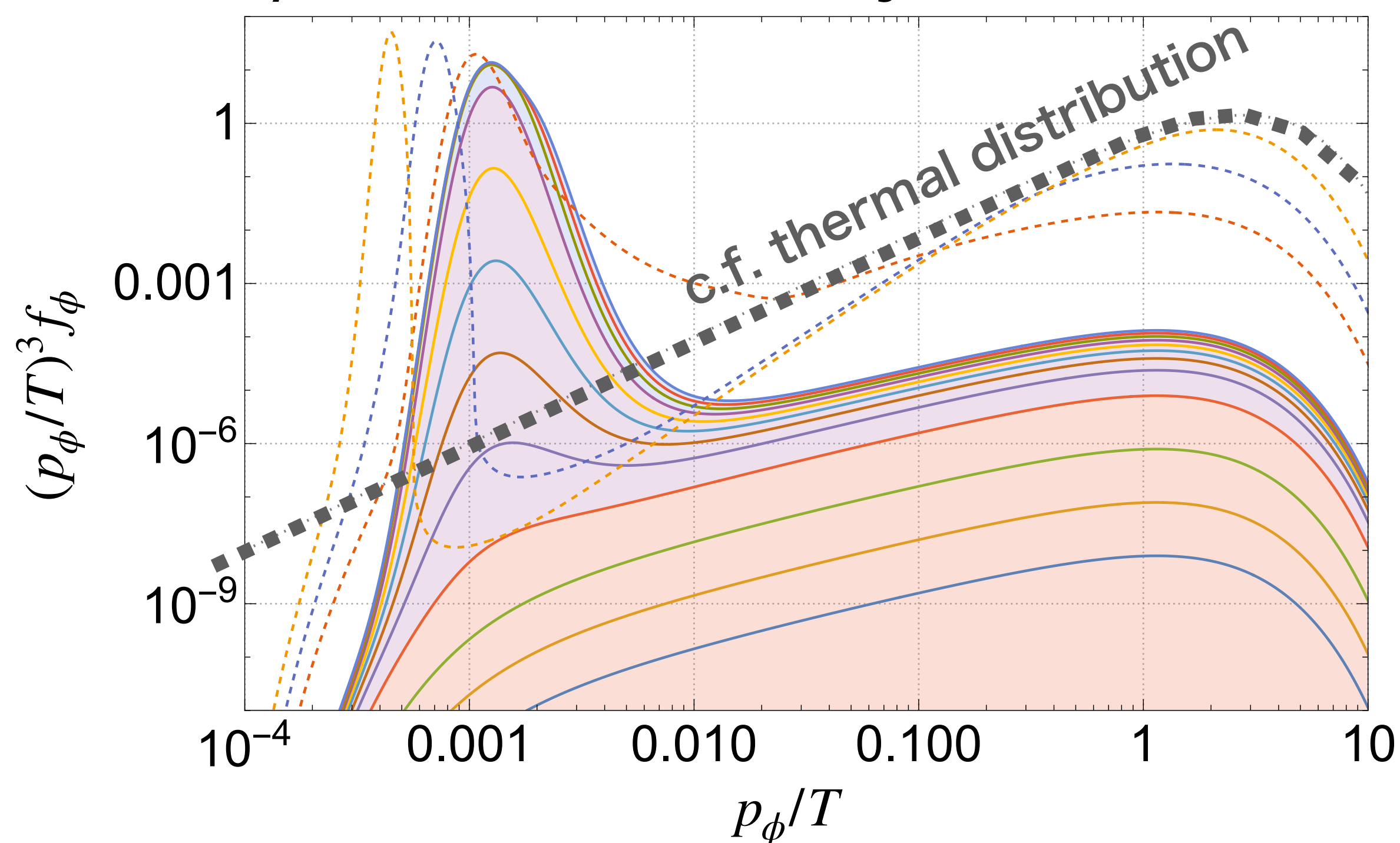
$$\dot{f}_\phi[p_\phi \sim p_\phi^{\text{burst}}] \sim 0$$

Stage 3: Saturation (quasi-equilibrium)

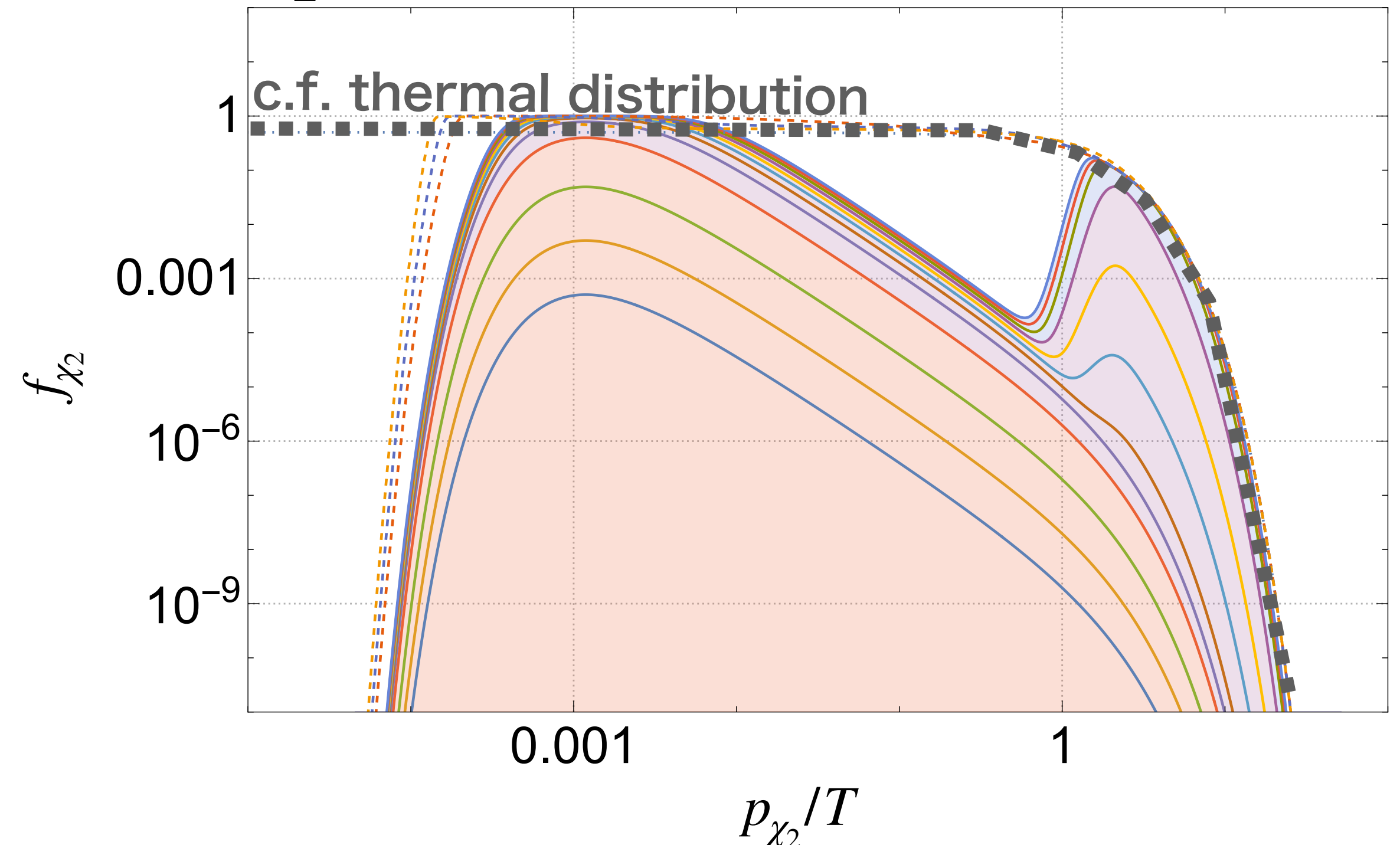
The number density of χ_2 at $p_{\chi_2} \sim T$ is T^3 . Since

$$\dot{n}_{\chi_2} = \dot{n}_\phi \text{ in } \chi_1 \leftrightarrow \chi_2 \phi,$$

ϕ number density



χ_2 (Dirac fermion) occupation#



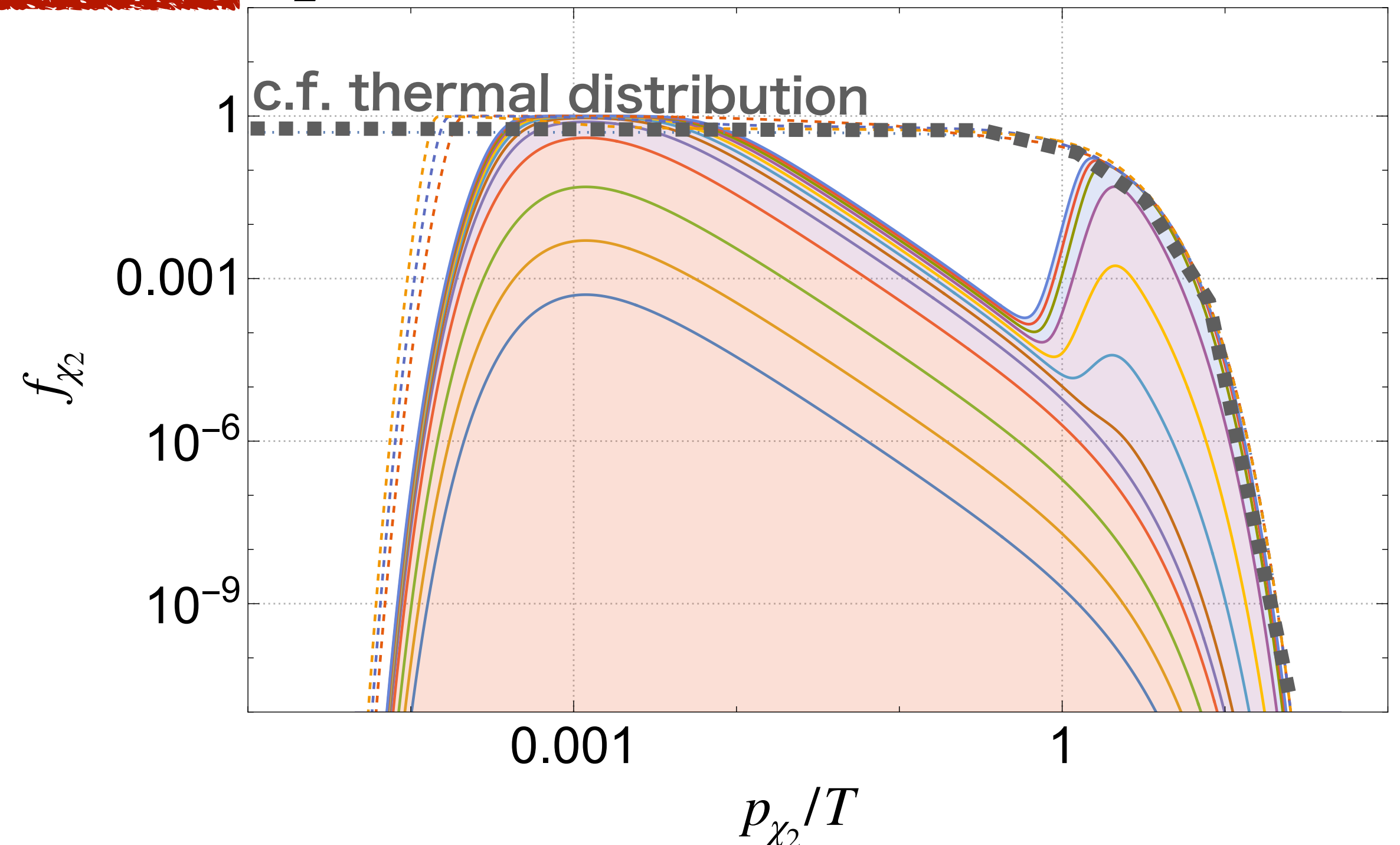
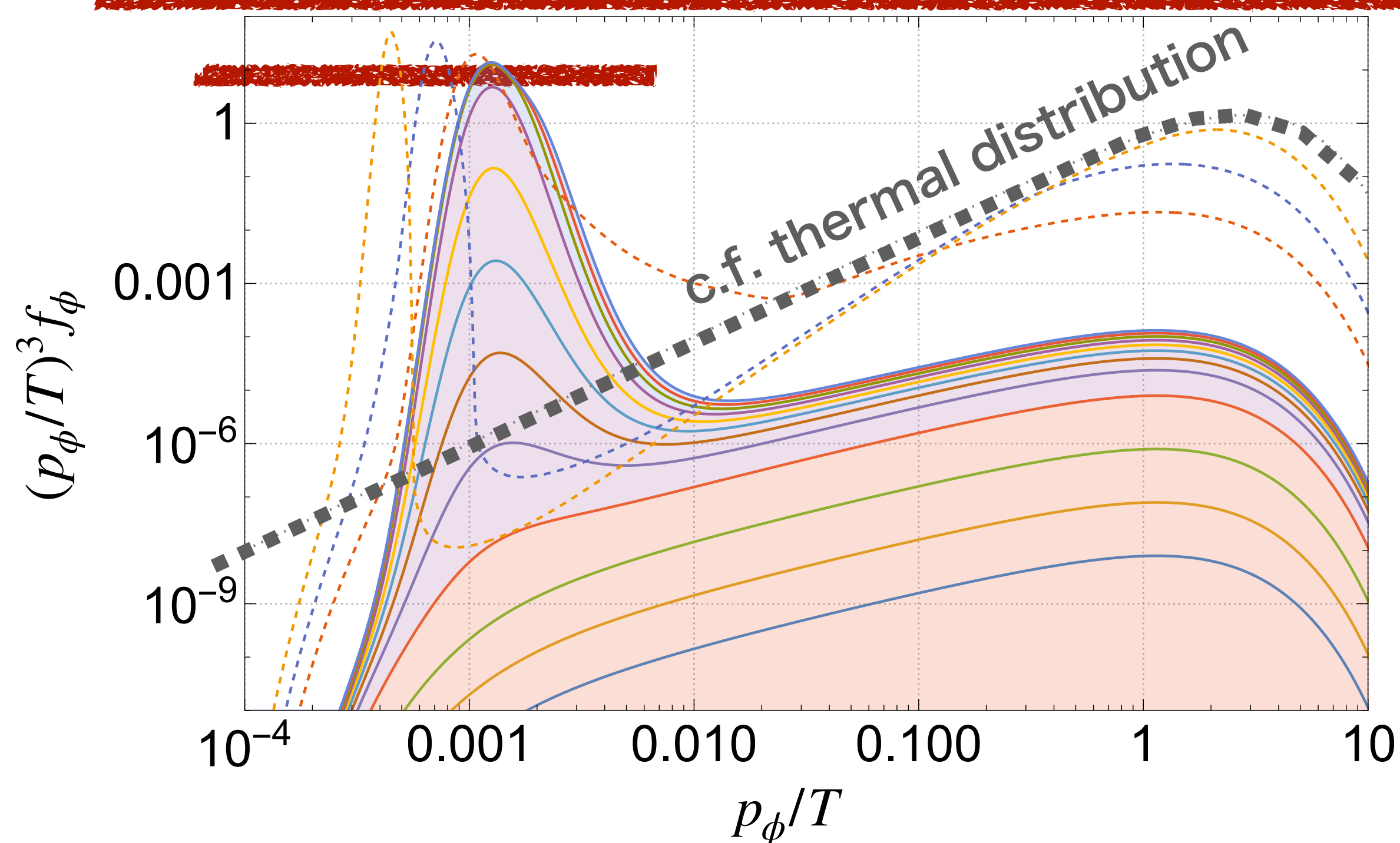
Stage 3: Saturation (quasi-equilibrium)

The number density of χ_2 at $p_{\chi_2} \sim T$ is T^3 . Since

$$\dot{n}_{\chi_2} = \dot{n}_\phi \text{ in } \chi_1 \leftrightarrow \chi_2 \phi,$$

$n_\phi \sim T^3, p_\phi \sim M_1^2/T$, which is cold

χ_2 (Dirac fermion) occupation#

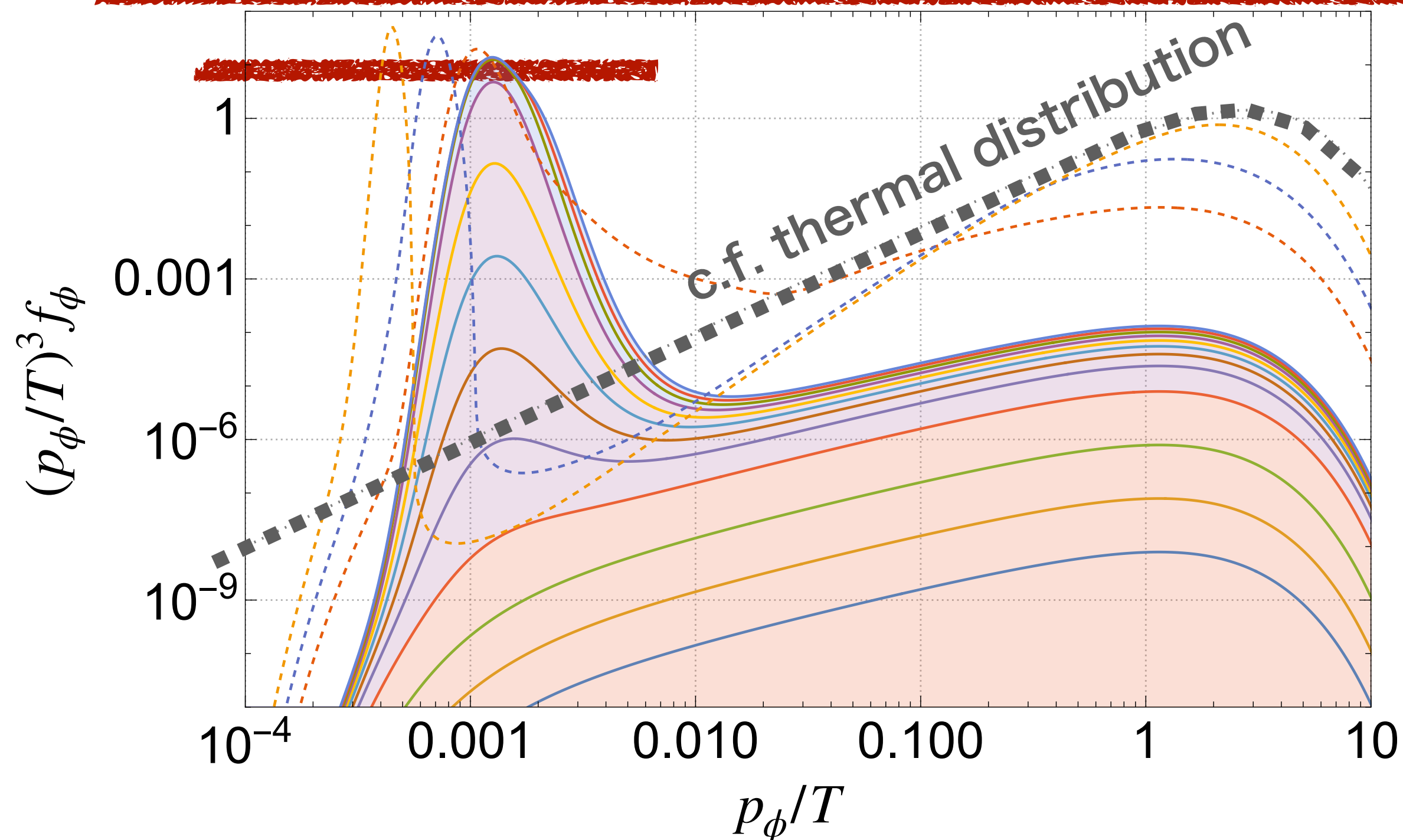


Stage 3: Saturation (quasi-equilibrium)

The number density of χ_2 at $p_{\chi_2} \sim T$ is T^3 . Since

$$\dot{n}_{\chi_2} = \dot{n}_\phi \text{ in } \chi_1 \leftrightarrow \chi_2\phi,$$

$$n_\phi \sim T^3, p_\phi \sim M_1^2/T, \text{ which is cold}$$

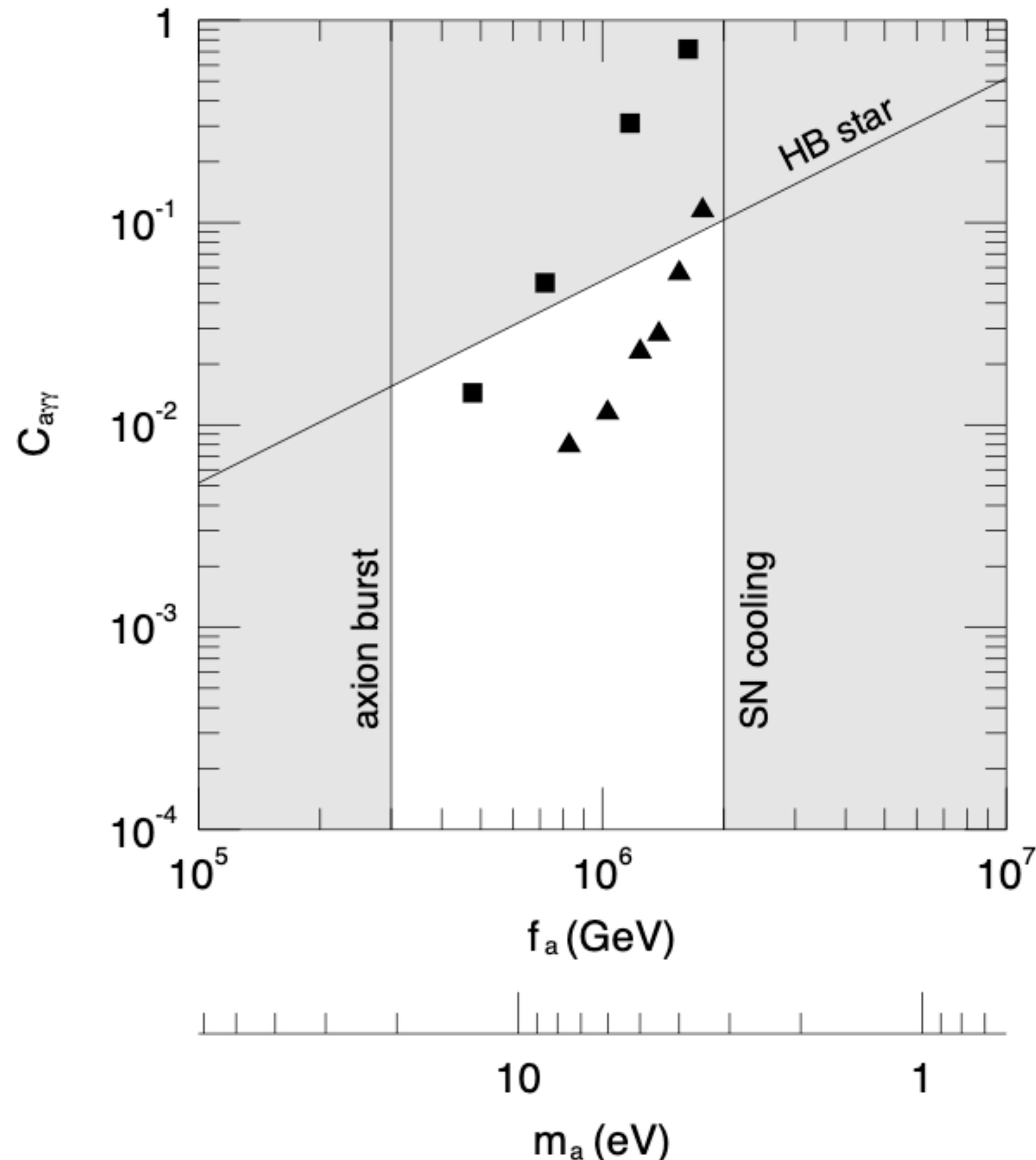


The quasi-equilibrium is kept on a very long time scale until

$$t \sim \left(\Gamma_{\text{decay}}^{(\text{proper})} \right)^{-1} \frac{T}{M_1} \sim \left(\frac{T}{M_1} \right)^4 \Delta t_{\text{ignition}}$$

1. Hadronic QCD axion window

[Chang:1993gm](#), [Moroi:1998qs](#)



QCD axion, coupled with hadrons, may change the measured duration of the neutrino burst from SN1987A.

Only relatively strong ($f_a < 10^6 \text{ GeV}$) or very weak ($f_a > 10^8 \text{ GeV}$) interaction is allowed.

The former has a window around eV.

- Hot DM bound?
 - >model-building can evade it.
- Updates of SN1987A bound close the window? ($f_a < 10^4 \text{ GeV}$? [Chang:2018rso](#))
 - >SN1987A bound to axion may be wrong... [Bar:2019ifz](#)
- Neutron star cooling bound?
 - Is there any study on the trapping regime?